ALFRED-WEGENER-INSTITUT
HELMHOLTZ-ZENTRUM FÜR POLAR- UND MEERESFORSCHUNG

780
2023

Berichte
zur Polar- und Meeresforschung

Reports on Polar and Marine Research

The Expedition PS136 of the Research Vessel POLARSTERN to the Fram Strait in 2023

Edited by

Thomas Soltwedel
with contributions of the participants

HELMHOLTZ

Die Berichte zur Polar- und Meeresforschung werden vom Alfred-Wegener-Institut, Helmholtz-Zentrum für Polar- und Meeresforschung (AWI) in Bremerhaven, Deutschland, in Fortsetzung der vormaligen Berichte zur Polarforschung herausgegeben. Sie erscheinen in unregelmäßiger Abfolge.

Die Berichte zur Polar- und Meeresforschung enthalten Darstellungen und Ergebnisse der vom AWI selbst oder mit seiner Unterstützung durchgeführten Forschungsarbeiten in den Polargebieten und in den Meeren.

Die Publikationen umfassen Expeditionsberichte der vom AWI betriebenen Schiffe, Flugzeuge und Stationen, Forschungsergebnisse (inkl. Dissertationen) des Instituts und des Archivs für deutsche Polarforschung, sowie Abstracts und Proceedings von nationalen und internationalen Tagungen und Workshops des AWI.

Die Beiträge geben nicht notwendigerweise die Auffassung des AWI wider.

Herausgeber
Dr. Horst Bornemann

Redaktionelle Bearbeitung und Layout
Susan Amir Sawadkuhi

Alfred-Wegener-Institut
Helmholtz-Zentrum für Polar- und Meeresforschung
Am Handelshafen 12
27570 Bremerhaven
Germany

www.awi.de
www.awi.de/reports

The Reports on Polar and Marine Research are issued by the Alfred Wegener Institute, Helmholtz Centre for Polar and Marine Research (AWI) in Bremerhaven, Germany, succeeding the former Reports on Polar Research. They are published at irregular intervals.

The Reports on Polar and Marine Research contain presentations and results of research activities in polar regions and in the seas either carried out by the AWI or with its support.

Publications comprise expedition reports of the ships, aircrafts, and stations operated by the AWI, research results (incl. dissertations) of the Institute and the Archiv für deutsche Polarforschung, as well as abstracts and proceedings of national and international conferences and workshops of the AWI.

The papers contained in the Reports do not necessarily reflect the opinion of the AWI.

Editor
Dr. Horst Bornemann

Editorial editing and layout
Susan Amir Sawadkuhi

Alfred-Wegener-Institut
Helmholtz-Zentrum für Polar- und Meeresforschung
Am Handelshafen 12
27570 Bremerhaven
Germany

www.awi.de
www.awi.de/en/reports

Ökologische Langzeituntersuchungen am LTER Observatorium HAUSGARTEN
in der Framstraße vor Spitzbergen
(Foto: Thomas Soltwedel, AWI)

Long-term ecological studies at the LTER observatory HAUSGARTEN
in the Fram Strait off Spitsbergen.
(Photo: Thomas Soltwedel, AWI)

The Expedition PS136 of the Research Vessel POLARSTERN to the Fram Strait in 2023

Edited by

Thomas Soltwedel
with contributions of the participants

Please cite or link this publication using the identiiers
https://hdl.handle.net/10013/epic.96033001-dda8-4c57-864a-7ec4cac22bee
https://doi.org/10.57738/BzPM_0780_2023
ISSN 1866-3192

PS136

22 May 2023 – 19 June 2023

Bremerhaven – Tromsø

Long-Term Ecological Research at an Arctic marine Observatory

Chief scientist
Thomas Soltwedel

Coordinator
Ingo Schewe

Contents

1.	**Überblick und Fahrtverlauf**	**3**
	Summary and itinerary	**5**
2.	**Weather Conditions**	**6**
3.	**LTER HAUSGARTEN – Impact of Climate Change on Arctic Marine Ecosystems**	**8**
4.	**PEBCAO – Plankton Ecology and Biogeochemistry in the Changing Arctic Ocean**	**29**
5.	**Pelagic Biogeochemistry – Nutrients and Net Community Production**	**50**
6.	**Physical Oceanography**	**65**
7.	**Phytooptics**	**77**
8.	**FRAM Pollution Observatory – Monitoring Litter and Microplastic at HAUSGARTEN**	**89**
9.	**FLUX-ON-SITE – Greenhouse Gas Fluxes at Ocean-Sea Ice Interfaces in the Arctic Ocean**	**96**

APPENDIX **99**

A.1 Teilnehmende Institute / Participating Institutes **100**

A.2 Fahrtteilnehmer:innen / Cruise Participants **103**

A.3 Schiffsbesatzung / Ship‘s Crew **105**

A.4 Stationsliste / Station List PS136 **107**

1. ÜBERBLICK UND FAHRTVERLAUF

Thomas Soltwedel DE.AWI

Am Montag, den 22. Mai 2023 verließ die *Polarstern* Bremerhaven zur Expedition PS136, die sie in die Framstraße zwischen Grönland und Spitzbergen führte. Die 4-wöchige Expedition wurde genutzt, um Beiträge zu verschiedenen nationalen und internationalen Forschungs- und Infrastrukturprojekten (FRAM, MUSE, iFOODis, HiAOOS, ICOS-D, SIOS) sowie dem Forschungsprogramm „Changing Earth – Sustaining our Future" („Erde im Wandel – Unsere Zukunft nachhaltig gestalten") des AWI, zu leisten. Im Rahmen des Topic 6 "Marine and Polar Life: Sustaining Biodiversity, Biotic Interactions and Biogeochemical Functions" (Subtopics 6.1 "Future ecosystem functionality" und 6.3 "The future biological carbon pump") des Forschungsprogramms wurden die mit steigenden Wassertemperaturen und dem Rückgang des Meereises verbundenen Ökosystemverschiebungen im Pelagial und im tiefen Ozean ermittelt und quantifiziert und Rückkopplungsprozesse auf ozeanographische Prozesse untersucht. Diese Untersuchungen beinhalteten die Identifizierung räumlicher und zeitlicher Entwicklungen in der Funktion ausgewählter Plankton- und Benthos-Gemeinschaften. Im Rahmen des Subtopics 6.4 „Use and misuse of the ocean: Consequences for marine ecosystems" wurden darüber hinaus der Eintrag von Plastikmüll in den Ozean, vertikale Plastikflüsse von der Meeresoberfläche zum Meeresboden und die Wechselwirkungen zwischen anthropogenem Müll und marinen Organismen untersucht.

Die Arbeiten stellten einen weiteren Beitrag zur Sicherstellung der Langzeitbeobachtungen am LTER Observatorium HAUSGARTEN dar, in denen der Einfluss von natürlichen und durch den Menschen verursachten Umweltveränderungen auf ein arktisches Tiefseeökosystem erfasst und dokumentiert wird. Diese Arbeiten wurden in enger Zusammenarbeit der HGF-MPG Brückengruppe für Tiefsee-Ökologie und -Technologie und der Arbeitsgruppe PEBCAO („Phytoplankton Ecology and Biogeochemistry in the Changing Arctic Ocean") des AWI durchgeführt.

Die Expedition wurde darüber hinaus genutzt, um weitere Installationen im Rahmen der HGF Infrastrukturmaßnahme FRAM (Frontiers in Arctic marine Monitoring) vorzunehmen. Das FRAM Ocean Observing System ermöglicht kontinuierliche Untersuchungen von der Meeresoberfläche bis in die Tiefsee und liefert zeitnah Daten zur Erdsystem-Dynamik sowie zu Klima- und Ökosystem-Veränderungen. Daten des Observatoriums werden zu einem besseren Verständnis der Veränderungen in der Ozeanzirkulation, den Wassermassen-Eigenschaften und des Meereisrückgangs sowie deren Auswirkungen auf das arktische, marine Ökosystem beitragen. FRAM führt Sensoren in Observationsplattformen zusammen, die sowohl die Registrierung von Ozeanvariablen, als auch physiko-chemischer und biologischer Prozesse im Ozean erlauben. Experimentelle und Ereignis-gesteuerte Systeme ergänzen diese Beobachtungsplattformen. Produkte der Infrastruktur umfassen hochaufgelöste Langzeitdaten sowie Basisdaten für Modelle und die Fernerkundung.

Die wissenschaftlichen Arbeiten während der *Polarstern* Expedition PS136 wurden (ein weiteres Mal) in erheblichen Maßen durch die so früh im Jahr vorherrschenden schwierigen Eisbedingungen in der Framstraße beeinträchtigt. Aufgrund der Eisverhältnisse konnte das

Schiff nur mit der im Eis gebotenen Geschwindigkeit von maximal 7 Knoten operieren, so dass das geplante Forschungsprogramm der Reise nicht voll umfänglich durchgeführt werden konnte und einzelne Standard-Stationen des HAUSGARTEN-Observatoriums sogar komplett gestrichen werden mussten. Insbesondere der Einsatz von geschleppten Geräten (Trawls, Kamerasysteme), der Austausch von Verankerungen und der sichere Einsatz des Autonomen Unterwasserfahrzeugs (Autonomous Underwater Vehicle, AUV) der Tiefseegruppe des AWI war nur eingeschränkt möglich – und z.T. auch unmöglich. Nichtsdestotrotz sind wir mit dem Erreichten insgesamt zufrieden. So konnte u.a. ein sehr komplexes und teures Großgerät der Tiefseegruppe des AWI, ein Meeresboden-Kettenfahrzeug (Benthic Crawler), das auf einer *Merian* Expedition MSM108 im Sommer 2022 ausgebracht wurde, während der PS136 erfolgreich geborgen werden. Die *Polarstern* Expedition PS136 endete am Montag, den 19. Juni 2023 in Tromsø, Norwegen (Abb. 1.1).

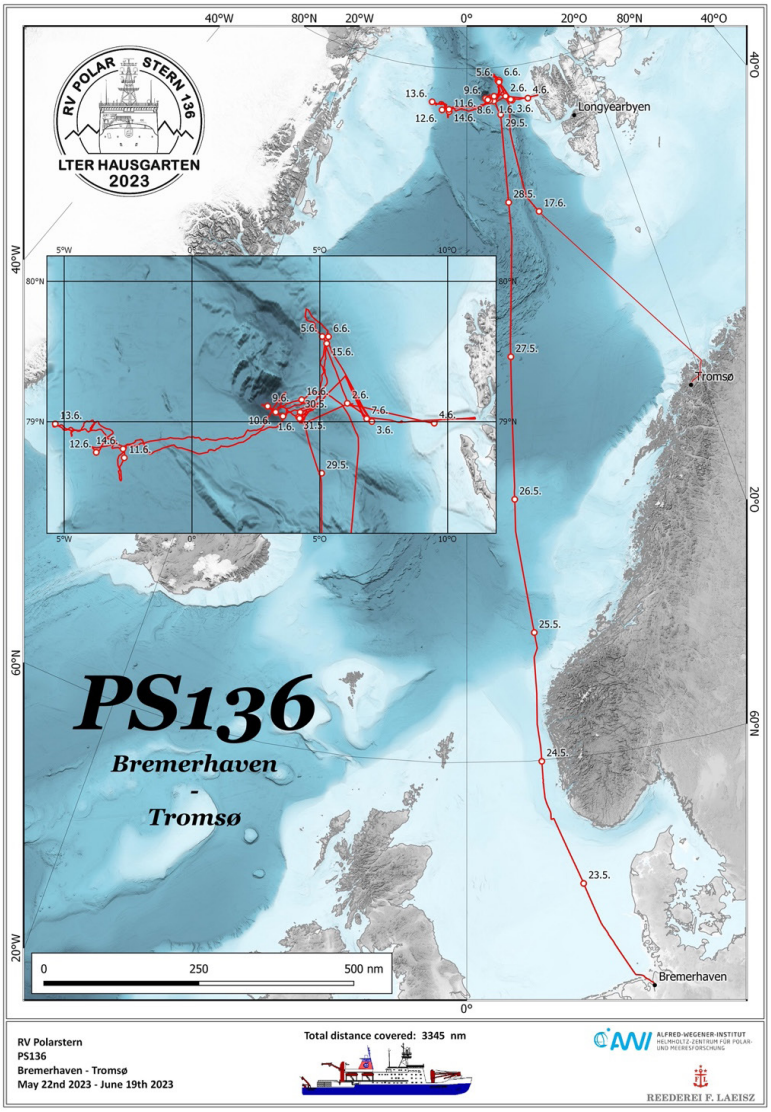

Abb. 1.1: Fahrtverlauf der Expedition PS136 vom Bremerhaven nach Tromsø. Siehe https://doi.pangaea.de/10.1594/PANGAEA.962551 für eine Darstellung des Master tracks in Verbindung mit der Stationsliste für PS136.

Fig. 1.1: Cruise tack of expedition PS136 from Bremerhaven to Tromsø. See https://doi.pangaea.de/10.1594/PANGAEA.962551 to display the master track in conjunction with the station list for PS136.

SUMMARY AND ITINERARY

The *Polarstern* expedition PS136 started on Monday, 22 May 2023 in Bremerhaven and lead to the Fram Strait between Greenland and the Svalbard archipelago. The 4-weeks expedition contributed to various large national and international research and infrastructure projects (FRAM, MUSE, iFOODis, HiAOOS, ICOS-D, SIOS) as well as to the new research programme „Changing Earth – Sustaining our Future" of the AWI. Within Topic 6 "Marine and Polar Life: Sustaining Biodiversity, Biotic Interactions and Biogeochemical Functions" (Subtopics 6.1 "Future ecosystem functionality" and 6.3 "The future biological carbon pump") of the new research programme, ecosystem shifts in the pelagic and deep ocean associated with water temperature increase and sea-ice retreat were identified and quantified, feedback processes on oceanographic processes were investigated. These studies included the identification of spatial and temporal developments in the function of selected pelagic and benthic communities. Within Subtopic 6.4 "Use and misuse of the ocean: Consequences for marine ecosystems", the input of plastic waste into the ocean, the vertical fluxes of plastic from the sea surface to the seafloor, and the interaction between plastic and marine biota were investigated.

The work supported the time-series studies at the LTER (Long-Term Ecological Research) observatory HAUSGARTEN, where we document natural and Global Change induced environmental variations on a polar deep-water ecosystem. This work was carried out in close co-operation between the HGF-MPG Research Group on Deep-Sea Ecology and Technology and the Working Group PEBCAO ("Phytoplankton Ecology and Biogeochemistry in the Changing Arctic Ocean") at AWI.

The expedition was further used to accomplish installations for the HGF infrastructure project FRAM (Frontiers in Arctic marine Monitoring). The FRAM Ocean Observing System aims at permanent presence at sea, from surface to depth, for the provision of near real-time data on Earth system dynamics, climate variability and ecosystem change. It serves national and international tasks towards a better understanding of the effects of change in ocean circulation, water mass properties and sea-ice retreat on Arctic marine ecosystems and their main functions and services. FRAM implements existing and next-generation sensors in observatory platforms, allowing synchronous observation of relevant ocean variables as well as the study of physical, chemical and biological processes in the ocean. Experimental and event-triggered platforms complement the observational platforms. Products of the infrastructure are continuous long-term data with appropriate resolution in space and time, as well as ground-truthing information for ocean models and remote sensing.

The scientific work during *Polarstern* Expedition PS136 was (again) significantly affected by the difficult ice conditions in the Fram Strait so early in the year. Due to the ice conditions, the ship could only operate at the appropriate maximum speed of 7 knots in the ice, so that the research programme during PS136 could not be fully carried out and individual standard stations of the HAUSGARTEN observatory even had to be cancelled completely. In particular, the use of towed equipment (trawls, camera systems), the replacement of moorings and the safe use of the Autonomous Underwater Vehicle (AUV) was only possible to a limited extent, or even impossible. Nevertheless, we are satisfied overall with what was achieved. For example, a very complex and expensive large-scale device of the AWI's Deep-Sea Research Group, a mobile seafloor platform (benthic crawler), which was deployed on a *Merian* expedition MSM108 in summer 2022, was successfully recovered during PS136. *Polarstern* Expedition PS136 ended on Monday 19 June 2023 in Tromsø, Norway (Fig. 1.1).

2. WEATHER CONDITIONS

Julia Wenzel[1], Christian Rohleder[1] [1]DE.DWD

Grant-No. AWI_PS136_00

The transit from Bremerhaven to the working area in the Fram Strait between Svalbard and Greenland started on 22 May and lasted one week. During the journey, *Polarstern* was influenced by a storm moving from Iceland to the northeast and filling up east of Svalbard from 27 May. When crossing its frontal system on 23 May the wind and the sea state temporarily increased to 8 Bft and 3 m. The low also caused a mean wind of 7 Bft and a significant wave height of 5 m (wind sea and swell) on 25 and 26 May. By reducing the ship's speed, an even higher swell could be avoided.

The occluding frontal system of another low near Iceland with a similar track as the previous one crossed *Polarstern* in the Norwegian Sea on 27 May, with the wind shifting to the east and temporarily increasing to 8 Bft. Continuing northward, wind and sea state decreased steadily. On 29 May *Polarstern* reached the working area in the Fram Strait. There, a significant wave height of 1 m or less occurred most of the time, and with travelling to the west, *Polarstern* was protected from wave development in the ice for several days. With a few exceptions (described below), the wind speed was between 2 and 4 Bft on most of the time.

The above mentioned low reached Franz-Josef-Land on 31 May, weakened slowly during the following days and filled up until 6 June. Originating from a high south of Iceland, a ridge extended into the western Fram Strait on 31 May, from which an own high developed over the Fram Strait on 2 June. As a result, the wind shifted to the north and temporarily increased to 8 Bft on 31 May with a resulting wind sea of 2 m.

The following days were characterized by calmer high-pressure weather, maintained by a high-pressure bridge between the high south of Iceland and a high over the northern part of Greenland. Due to local effects caused by the orography and proximity to Svalbard, the wind temporarily increased to 6 Bft on 4 June. From 8 June onwards, the high south of Iceland shifted eastward together with the northward reaching ridge.

In the night to 8 June, a low formed off the east coast of Greenland at the latitude of Iceland and moved north-eastward while deepening. It crossed the Fram Strait on 11 June and reached Svalbard on 12 June. It transported a more humid and warmer air mass into the Fram Strait, resulting in dense fog on 10 and 11 June and no suitable flight conditions for helicopter operations until 12 June. Upon reaching the back side of the low, the wind shifted to northwest and increased to 7 to 8 Bft on 12 June. Since *Polarstern* was in the ice at that time, this had no significant effect on the sea state in the vicinity of the ship.

The low moved into the Barents Sea on 13 June while weakening. On the same day, a ridge extending northward from a high-pressure system over the Norwegian Sea crossed the Fram Strait. This short weather window could again be used for helicopter flights. From 13 to 14 June a low-pressure system moved from North Greenland to Svalbard. In the night to 14 June

it transported low clouds in and caused north-westerly winds up to 7 Bft on 14 June. From 14 to 16 June another high-pressure ridge moving from west to east brought again calmer weather conditions.

On 16 June the return journey to Tromsø (Norway) began. During the whole cruise the significant wave height mostly was about 1 m. After having been crossed in the night to 17 June by the warm front of a low-pressure system that was moving from the east coast of Greenland to the western Fram Strait (prefrontal backing of the wind to Southeast and increase to 6 Bft, postfrontal wind from Southwest with 4 to 5 Bft), *Polarstern* approached the high-pressure system over the Norwegian Sea while travelling southward. While crossing the high on 18 June fog occurred accompanied with weak variable winds. Just off the Norwegian coast on the southern side of the high, the wind shifted to the northeast to east and temporarily increased to 6 Bft. In the morning of 19 June *Polarstern* reached Tromsø.

3. LTER HAUSGARTEN – IMPACT OF CLIMATE CHANGE ON ARCTIC MARINE ECOSYSTEMS

Christiane Hasemann[1], Maikani Andres[2], Volker Asendorf[3], Alexandra Aves[4], Saskia Brix[5], Michael Busack[1], Jennifer Dannheim[1], Konstantin Flegar[1], Jonas Hagemann[1], Katharina Kistrup[1], Sascha Lehmenhecker[1], Katrin Linse[6], Normen Lochthofen[1], Janine Ludszuweit[1], Anneke Neber[7], Autun Purser[1], Sonja Rückert[8], Ingo Schewe[1], Lydia Schmidt[9], Maximilian Schrade[1], Kharis Schrage[2], Thomas Soltwedel[1];
not on board: Deonie Allen[4], Melanie Bergmann[1], Kirstin Meyer-Kaiser[2], Frank Wenzhöfer[1]

[1]DE.AWI
[2]US.WHOI
[3]DE.MPIMM
[4]NZ.UCANT
[5]DE.SENCKENBERG
[6]UK.BAS
[7]DE.HS-BHV
[8]DE.UNI-DUE
[9]DE.UNI-ROS

Grant No. AWI_PS136_01

Objectives and scientific programme

The marine Arctic has played an essential role in the history of our planet over the past 130 million years and contributes considerably to the present functioning of the Earth and its life. The past decades have seen remarkable changes in key Arctic variables, including a decrease of sea-ice extent and sea-ice thickness, changes in temperature and salinity of Arctic waters, and associated shifts in nutrient distributions. Since Arctic organisms are highly adapted to extreme environmental conditions with strong seasonal forcing, the accelerating rate of recent climate change challenges the resilience of Arctic life. The stability of a number of Arctic populations and ecosystems is probably not strong enough to withstand the sum of these factors, which might lead to a collapse of subsystems.

Benthos, particularly in deep waters, is a robust ecological indicator for environmental changes, as it is relatively stationary and long-lived, and reflects changes in ecological conditions in the oceans (e.g. organic flux to the seabed) at integrated scales (Gage and Tyler 1991; Piepenburg 2005). To detect and track the impact of large-scale environmental changes in the transition zone between the northern North Atlantic and the central Arctic Ocean, and to determine experimentally the factors controlling deep-sea biodiversity, the Alfred Wegener Institute Helmholtz Center for Polar and Marine Research (AWI) established the deep-sea observatory HAUSGARTEN, which constitutes the first, and until now only open-ocean long-term observatory in a polar region (Soltwedel et al. 2016).

HAUSGARTEN is located in the eastern Fram Strait and includes 21 permanent sampling sites along a depth transect (250 - 5,500 m) and along a latitudinal transect following the 2,500 m isobath crossing the central HAUSGARTEN station (Fig. 3.1). Multidisciplinary research activities at HAUSGARTEN cover almost all compartments of the marine ecosystem from the pelagic zone to the benthic realm. Regular sampling as well as the deployment of moorings and different stationary and mobile free-falling systems (Bottom-Lander, Benthic Crawler), which

act as local observation platforms, have taken place since the observatory was established in 1999. Frequent visual observations with towed photo/video systems allow the assessment of large-scale epifauna distribution patterns as well as their temporal development.

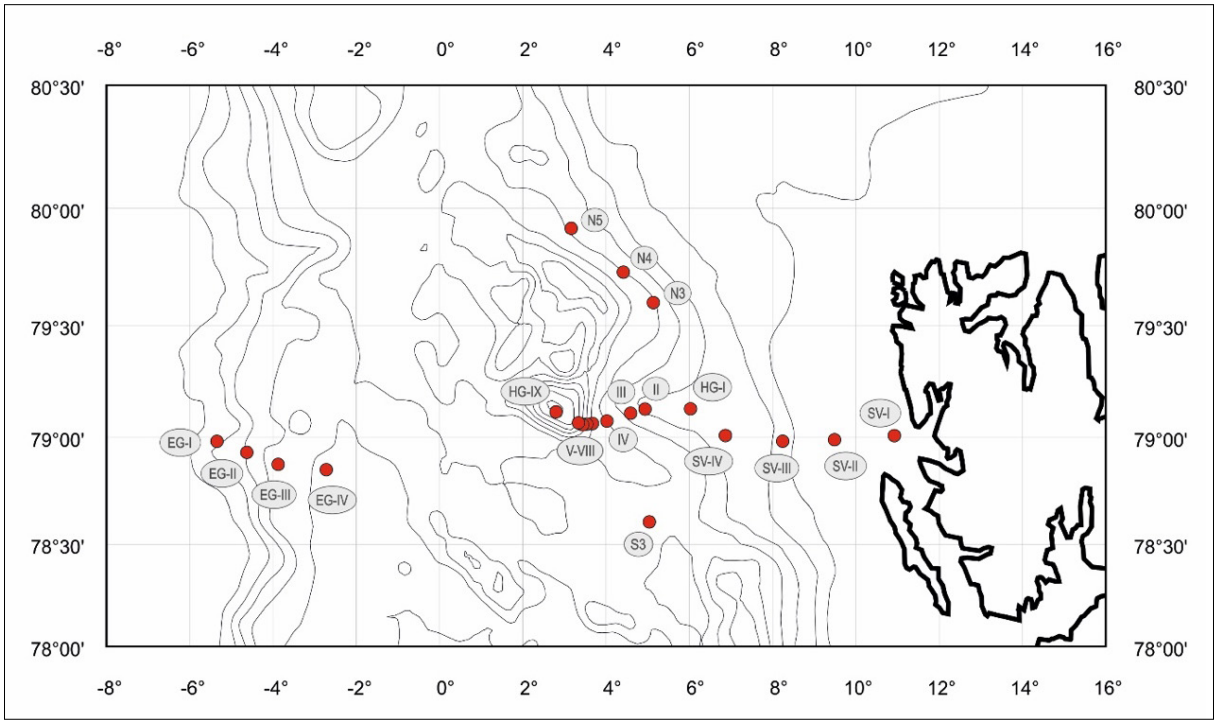

Fig. 3.1: Permanent sampling sites of the LTER Observatory HAUSGARTEN in the Fram Strait

Geographical features in the HAUSGARTEN area provide a variety of contrasting marine landscapes and landscape elements (e.g. banks, troughs [marine valleys], ridges and moraines, canyons and pockmarks) that generally shape benthic communities over a variety of different scales (Buhl-Mortensen et al. 2010, 2012). The habitat-diversity (heterogeneity) hypothesis states that an increase in habitat heterogeneity leads to an increase in species diversity, abundance and biomass of all fauna groups (Whittaker et al. 2001; Tews et al. 2004). Improved technologies, particularly the recent deployment of acoustic and side-scan sonar systems at depth by an Autonomous Underwater Vehicle (AUV) and towed camera sleds within AWI's Deep-Sea Research Group (Purser et al. 2018) have indicated the high-resolution topographical variability of many deep-sea areas, including HAUSGARTEN (Schulz et al. 2010; Taylor et al. 2016; Purser et al. 2021). So far, the time-series stations maintained across the region do not capture the high degree of local heterogeneity (in terms of physical seafloor terrain variables such as slope, rugosity, aspect, depth). Therefore, during *Polarstern* expedition PS136, dedicated attempts to collect spatial data to capture the role of this heterogeneity in biodiversity and biomass estimation are planned to complement investigations on the temporal variability of benthos in the HAUSGARTEN area.

Early life history ecology of benthic invertebrates remains virtually unknown in the Arctic deep sea. The research at HAUSGARTEN observatory and surrounding waters has revealed much about the distribution and ecology of invertebrate organisms living on the seafloor, but without knowing their origins it will still be difficult to fully assess how the populations may change in the face of Climate Change. By studying the larvae of these organisms, we hope to shine light on how these organisms reproduce, where they may disperse to, and how these things

may change in the future. Studying surface waters allowed us to study two distinct groups of organisms. Planktonic larvae of deep-sea organisms local to the HAUSGARTEN may go to the surface to feed. In addition, non-local species may be advected through the area. If they are shallow water organisms they may die before reaching suitable habitat. By studying their distribution as well as the currents we may better understand their dispersal potential as well as larval mortality. In addition, some larvae may be species invading from the south, so understanding their current dispersal may help inform future non-native and invasive species distributions in the area.

Work at sea

Larval biology in the Fram Strait

In order to collect larvae from throughout the water column, three collection devices were employed. First, a WTS-LV pump (McLane Research Laboratories, USA) was deployed to the seafloor on a free-falling system (bottom lander). Three of the four planned deployments were carried out and were successful (planned deployments at N3 and N5 could not be carried out due to the ice cover). Lander deployments took place at S3, HG-IV, and a new location between and north of the HG-IV and SV-IV stations that was of similar depth to the other stations (Fig 3.1; Table 3.1). The second equipment deployed regularly was the multi-net. The five nets had a mesh size of 150 µm and was deployed at depth bins of 1,500–1,000, 1,000 – 500, 500 –200, 200 – 50, and 50 – 0 m. Multi-nets were deployed at S3, HG-IV, N3, and N4 (Tab. 3.1). The final equipment used was a 63 µm mesh hand-net deployed to 20 m over the side off the D deck during CTD/Rosette Water Sampler deployments at 17 stations (Tab. 3.1). In addition to deployment of these different systems to collect larvae, biofouling species were opportunistically collected from moorings and lander systems being recovered during PS136.

Tab. 3.1: Equipment deployments and collections to study larval biology during PS136

Event number	Sample code	Station	Date	Gear	Latitude	Longitude	Sample depth [m]
PS136_4-1	S3_LL	S3	29/05/23	Larvae-Lander	78.616063	5.000583	2350
PS136_4-4	S3_HN	S3	29/05/23	Hand-net	78.609755	5.067711	20
PS136_4-6	S3_MN	S3	29/05/23	Multi-net	78.609776	5.067434	1500
PS136_5-6	HGIV_MN	HG-IV	30/05/23	Multi-net	79.074891	4.240551	1500
PS136_5-8	HGIV_LL	HG-IV	30/05/23	Larvae-Lander	79.072496	4.259397	2376
PS136_7-3	HGIII_HN	HG-III	31/05/23	Hand-net	79.106934	4.596983	20
PS136_8-3	HGIV_BF	HG-IV	01/06/23	Long-term-Lander	79.037235	4.185137	2500
PS136_10-2	HGI_HN	HG-I	01/06/23	Hand-net	79.131089	4.916879	20
PS136_12-5	SVIV_HN	SV-IV	03/06/23	Hand-net	79.029306	6.998891	20
PS136_13-3	SVIII_HN	SV-III	03/06/23	Hand-net	79.000115	8.225245	20
PS136_14-3	SVI_HN	SV-I	04/06/23	Hand-net	79.028059	11.07844	20
PS136_15-4	SVII_HN	SV-II	04/06/23	Hand-net	78.979882	9.512964	20
PS136_12-2	F4S-6_BF	F4S-6	03/06/23	Mooring	79.007872	6.964353	1280
PS136_17-3	N3_MN	N3	05/06/23	Multi-net	79.605823	5.097895	1500
PS136_17-9	N3_HN	N3	05/06/23	Hand-net	79.62238	5.072646	20
PS136_18-4	N4_HN	N4	05/06/23	Hand-net	79.740314	4.478702	20
PS136_18-8	N4_MN	N4	06/06/23	Multi-net	79.772491	4.44858	1500

Event number	Sample code	Station	Date	Gear	Latitude	Longitude	Sample depth [m]
PS136_21-1	Surprise_ LL	Surprise	06/06/23	Larvae-Lander	79.334254	6.000073	1715
PS136_23-3	HGV_HN	HG-V	07/06/23	Hand-net	79.055213	3.669202	20
PS136_24-3	HGVI_HN	HG-VI	08/06/23	Hand-net	79.042029	3.544632	20
PS136_25-3	HGVII_ HN	HG-VII	08/06/23	Hand-net	79.059469	3.446685	20
PS136_27-3	HGIX_HN	HG-IX	09/06/23	Hand-net	79.125603	2.968555	20
PS136_30-5	EGIV_HN	EG-IV	11/06/23	Hand-net	78.76751	-2.64468	20
PS136_31-3	EGIII_HN	EG-III	12/06/23	Hand-net	78.811858	-3.91674	20
PS136_32-3	EGII_HN	EG-II	12/06/23	Hand-net	78.925963	-4.72543	20
PS136_33-2	EGI_HN	EG-I	13/06/23	Hand-net	78.988866	-5.37904	20

Benthic bacteria, parasites, meiobenthos, and biogenic sediment compounds

Virtually undisturbed sediment samples were taken using a multiple corer (MUC; Fig. 3.2). Various biogenic compounds from these sediments were analysed to estimate the input of organic matter to the seafloor as well as benthic activities (i.e. bacterial exoenzymatic activity) and the total biomass (i.e. particulate proteins, phospholipids) of the smallest sediment-inhabiting organisms (Tab. 3.2).

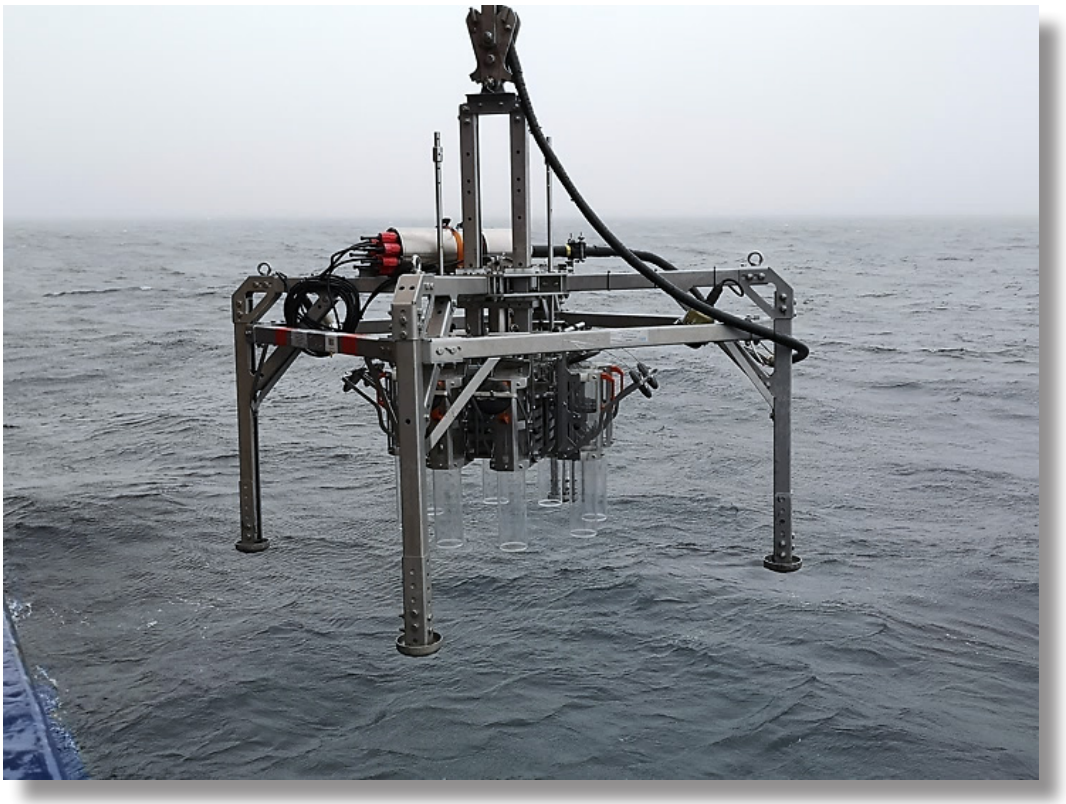

Fig. 3.2: Deployment of the video-controlled multiple corer (OKTOPUS GmbH) during Polarstern expedition PS136

Tab. 3.2: HAUSGARTEN stations with station ID, date, geographic position and water depth [m] of PS136. Stations were sampled with multiple corer (MUC), box corer (BC), as well as two deployments (L-RE) and one recovery (L-RC) of the arcFOCE-Lander for experiments; (f) = box corer failed

Site	Station ID	Date	Latitude	Longitude	Depth [m]	Gear
SV-I	PS136_14-7	04/06/2023	79° 01.71‘ N	011° 04.62‘ E	287	MUC
SV-II	PS136_15-5	04/06/2023	78° 58.80‘ N	009° 30.89‘ E	230	MUC
SV-IV	PS136_12-8	03/06/2023	79° 01.77‘ N	006° 59.98‘ E	1296	MUC
SV-IV	PS136_12-9	03/06/2023	79° 01.78‘ N	006° 59.92‘ E	1296	BC
HG-I	PS136_11-9	02/06/2023	79° 08.01‘ N	006° 05.47‘ E	1271	BC
HG-I	PS136_11-10	02/06/2023	79° 08.00‘ N	006° 05.50‘ E	1272	MUC
HG-I	PS136_11-11	02/06/2023	79° 07.99‘ N	006° 05.52‘ E	1272	BC (f)
HG-I	PS136_11-11	02/06/2023	79° 07.96‘ N	006° 05.792 E	1272	BC
HG-II	PS136_10-4	02/06/2023	79° 07.90‘ N	004° 54.75‘ E	1523	MUC
HG-II	PS136_10-5	02/06/2023	79° 07.82‘ N	004° 54.08‘ E	1538	BC
HG-III	PS136_7-4	31/05/2023	79° 06.43‘ N	004° 36.26‘ E	1909	MUC
HG-III	PS136_7-5	01/06/2023	79° 06.52‘ N	004° 36.41‘ E	1887	BC
HG-IV	PS136_5-10	30/05/2023	79° 03.95‘ N	004° 09.69‘ E	2462	BC
HG-IV	PS136_5-11	31/05/2023	79° 03.89‘ N	004° 10.81‘ E	2450	MUC
HG-IV	PS136_5-12	31/05/2023	79° 03.97‘ N	004° 10.57‘ E	2450	BC
HG-V	PS136_23-6	08/06/2023	79° 03.19‘ N	003° 40.65‘ E	3031	MUC
HG-V	PS136_23-7	08/06/2023	79° 03.35‘ N	003° 41.70‘ E	2992	BC
HG-VI	PS136_24-5	08/06/2023	79° 02.82‘ N	003° 32.34‘ E	3601	MUC
HG-VI	PS136_24-6	08/06/2023	79° 02.18‘ N	003° 33.98‘ E	3519	BC
HG-VII	PS136_25-6	08/06/2023	79° 03.14‘ N	003° 26.49‘ E	4214	MUC
HG-VII	PS136_25-7	08/06/2023	79° 02.77‘ N	003° 28.97‘ E	4002	BC (f)
HG-VII	PS136_25-8	09/06/2023	79° 03.06‘ N	003° 26.59‘ E	4126	BC (f)
HG-VIII	PS136_26-2	09/06/2023	79° 03.96‘ N	003° 19.88‘ E	5032	MUC
HG-IX	PS136_27-10	09/06/2023	79° 07.97‘ N	002° 56.47‘ E	5529	MUC
HG-IX	PS136_27-11	10/06/2023	79° 08.14‘ N	002° 56.53‘ E	5531	BC
N3	PS136_17-5	05/06/2023	79° 36.83‘ N	005° 12.11‘ E	2736	MUC
N3	PS136_17-6	05/06/2023	79° 36.69‘ N	005° 08.22‘ E	2769	BC
N4	PS136_18-9	06/06/2023	79° 47.62‘ N	004° 27.51‘ E	2356	MUC
N4	PS136_18-10	06/06/2023	79° 48.44‘ N	004° 28.13‘ E	2288	BC
S3	PS136_4-12	29/05/2023	78° 36.61‘ N	005° 04.04‘ E	2325	MUC
S3	PS136_4-13	29/05/2023	78° 36.64‘ N	005° 03.74‘ E	2326	BC
EG-I	PS136_33-10	13/06/2023	78° 57.97‘ N	005° 25.81‘ W	927	MUC
EG-I	PS136_33-11	13/06/2023	78° 57.85‘ N	005° 25.50‘ W	925	BC
EG-II	PS136_32-4	13/06/2023	78° 54.55‘ N	004° 43.45‘ W	1432	MUC
EG-II	PS136_32-5	13/06/2023	78° 54.08‘ N	004° 42.06‘ W	1443	BC
EG-III	PS136_31-5	12/06/2023	78° 48.58‘ N	003° 54.35‘ W	1970	MUC
EG-III	PS136_31-6	12/06/2023	78° 47.18‘ N	003° 48.47‘ W	2011	BC

Site	Station ID	Date	Latitude	Longitude	Depth [m]	Gear
EG-IV	PS136_30-8	11/06/2023	78° 39.89‘ N	002° 48.56‘ W	2524	MUC
EG-IV	PS136_30-9	11/06/2023	78° 38.49‘ N	002° 49.02‘ W	2513	BC
HG-II	PS136_10-6	02/06/2023	79° 07.86‘ N	004° 53.87‘ E	1538	L-RE
		07/06/2023	79° 07.87‘ N	004° 54.38‘ E	1532	L-RC
HG-II	PS136_37-1	15/06/2023	79° 08.10‘ N	004° 52.85‘ E	1494	L-RE

Sediment-bound chloroplastic pigments (chlorophyll *a* and its degradation products) represent a suitable indicator for the input of phytoplanktonic detritus to the seafloor, representing the major food source for benthic organisms. They can be analysed with high sensitivity by fluorometric methods. To estimate the potential heterotrophic activity of bacteria, we measured cleaving rates of extracellular enzymes using the model-substrate FDA (fluorescein-di-acetate) in incubation experiments. Results will help to describe ecosystem changes in the benthal of the Arctic Ocean.

Additional samples were taken to analyse the abundance and biomass of bacteria as well as meiofauna densities and the diversity patterns of nematodes. Moreover, samples were taken to study, for the first time, the potential diversity of parasitic protists associated with benthic organism in four different sampling approaches:

1. The upper 2 cm of two cores retrieved by the MUC at each station were sieved through a 125 µm sieve and then fixed in ethanol and Histofix (one sample each). These will be analysed for meio- and macrofauna. Once sorted, collected invertebrates will be dissected to isolate parasitic protists, e.g. gregarine apicomplexans.

2. In addition, a small duplicate sample of sediment from the middle of each of the two cores was fixed in RNA/DNA Shield for amplicon sequencing to identify any parasitic protists present in the benthos that could not be detected by dissections.

3. The supernatant of one core was collected at six stations (i.e. HG-I, HG-IV, HG-VII, HG-IX, EG-I, EG-IV). 600 ml of the supernatant were filtered through 0.45-µm cellulose nitrate membrane filters (diameter 47 mm; Nalgene) for later DNA extraction and amplicon sequencing to identify potential traces of parasitic protists.

4. Sediment retrieved from two box corers at two stations (HG-I and HG-IV) was sieved through a 500-µm sieve and fixed in ethanol and Histofix. The samples will be sorted to collect benthic invertebrates. The invertebrates will later be dissected to isolate parasitic protists.

Bacterial activities and chloroplastic pigments were analysed on board. All other sub-samples were stored for later analyses of the meiobenthic fauna and various biochemical bulk parameters at the home lab.

Macrobenthos

We were able to take a total of 17 box corer samples at 16 sites (20 deployments of which one failed and two were only used qualitatively due to uneven seafloor or gear failure; see Tab. 3.2). At HAUSGARTEN station HG-VII the box corer did not close properly due to uneven seafloor and was washed out when setting down on deck, thus the sample was sieved but is only useful for presence-absence data analysis.

Macrobenthic samples were obtained by USNEL box corer (0.25 m²; Fig. 3.3), a preferred sampling gear in deep waters, as it provides reliably deep and relatively undisturbed sediment samples adequate for macrofauna sampling. The samples allow a continuation of the long-term series along depth gradients from the top to deeper adjacent areas and a comparison between samples of ice-free zones and stations covered mainly by ice throughout most of the year.

Fig. 3.3: Recovery of the USNEL giant box corer deployed from the aft of Polarstern

Box-corer samples were divided into eight equal subsamples. The upper 12 cm of each subsample sediment and the supernatant seawater to catch epibenthic animals from the fluffy layer on top of the sediment, were taken for further sample processing. Quantitative and qualitative samples were sifted over a 500 µm mesh size sieve and sieve residues were preserved in 4% buffered formalin. In the laboratory at AWI, species will be determined to the lowest possible taxonomic level, counted and wet weights per species will be determined.

Further macrofauna was sampled using an Epibenthic Sledge (EBS) with a bottom shovel to open the sampler box doors on the seafloor only are proven sampling devices to collect macrofaunal organisms on and above the seafloor (Brandt and Barthel 1995; Kaiser and Brenke 2016). During PS136, a double, supra- and epi-sampler EBS *sensu* Brenke (2005), named BERTA (Fig. 3.4) was deployed at a total of six HAUSGARTEN sites (Tab. 3.3). BERTA was equipped with a bracket to hold an Aanderaa Seaguard RCM DW CTD to further characterize environmental parameters of pressure, temperature, salinity, turbidity and current/current direction by the latter as well as seafloor habitat heterogeneity by the former. The sampler boxes are of the same size to allow for comparison between samples. The lower sampler, its net and cod end are referred to as epi-net, while the upper sampler, its net and cod end are referred to as supra-net. The mesh size of the nets is 500 µm. The cod ends are equipped with net-buckets containing a 300-µm mesh window (Brenke 2005).

Fig. 3.4: Deployment of the Epibenthic Sledge BERTA during Polarstern cruise PS136

Tab. 3.3: EBS stations.

Area	Station	Date	Latitude	Longitude	Depth [m]	Gear
S3	PS136_4-11	29/05/2023	78° 36.172' N 78° 37.079' N	005° 08.807' E 005° 07.750' E	2336 2328	EBS start EBS end
HG-IV	PS136_5-9	30/05/2023	79° 04.459' N 79° 05.547' N	004° 15.343' E 004° 15.419' E	2372 2382	EBS start EBS end
HG-I	PS136_11-14	03/06/2023	79° 07.336' N 79° 07.304' N	006° 08.619' E 006° 10.552' E	1255 1254	EBS start EBS end
N3	PS136_19-1	06/06/2023	79° 36.889' N 79° 36.790' N	005° 19.684' E 005° 18.922' E	2560 2587	EBS start EBS end
HG-IX	PS136_27-12	10/06/2023	79° 07.457' N 79° 07.439' N	002° 45.057' E 002° 46.163' E	5409 5414	EBS start EBS end
EG-IV	PS136_30-10	11/06/2023	78° 36.467' N 78° 35.108' N	002° 46.748' W 002° 46.137' W	2545 2551	EBS start EBS end

The position of the EBS deployments were chosen based on the most available box corer data in the HAUSGARTEN area to allow a biodiversity comparison of the qualitative box corer sampling to the semi-qualitative EBS deployment over a larger distance. Deployments took between 2.5 and 3.5 hours and calculated trawling distance varied between approx. 500 and 2,000 m. The trawled distanced were planned to be either parallel or in min. 1 nm distance to the OFOBS transect lines to enable a collection of reference specimens next to a visual description of the sampled area by still and video imagery (reference to OFOBS dives). The EBS was deployed via the A-frame of *Polarstern* following a standard protocol in ice-free areas and an adapted "flexible" protocol to allow sampling with the ice drift in ice covered areas:

1. *Polarstern* holding on start position (in sea-ice drifting with the ice)
2. Lower with 0.5 m/s (max. 0.8 m/s) to 300 m over ground (in sea-ice conditions depending on the drift speed)
3. Winch stopped for 1 min. to stop swinging of EBS and letting the gear flowing behind the vessel in the right direction in the water column
4. *Polarstern* moving forward with 1 kt over ground, while lowering with 0.5 m/s until 1,500 m cable length over water depth or cable length depending on space of free water between the ice floats. The winch speed on stations in the ice depended on the speed of the ice drift as well as the position holding or letting *Polarstern* drifting with the ice during deployment
5. Winch stopped
6. *Polarstern* moving with 1 kt for 10 min. (In sea ice conditions vessel speed according to ice drift speed)
7. *Polarstern* stopped (step omitted in sea ice conditions or vessel operating against the drift to secure the wire)
8. Heaven with 0.3 m/s (max. 0.4) until EBS leaves seafloor
9. Raise heaving speed to 1.0 m/s until deck
10. On deck the EBS will be secured in a hanging position to enable cleaning of nets prior to removal of cod ends and empty of sediment in nets into rectangular rubber tubs

Landing of the EBS on ground and lift off ground were monitored by the vessels tension meter system digitally and on paper.

The trawl lengths were calculated using the following formula:

$$s = v1 \times t1 + v2 \times t2 + v3 \times t3$$

s= trawl length, t1 = vessel trawl time (min), t2 = vessel haul (min), t3 = winch haul time (min), v1 = vessel trawl speed (m/s), v1 = vessel haul speed (m/s), v1 = winch haul speed (m/s).

Upon arrival on deck, the cod ends were retrieved from the nets and immediately transported to the cooling container (+4°C). Here, samples were sieved in pre-cooled filtered seawater over a 300 µm mesh. Organisms visible to the eye were removed from the sieve for live sorting of all possible invertebrate taxa. The remaining samples from the cod ends were fixed in pre-cooled denaturated 96 % ethanol.

When available, net supernatant was sieved on deck at the sieving table with filtered seawater over stacked 1,000 µm, 500 µm and 300 µm sieves. Organisms visible to the eye were removed from the sieve. The remaining samples per sieving fraction were fixed either in 4 % formosaline solution or in denatured 96% ethanol depending on the size of the sample.

The decanted fraction of the sieves was caught via a small plankton sieve to focus on copepod crustaceans in collaboration with the BIOPOL project. These were sorted independently from the live picked samples and frozen for biochemical analyses. For the macrofauna live picked

specimens, if > 3 specimens were found of the same morphotype, one was fixed in 96 % non-denatured ethanol, one was frozen at -80°C and one preserved in RNA later, to enable additional transcriptome and genome studies as well as lipid analyses (BIOPOL: responsible person Katrin Linse). Furthermore, selected individuals were frozen at -20°C for microplastic analyses (Alexandra Aves for Melanie Bergmann) after a specific treatment of sample picking avoiding plastic contamination and using plastic-free funnels and glass tubes or tins. If less than three specimens per morphospecies were found, the first specimen was fixed in ethanol, the second in RNAlater or frozen. All these specimens were catalogued for the DZMB sample database and documented photographically. Specific samples were given out to cooperating scientists and participants directly on *Polarstern* (Copepods also to Barbara Niehoff, parasites to Sonja Rückert, Ophiurids to Lydia Schmidt, etc.).

The remaining samples from the net and subsample were fixed in pre-cooled denaturated 96 % ethanol and kept at -20°C for 48 h. During the first 12 h, samples were gently moved every three hours to avoid freezing of the samples. After 24 h the ethanol concentration was measured and the sorting process could be started when 90 % was exceeded. Samples with ethanol concentration lower than 85 % were re-fixed to keep ethanol at high concentrations. The samples were sorted to higher taxon level (phylum, class, order) and selected groups (isopods, bivalves and ophiurids) to family, genus and in some cases to species level. Sorted specimens were transferred to 96% non-denaturated ethanol, and kept cool during the entire process.

Megafauna and seafloor mapping

During the PS136 expedition the Autonomous Underwater Vehicle (AUV) “PAUL” (Fig. 3.5) was deployed three times to carry out seafloor imaging and mapping: at HAUSGARTEN stations S3 and HG-IV as well as across unusual ‘pockmark’ features near HAUSGARTEN site SV-IV (Tab. 3.4). In addition, there were nine successful deployments of the Ocean Floor Observation and Bathymetry System (OFOBS; Fig. 3.6) made during the expedition (Tab. 3.5). The considerable ice cover encountered during the cruise precluded further AUV deployments at other stations, though the system operated well. Problems with the underwater communication system POSIDONIA system and its integration into the OFOBS platform following a software update of the IXBLUE hardware prevented the collection of high-resolution bathymetric data during all deployments, except the final deployment at HAUSGARTEN station HG-IX, prior to which a workaround solution had been devised. During five OFOBS dives, the miniROV “Remora” was attached to OFOBS and test deployments of the new height maintenance system tested.

Fig. 3.5: Deployment of the Autonomous Underwater Vehicle “PAUL”

Fig. 3.6: Deployment of the Ocean Floor Observation and Bathymetry System (OFOBS)

Tab. 3.4: HAUSGARTEN stations with AUV deployments conducted during PS136; the distance travelled, number of images and sonar files collected is also given.

Site	Station ID	Date	Lat. °N	Lon. °E	Depth [m]	Dist. km	Image no.	Sonar files
S3	PS136_4-10	29/05/2023	78.661	5.0772	2326	01.6	971	14
HG-IV	PS136_8-6	01/06/2023	79.0746	4.1491	2460	39.8	8	455
Pocks	PS136_22-2	07/06/2023	79.0426	6.6951	1230	32.7	18678	171

Tab. 3.5: OFOBS deployments made at HAUSGARTEN stations during PS136 with station ID, dates and times at seafloor, geographic start and end coordinates and water depths.

Station ID	Date	Time (UTC)	Latitude	Longitude	Depth [m]	Notes
PS136_4-14	30/05/2023	00:04	78° 37.037‘ N	005° 08.619‘ E	2338	Start
	30/05/2023	03:00	78° 37.042‘ N	005° 00.162‘ E	2350	End
PS136_6-4	31/05/2023	12:12	79° 02.091‘ N	004° 10.260‘ E	2607	Start
	31/05/2023	16:33	79° 03.334‘ N	004° 15.247‘ E	2462	End
PS136_11-12	02/06/2023	23:39	79° 07.948‘ N	006° 06.976‘ E	1267	Start
	03/06/2023	03:21	79° 07.950‘ N	006° 17.681‘ E	1335	End
PS136_13-6	04/06/2023	00:04	78° 59.994‘ N	008° 09.671‘ E	976	Start
	04/06/2023	02:26	79° 00.027‘ N	008° 14.017‘ E	910	End
PS136_15-1	04/06/2023	12:28	78° 58.788‘ N	009° 25.774‘ E	233	Start
	04/06/2023	15:10	78° 58.666‘ N	009° 31.810‘ E	233	End
PS136_22-1	07/06/2023	02:41	79° 02.559‘ N	006° 41.403‘ E	1229	Start
	07/06/2023	06:19	79° 01.544‘ N	006° 46.705‘ E	1225	End
PS134_34-1	14/06/2023	06:25	78° 50.241‘ N	003° 02.214‘ W	2427	Start
	14/06/2023	08:20	78° 49.216‘ N	003° 05.156‘ W	2422	End
PS136_36-1	15/06/2023	13:15	79° 34.220‘ N	005° 14.418‘ E	2590	Start
	15/06/2023	15:22	79° 34.984‘ N	005° 12.683‘ E	2619	End
PS136_39-1	16/06/2023	04:55	79° 06.518‘ N	003° 23.249‘ E	4929	Start
	16/06/2023	08:16	79° 06.221‘ N	003° 25.344‘ E	4900	End

The ‘pockmark’ features running south-east of the HAUSGARTEN sites HG-II and HG-III were successfully mapped and imaged across a number of km with both the AUV and the OFOBS systems. The data collected during PS136 complements that collected during *Maria S. Merian* cruise MSM108 and it is intended to write a descriptive paper on the topography and fauna of this ecosystem. Further, the data will be discussed with geologist colleagues in Bremen and Norway to better understand the underlying structure of this interesting region of seafloor. Numerous fish species, worms and bacterial mats seem to be locally unique to the close vicinity of these pockmark features and active fluid flow is indicated by the staining of seafloor sediments observed in numerous collected images.

A number of stations imaged previously by OFOS and OFOBS were revisited, with comparable image data collected for later analysis and comparison for fauna and litter abundance across stations and temporally. This comparison work will commence on return to shore. A long and successful dive at the Molloy Deep (HG-IX) was conducted, but not across the traditional OFOBS transect as ice prevented deployment and transit in that region. Because of this a

0.4 kt drift deployment was made. The drift track directed the OFOBS device from the Molloy Deep seafloor on a route which started the sloped ascent of the eastern slope flank of the feature. A particularly unusual observation was made here of a sizable lump of compressed sediments, estimated to be 3 to 4 m in height and covering an area of approximately 15 m of seafloor was made. Within, beneath and surrounding this feature were several pieces of wood, which looked both degraded and shaped. Numerous images, video and acoustic records of this feature were collected and are being discussed at present with marine archaeologists in case they represent the remains of a vessel which may have suck to the east, then slipped down the Molloy Deep slope following the dislodging of higher compacted sediments. During a approx. four-hour seafloor deployment, no further comparable structures were observed, either on the Molloy Deep floor or slope.

Experimental work at the deep seafloor

Ocean acidification has been identified as a risk to marine ecosystems, and substantial scientific effort has been expended on investigating its effects, mostly in laboratory manipulation experiments. Experimental manipulations of CO_2 concentrations in the field are difficult, and the number of field studies are limited to a few locations. The LTER observatory HAUSGARTEN was extended with an experimental system (Fig. 3.7) to study impacts of ocean acidification on benthic organisms and communities for the first time in deep Arctic waters with an autonomous system. The arcFOCE (Arctic Free Ocean Carbon Enrichment) system was developed to create semi-enclosed test areas on the seafloor where the seawater's pH (an indicator of acidity) can be precisely controlled for weeks or months at a time. The implementation of an arcFOCE for long-term experiments will enable us to generate data on the resistance of Arctic marine benthic organisms and communities to a reduction in ocean pH. A short test deployment was performed close to HAUSGARTEN site HG-II. Following the successful test, the system was deployed again for a year at 1,500 m water depth, with a several months operation time-period at the end of the one-year deployment.

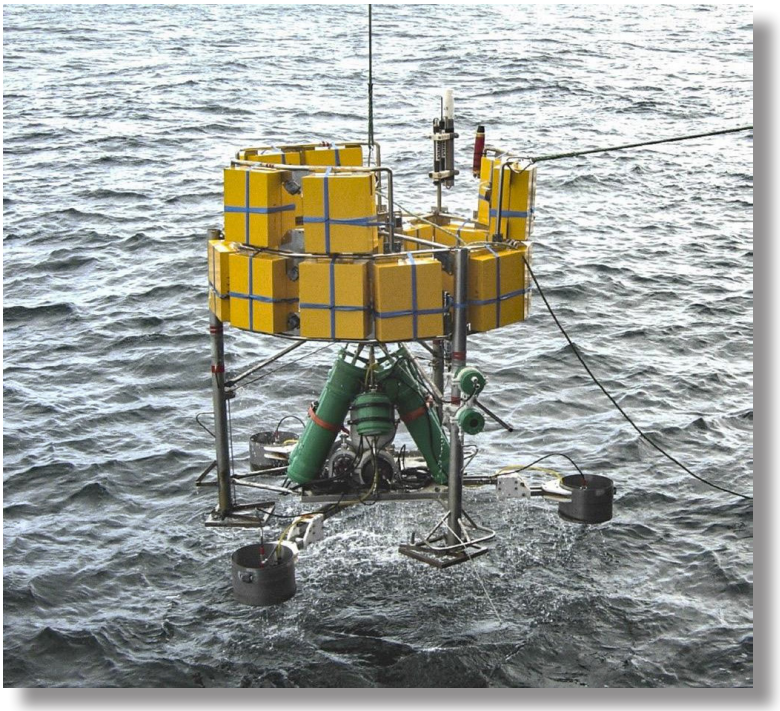

Fig. 3.7: Recovery of the arcFOCE experimental set-up after a test deployment at 1,500 m water depth during Polarstern expedition PS136

Preliminary (expected) results

Larval biology

We collected over 4,000 specimens of larvae at HAUSGARTEN observatory. All species will be identified to the lowest taxonomic level possible using both morphological and genetic approaches. We found over 100 distinct morphotypes, showing the huge diversity of organisms with meroplanktonic larvae using the Fram Strait.

Most larvae we found were in hand net hauls, even though the volume filtered with a hand net was approximately one third that filtered with the bottom lander based deep-sea pumps, showing that there is far more biomass and diversity of meroplankton at the sea surface than near the seafloor. This pattern was reflected in the multi-net hauls. The most individuals were found in the surface nets and counts and diversity decreased with depth (Fig. 3.8).

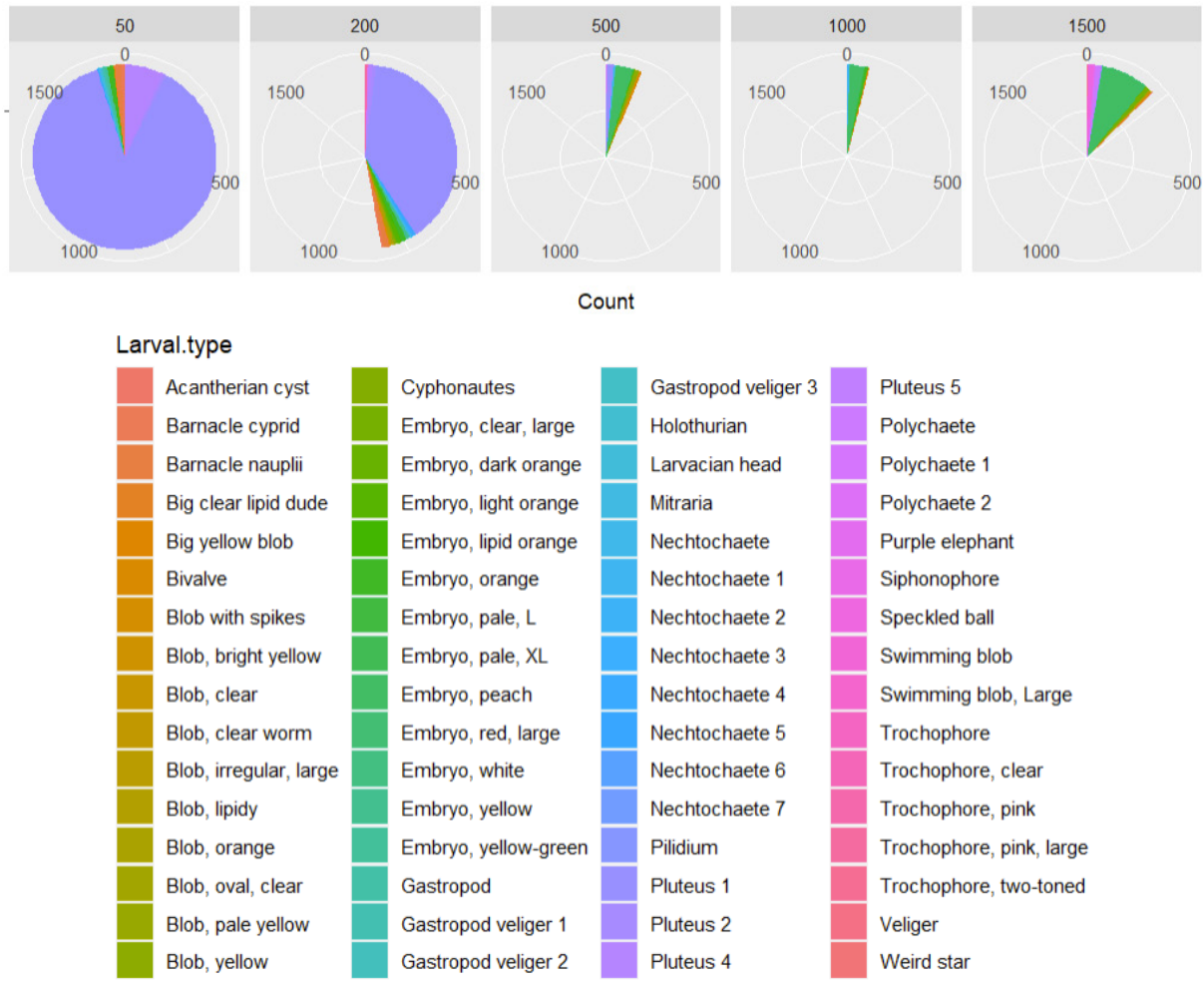

Fig. 3.8: Pie charts representing the distribution of morphotypes with depth from multi-net deployments at S3, HG-IV, N3, and N4. Each colour represents a morphotype

- Dominant taxa:

Each station had a unique assemblage of organisms but with similarities in dominant taxa at some stations. We found Pluteus 1 at 16 of our 18 surface stations in quantities ranging from

1 to 882 individuals in a single net (Fig. 3.9). They ranged in developmental stage from a few days old (Fig. 3.10 A) to metamorphosing into a juvenile (Fig. 3.10 B). Further analysis will evaluate patterns in size distribution throughout the Fram to inform possible origins.

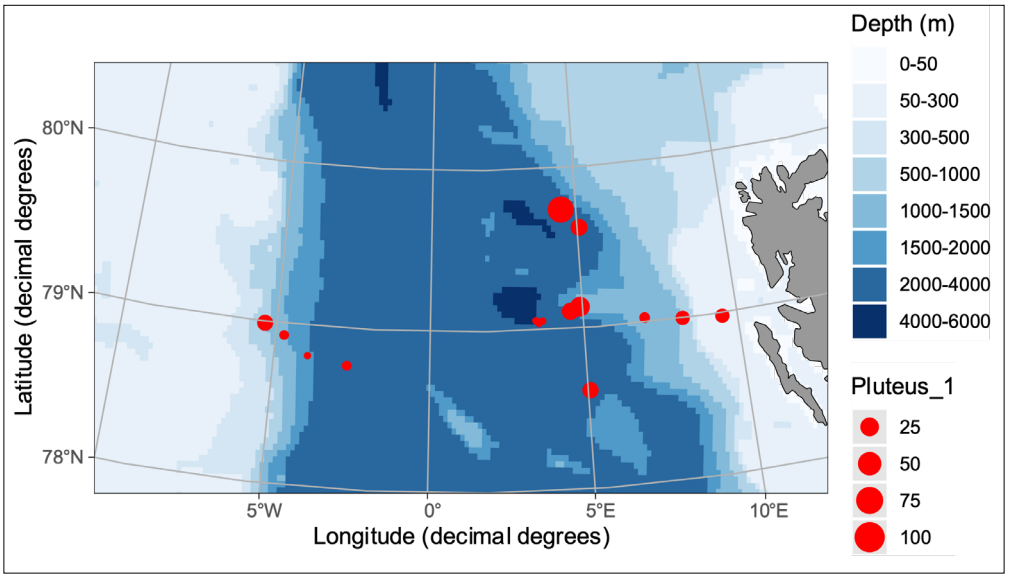

Fig. 3.9: Map of the abundance and distribution of our most common larvae, Pluteus_1, which we suspect to be the larval form of the brittle star Ophiocten gracilis

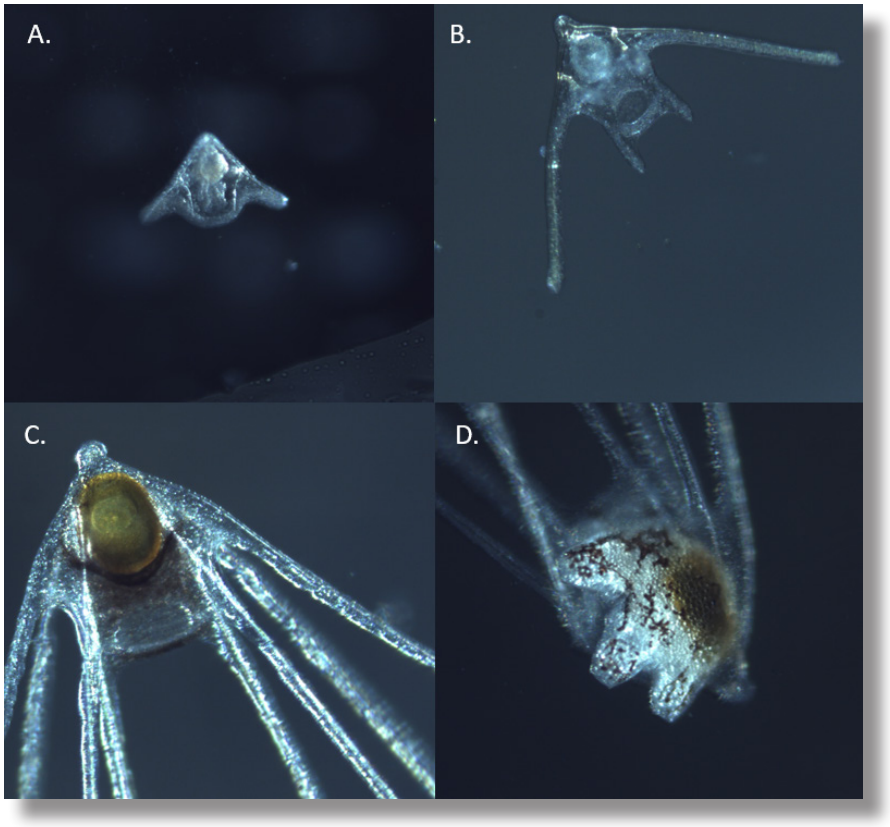

Fig. 3.10: Pluteus larvae found at different developmental stages from (A) a few days old to (D) metamorphosing into a juvenile. We suspect it to be the larval form of the brittle star Ophiocten gracilis.

Some morphotype groups contained a few distinct morphotypes, but in general, our four most common groups (by number of stations) were pluteus, nauplii, trochophores, and bivalves (Tab. 3.6, Fig. 3.11). Fewer than 20 individual morphotypes were found at five stations or more, demonstrating the importance of sampling widely to capture the diversity of the region.

Tab. 3.6: Most common morphotype groups.

Morphotype group	Stations present	Count range when present	Sum
Pluteus (Fig. 3.11 A)	17	1-882	2573
Trochophore (Fig. 3.11 B)	13	1-134	236
Nauplii (Fig. 3.11 C)	10	1-141	294
Bivalves (Fig. 3.11 D)	9	1-189	383

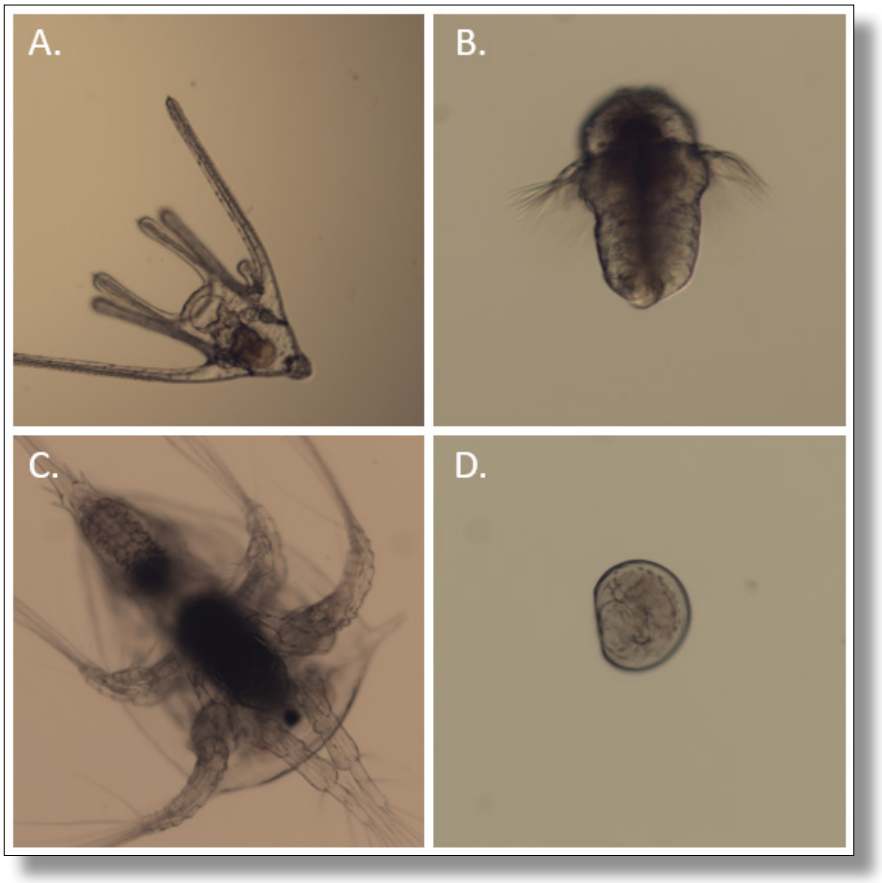

Fig. 3.11: The four most common morphotype groups found at HAUSGARTEN observatory (by frequency of occurrence); A. Pluteus, B. Trochophore, C. nauplii, D. bivalve veliger

- Non-dominant taxa:

Most morphotypes were found at fewer than five stations. Some examples are shown in Figure 3.12. Many of these were in low quantities with 35 morphotypes being recorded only once. These were mostly embryos, blob, and trochophores which were difficult to distinguish so some may end up being the same as other named morphotypes. For more unique morphotypes, we found only five each of mitraria (Fig. 3.12 D), zoea (Fig. 3.12 G), and cyphonautes (Fig. 3.12 J), and six pilidium (Fig. 3.12 E). Overall, we hope to more completely

analyse the species makeup and distribution of the area and compare it to adult populations in the region to assess connectivity and dispersal.

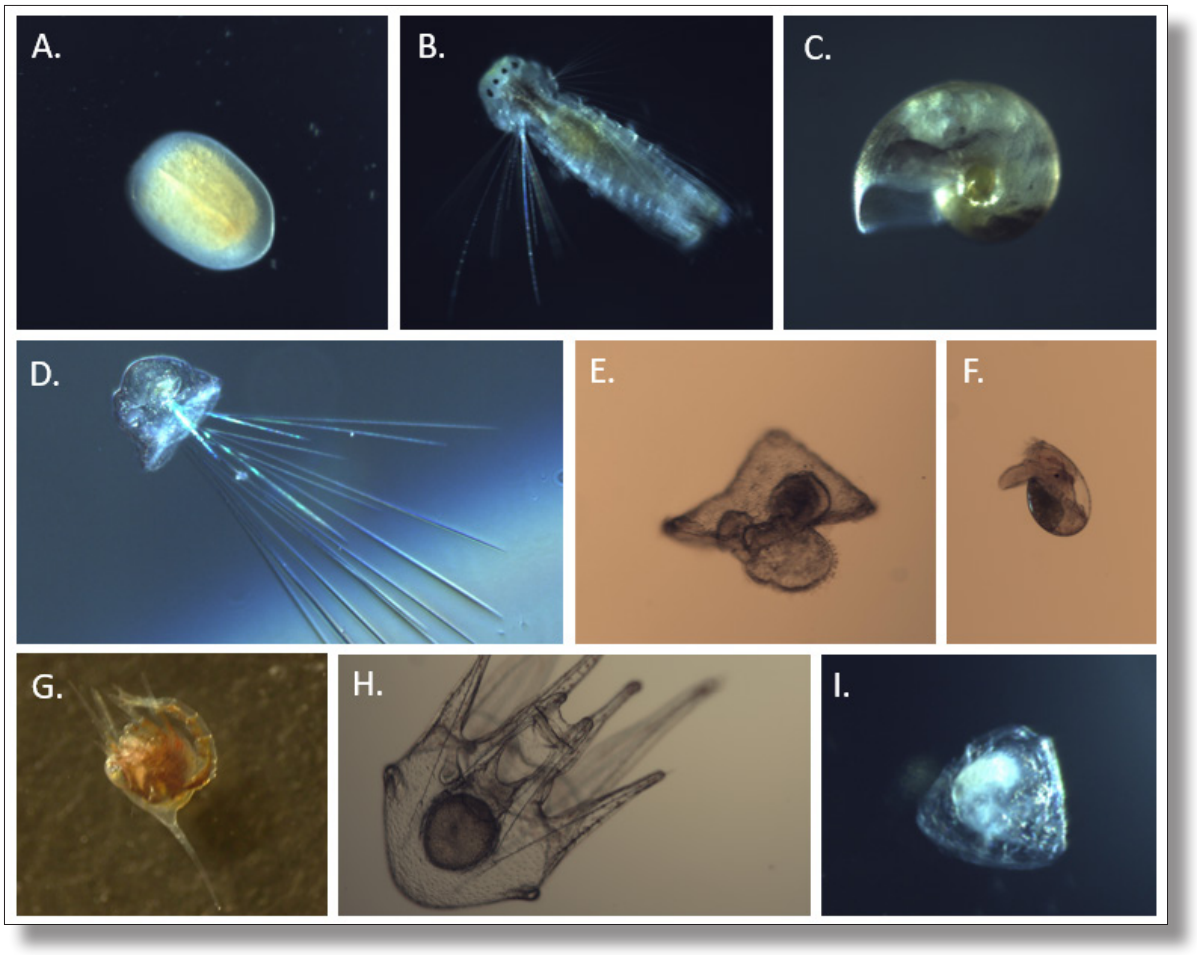

Fig. 3.12: Assortment of larvae collected from multi-net and hand-net deployments at HAUSGARTEN; A. Unknown swimming blob, B. Polychaete nechtochaete, C. Gastropod veliger, D. Polychaete mitraria, E. Nemertine pilidium, F. Gastropod veliger, G. Crab zooea, H. Urchin pluteus, and I. Bryozoan cyphonautes

Biogenic sediment compounds

Except for one station at a shallow-water site on the Svalbard shelf (SV-III), we were able to successfully sample all HAUSGARTEN stations. Comparing the concentrations of sediment-bound pigments and potential bacterial activities along the bathymetric transect across the Fram Strait and along the latitudinal transect with stations at different distances from the ice edge in the northern parts of the strait, we found noticeable differences (Fig. 3.13). Irrespective of the depth of the station, all sites on the East Greenland continental margin generally had lower pigment concentrations than the stations off Svalbard. Neglecting station HG-II, pigment concentrations and bacterial activities showed a general trend of decreasing values with increasing water depth along the HAUSGARTEN depth transect. However, the deepest station along the HAUSGARTEN depth transect (HG-IX) showed conspicuously elevated values.

Station HG-IX is located at Molloy Hole, a deep depression with a maximum water depth of 5,600 m. Such an increase at great depth is a feature that has been observed in other

deep trenches. The Molloy Hole appears to act as a depositional centre for organic matter, suggesting that it acts as a huge natural trap for organic matter at abyssal depths in the Fram Strait. On the East Greenland continental shelf, the highest values for pigment concentrations and bacterial activity were observed at the deepest station EG-IV, which may be explained by its location close to the ice edge in the western parts of the Fram Strait. Generally increased primary production in the Marginal Ice Zone (MIZ) and subsequent increased sedimentation of phytodetritus, a potential food source for benthic organisms, could explain the increased pigment and activity values found at EG-IV. Values along the latitudinal transect showed no clear trend.

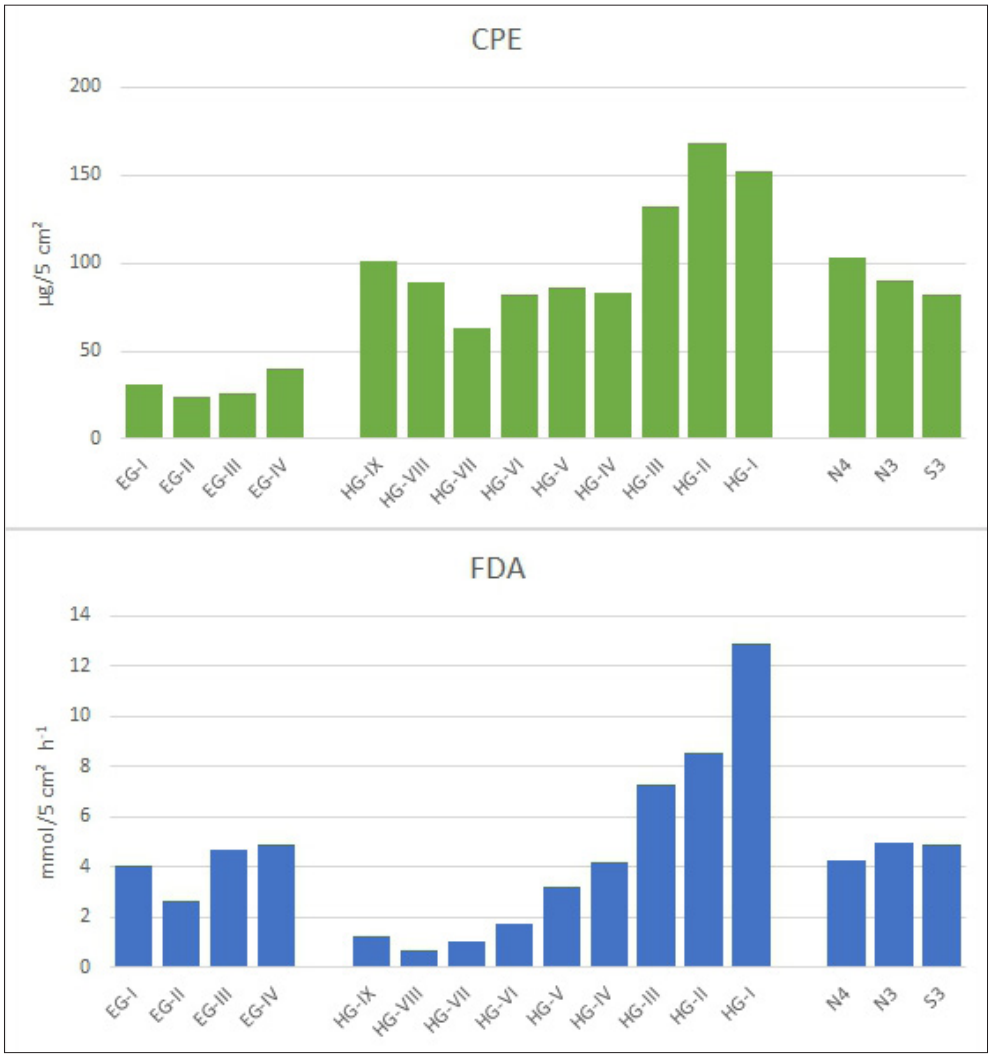

Fig. 3.13: Preliminary results from on-board pigment measurements (top: Concentrations of chloroplastic pigment equivalents, CPE) and bacterial activity assessments (bottom: degradation of the artificial substrate fluorescein-di-acetate, FDA)

Macrobenthos

Six epibenthic sledge samples were taken at selected stations (HG-I, HG-IV, HG-IX, N3, S3, and EG-IV (Tab. 3.2). Figure 3.14 shows temperatures and conductivity data from the CTD attached to the EBS and Figure 3.15 displays a collection of macrofauna organisms sampled with the EBS.

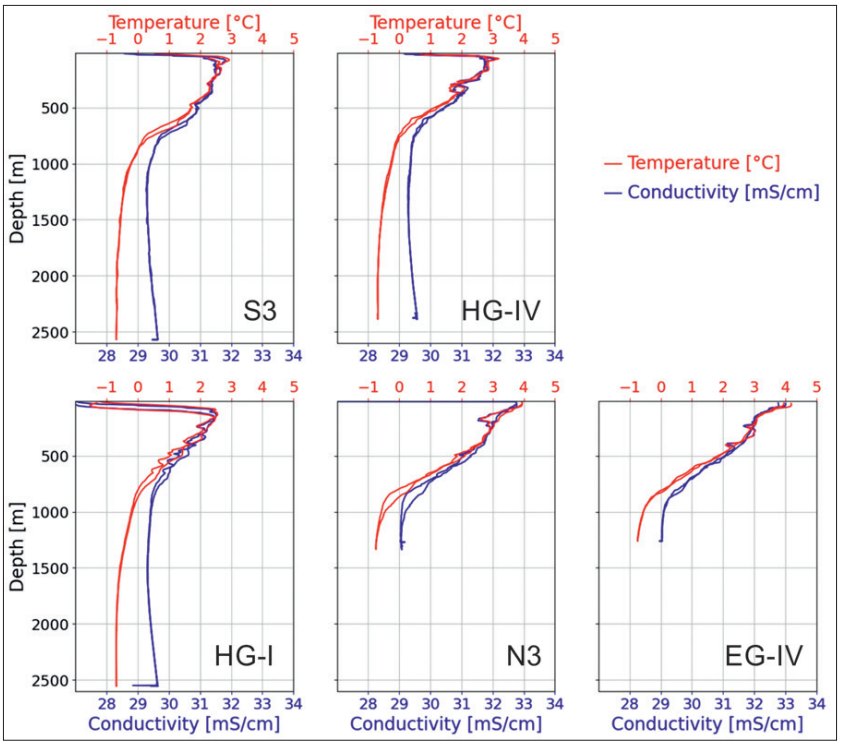

Fig. 3.14: CTD data registered during EBS deployments at five HAUSGARTEN station (no data for HG-IX, because the pressure housing was not depth-rated to 6,000 m water depth)

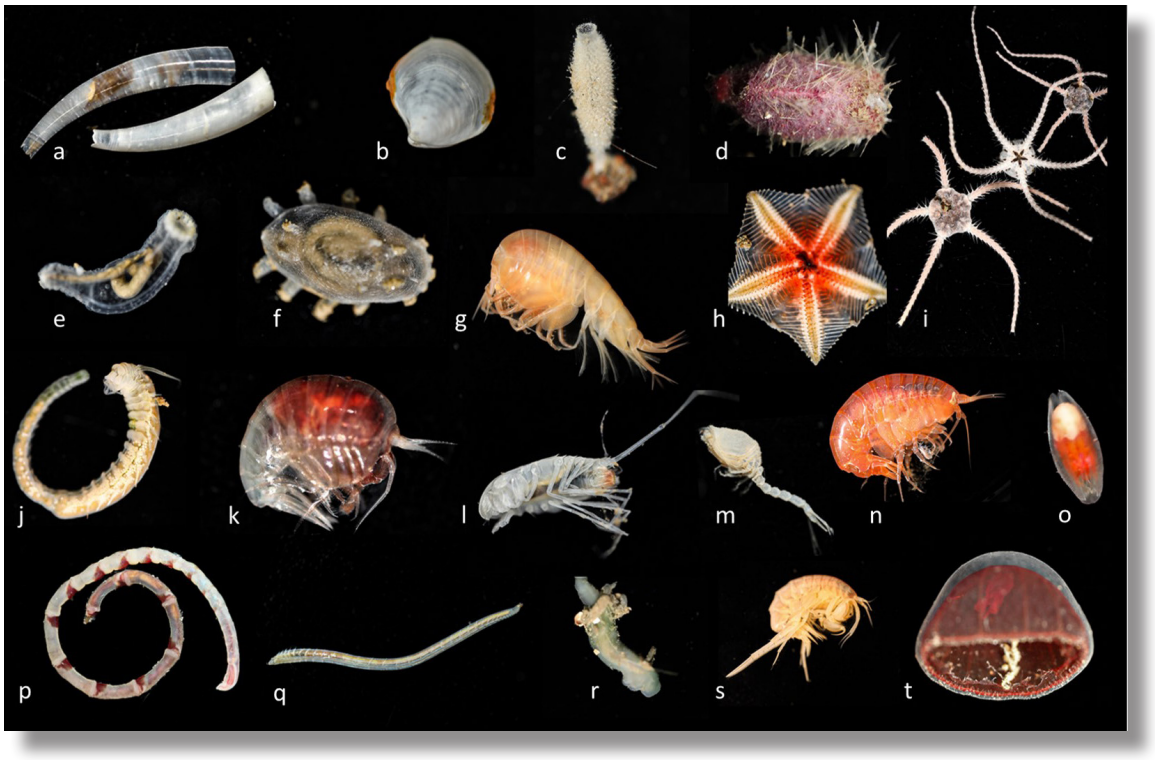

Fig. 3.15: Selected live photographed specimens. a. Scaphopoda, b. Bivalvia, c. Porifera, d. Echinodermata, e. Holothuria, f. Holothuria (Elpidia), g. Amphipoda, h. Echinodermata, i. Ophiuroidea, j. Polychaeta, k. Amphipoda, l, Isopoda (Munnopsidae), m. Cumacea, n. Amphipoda, o. Ostracoda, p. Polychaeta (Maldanidae), q. Polichaeta (Owniidae), r. Proapulida, s. Apmphipoda, t. Cnidaria (Medusa)

Data management

The sorting on species level and final species identification of the ethanol and formalin fixed macrofauna from box corer and EBS deployments will happen in the home laboratories at AWI and the DZMB Hamburg, Germany. Sample processing of the meiofauna and biogenic sediment compounds will be carried out at AWI. Identifications of larvae will take place at the WHOI, USA.

Many of the samples will be processed and further analysed at AWI, DZMB, and WHOI within approximately one year after the crise. We plan that the full data set will be available at latest about 2-3 years after the cruise. Faunal and environmental data as well as all acoustic and image data collected by the AUV and the towed camera systems during *Polarstern* expedition PS136 will be archived, published and disseminated according to international standards by the World Data Center PANGAEA Data Publisher for Earth & Environmental Science (https://www.pangaea.de). The CC-BY license will be applied after publication.

All benthic data will further be deposited in the data repository CRITTERBASE at AWI, while seafloor still images will also be uploaded to the online image database BIIGLE to enable easy access by other parties.

Molecular data (DNA and RNA data) will be archived, published and disseminated within one of the repositories of the International Nucleotide Sequence Data Collaboration (INSDC, www.insdc.org) comprising of EMBL-EBI/ENA, GenBank and DDBJ.

Any other data will be submitted to an appropriate long-term archive that provides unique and stable identifiers for the datasets and allows open online access to the data.

The expedition will be supported by the Helmholtz Research Programme “Changing Earth – Sustaining our Future” Topic 6, Subtopics 6.1, 6.3 and 6.4.

In all publications, based on this cruise, the Grant No. **AWI_PS136_01** will be quoted and the following publication will be cited:

Alfred-Wegener-Institut Helmholtz-Zentrum für Polar- und Meeresforschung (2017). Polar Research and Supply Vessel POLARSTERN Operated by the Alfred-Wegener-Institute. Journal of large-scale research facilities, 3, A119. http://dx.doi.org/10.17815/jlsrf-3-163.

References

Brandt A, Barthel D (1995) an improved supra- and epibenthic sledge for catching Peracarida (Crustacea, Malacostraca). Ophelia, 43 (1), 15-23.

Brenke N (2005) An epibenthic sledge for operations on marine soft bottom and bedrock. Marine Technology Society Journal 39, (2), 11-21.

Buhl-Mortensen L, Buhl-Mortensen P, Dolan MFJ, Dannheim J, Bellec V, Holte B (2012) Habitat complexity and bottom fauna composition at different scales on the continental shelf and slope of northern Norway. Hydrobiologia, 685 (1), 191-219.

Buhl-Mortensen L, Vanreusel A, Gooday AJ, Levin LA, Priede IG, Buhl-Mortensen P, Gheerardyn H, King NJ, Raes M (2010) Biological structures as a source of habitat heterogeneity and biodiversity on the deep ocean margins. Marine Ecology - an Evolutionary Perspective, 31 (1), 21-50.

Gage JD, Tyler PA (1991) Deep-sea biology: a natural history of organisms at the deep-sea floor. London: Cambridge University Press.

Kaiser S, Brenke N (2019) Chapter 9: Epibenthic sledges. In: Clarke MR, Consalevey M, Rowden AA (eds) Biological sampling in the Deep Sea. https://doi.org/10.1002/9781118332535.ch9

Piepenburg D (2005) Recent research on Arctic benthos: common notions need to be revised. Polar Biology, 28 (10), 733-755

Purser A, Marcon Y, Dreutter S, Hoge U, Sablotny B, Hehemann L, Lemburg J, Dorschel B, Biebow H, Boetius A (2018) OFOBS – Ocean Floor Observation and Bathymetry System: A new towed camera / sonar system for deep sea exploration and survey. IEEE Journal of Oceanic Engineering, https://doi.org/10.1109/JOE.2018.2794095

Purser A, Hoge U, Busack M, Hagemann J, Lehmenhecker S, Dauer E, Korfman N, Boehringer L, Merten V, Priest T, Dreutter S, Warnke F, Hehemann L (2021) Arctic Seafloor Integrity, Cruise No. MSM95 – (GPF 19-2_05), 09.09.2020 – 07.10.2020, Emden (Germany) – Emden (Germany). https://doi.org/10.48433/cr_msm95

Schulz M, Bergmann M, von Juterzenka K, Soltwedel T (2010) Colonisation of hard substrata along a channel system in the deep Greenland Sea. Polar Biology, 33, 1359-1369.

Soltwedel T, Bauerfeind E, Bergmann M, Bracher A, Budaeva N, Busch K, Cherkasheva A, Fahl K, Grzelak K, Hasemann C, Jacob M, Kraft A, Lalande C, Metfies K, Nöthig E-M, Meyer K, Quéric N-V, Schewe I, Wlodarska-Kowalczuk M, Klages M (2016) Natural variability or anthropogenically-induced variation? Insights from 15 years of multidisciplinary observations at the arctic marine LTER site HAUSGARTEN. Ecological Indicators, 65, 89-102.

Taylor J, Krumpen T, Soltwedel T, Gutt J, Bergmann M (2016) Regional- and local-scale variations in benthic megafaunal composition at the Arctic deep-sea observatory HAUSGARTEN. Deep-Sea Research Part I: Oceanographic Research Papers, 108, 58-72.

Tews J, Brose U, Grimm V, Tielbörger K, Wichmann MC, Schwager M, Jeltsch F (2004) Animal species diversity driven by habitat heterogeneity/diversity: the importance of keystone structures. Journal of Biogeography, 31 (1), 79-92.

Whittaker RJ, Willis KJ, Field R (2001) Scale and species richness: towards a general, hierarchical theory of species diversity. Journal of Biogeography, 28 (4), 453-470.

4. PEBCAO – PLANKTON ECOLOGY AND BIOGEOCHEMISTRY IN THE CHANGING ARCTIC OCEAN

Katja Metfies[1], Natasha Bryan[1], Sophia Hirschmann[2], Tania Klüver[2], Nadine Knüppel[1], Alexandra Kraberg[1], Barbara Niehoff[1], Benjamin Pontiller[2], Antonia Thielecke[1], Kim Vane[1], Yara Zimmer[1];
not on board: Christina Bienhold[1], Astrid Bracher[1], Anja Engel[2], Maria Fernandez-Mendez[1], Morten Iversen[1], Christian Konrad[1], Eva-Maria Nöthig[1], Matthias Wietz[1]

[1]DE.AWI
[2]DE.GEOMAR

Grant-No. AWI_PS136_02

Outline

The Arctic Ocean has gained increasing attention in recent decades due to the ongoing significant changes in sea ice cover and increase in temperature, which is approximately twice as fast as the global average. It is also expected that the chemical equilibrium and the elemental cycling in the surface ocean changes due to ocean acidification. The PEBCAO group began its studies of plankton ecology in the Fram Strait (~ 79°N) in 1991 and intensified its efforts in 2009. Since then, classical mass measurements of biogeochemical parameters, microscopy, optical methods, satellite observations, and molecular genetic approaches have been combined in a holistic approach to collect comprehensive information on the variability of biodiversity, community structure, biomass and distribution of microbial plankton, primary production, bacterial activity, and zooplankton composition annually. As part of the PEBCAO contribution to the FRAM-observatory, this included the deployment of long-term sediment traps and automated water samples on long-term moorings.

The long-term observations and process studies of the past years have already given us first important insights into mechanistic linkages between environmental conditions, biodiversity and ecosystem functionality, but also ongoing change in the marine ecosystem of the Fram Strait. For instance, our results clearly indicate that chlorophyll *a* (Chl *a*) values increase in summer in the eastern but not in the western Fram Strait (Nöthig et al. 2015, 2020). This is in accordance with the increasing contributions of *Phaeocystis pouchetii* and nanoflagellates to the summer phytoplankton community in relation to diatoms. These changes might be related to decreasing availability of silicic acid in the water column. The amount of silicic acid entering the Eurasian Basin of the Arctic comes mainly from the North Atlantic Water (NAW) inflow (100 - 400 m depth) through the Fram Strait and the Barents Sea Opening and riverine input from the Laptev Sea. Recent analyses have shown that all these waters from mid-latitudes to subpolar regions in the North Atlantic are affected by decreasing trends in silicic acid concentrations up to 1–2 µm in 25 years (Hátún et al. 2017). This decrease is primarily attributed to reduced winter convection depths since the mid-1990s and an increased influence of nutrient-poor water of mid-latitudes origin (Hátún et al. 2017). Although nitrate limits the total annual NPP, spring diatom productivity, which is a major part of the total productivity, is strongly

controlled by silicic acid supply (Krause et al. 2019). The Fram Strait is an ideal location to study this ongoing decline in silicic acid concentrations and investigate potential effects on diatom silicification and phytoplankton community composition. Changes in phytoplankton composition are corroborated by variations in the biogeochemical flux composition (Lalande et al. 2016, 2019), as well as in large zooplankton species (caught as so-called “swimmers” in sediment trap samples), which have shown an increase of warm adapted organisms in recent years (Kraft et al. 2013; Bauerfeind et al. 2014; Busch et al. 2015; Ramondenc et al. 2022).

We were able to show that *Phaeocystis sp.* controls production of transparent exopolymer particles (TEP) in the Fram Strait (Engel et al. 2017). However, despite the observed shift in phytoplankton community composition the concentration of dissolved organic carbon (DOC) was relatively stable over the last two decades, but we observed a slight decrease in the particulate organic carbon (POC) during the summer months (Engel et al. 2019). Moreover, the data of our long-term sediment-trap program suggest that over the period 2009 - 2016 the abundance of *Micromonas polaris* and *Micromonas commoda*-like cells is positively correlated with lower standing stocks of phosphate and nitrate in the upper water-column at LTER observatory HAUSGARTEN, and that they are exported to the deep sea, despite of their small size (Bachy et al. 2022). All this suggests that already now the ecosystem in the Fram Strait is subject to profound changes, likely induced by changing climate conditions, which warrants further, sustained observation. Here it is of particular importance to quickly improve our understanding of the effects of variable sea-ice coverage and the Marginal Ice Zone (MIZ), respectively sea-ice melt on the ecosystems. These effects are predicted to prevail in larger areas of the AO in the future and the Fram Strait is an ideal site to study these effects. Its ecosystems are already strongly and regularly intensively affected by sea-ice related processes happening the MIZ.

The impact of these effects is expected to change in the future, also in the Fram Strait in consequence to further Arctic environmental change. Biogeographical studies of PEBCAO indicate that a year-round semi-stationary sea-ice edge serves as a strong biogeographical boundary between Atlantic conditions to the southeast and polar conditions to the Northwest of the Fram Strait (Metfies et al. 2016). In 2017, the MIZ extended further eastwards and southwards into the Fram Strait than in average years, with profound impacts on the ecosystems. Sea ice melt in a sub-mesoscale filament, characterized by a thin surface meltwater layer, led to comprehensive changes in plankton-biodiversity, carbon export and primary production in vicinity of the filament (Fadeev et al. 2021). Here, a combination of the latest biological and physical underway-measurements has proven very useful to map the physical environment and eukaryotic microbial community composition in a sub-mesoscale filament with high spatial resolution (Weiss et al., submitted).

PEBCAO contributed to year-round interdisciplinary observations indicating that increased meltwater-stratification during spring/summer of 2017 slowed down the biological carbon pump in AW the central Fram Strait with significant impacts for on pelagic and benthic communities in comparison to the warmer year 2018 (von Appen et al. 2021). Furthermore, based on our year-round automated water-sampling we characterized the annual succession of microbial communities at a station in West Spitsbergen Current (WSC) and East Greenland Current (EGC). The ice-free West Spitsbergen Current displayed a marked separation into a productive summer (dominated by diatoms and carbohydrate-degrading bacteria) and regenerative winter state (dominated by heterotrophic Syndiniales, radiolarians, chemoautotrophic bacteria, and archaea). In the East Greenland Current, deeper sampling depth, ice cover and polar water masses concurred with weaker seasonality and a stronger heterotrophic signature. Low ice cover and advection of Atlantic Water coincided with diminished abundances of chemoautotrophic bacteria while others such as *Phaeocystis* increased, suggesting that “Atlantification” alters microbiome structure and eventually the biological carbon pump (Wietz

et al. 2021). Seasonal succession of prokaryotic microbes in the Fram Strait is related to a succession in the biopolymer pool, which indicates seasonally distinct metabolic regimes (von Jackowski et al. 2022), and is further reflected in clear differences in the particle dynamics between summer and autumn in the Fram Strait (von Jackowski et al. 2020).

On PS136, PEBCAO continued these annual time-series observations of biological and biogeochemical parameters, complemented by experimental studies of trophic interactions within the planktonic food web.

Objectives

The effects of changes on the polar plankton ecology and biogeochemical processes (PEBCAO) can only be detected through a combination of dedicated interdisciplinary process studies and long-term observations, as implemented by PEBCAO within the framework of LTER HAUSGARTEN and the FRAM observatory for more than a decade. Overall, the overarching objectives of PEBCAO are to improve the mechanistic understanding of biogeochemical and microbiological feedback processes in the changing Arctic Ocean, to document ongoing and long-term changes in the biotic and abiotic environment and to assess the potential future consequences of these changes. In particular we aim to identify climate-induced changes in the biodiversity of pelagic ecosystems and, concomitantly, in carbon cycling and sequestering and improve our mechanistic understanding of linkages between key environmental parameters and ecosystem functionality in the Arctic Ocean. The overall objectives were addressed using a range of methodologies:

Primary production is expected to increase in the changing Arctic Ocean, however, it is currently unclear if this will lead to increased export of particulate organic carbon or if organic carbon will remain at the surface, fuelling heterotrophic bacteria. Heterotrophic bacteria play a vital role in global biogeochemical cycles. To better understand bacterial activity, we will determine bacterial abundance, biodiversity and bacterial production. By linking compound dynamics with rate measurements and community structure, we will gain further insights into the flow of carbon through the Arctic food web. To address the effects of global change on microbial biogeochemistry in the Arctic Ocean, we will also continue to monitor concentrations of organic carbon, nitrogen, and phosphorus, as well as specific compounds like amino acids, carbohydrates, and gel particles. To assess cell abundances, we will sample for microscopic counts and flow cytometry that allows us determining phytoplankton (< 50 µm), bacteria, and viral abundances. Phytoplankton primary production will be determined by radioisotopes (14C-incorporation) and distinguished into particulate primary production (carbon remaining in the cells) and dissolved primary production (organic carbon subsequently released by cells). In addition, primary production will be assessed in situ using fast repetition rate fluorometry (FRRF) with the FastOcean ADP profiling system.

Silicic acid availability constrains the expected increase in primary productivity in consequence to elevated light availability as the sea-ice retreats. Diatoms, compared to other microalgae groups, will likely lower their cell-specific carbon, nitrate and silicic acid uptake rates under silicic limitation or shift towards smaller and less-silicified species, and non-silicifying microalgae will consequently contribute the most to primary productivity. To assess this, we will measure carbon and nutrient uptake rates for bulk and single cell phytoplankton under different silicic acid concentrations using stable isotope incubations. In addition, we will conduct incubations with a stain for silicate frustules (PDMPO) to assess the silicification degree of diatoms under different silicic acid concentrations.

We expect that the small algae at the base of the food web gain importance in mediating element and matter turnover as well as energy fluxes in Arctic pelagic systems. In order to detect changes, also in this smallest fraction of the plankton, traditional microscopy will be

complemented by molecular methods that are independent of cell-size and morphological features, and we will determine their contribution to phtototrophic biomass. Changes in Eukaryotic microbial communities are tightly linked to prokaryotic community composition. The assessment of the biodiversity and biogeography of Arctic Eukaryotic microbes, including phytoplankton and their linkages to Prokaryotic microbial communities, will be based on analyses of eDNA via 16S and 18S meta-barcoding. A suite of automated sampling devices will be used in addition to classical sampling at selected sites via Niskin bottles attached to a CTD/ Rosette Water Sampler to collect samples for eDNA analyses. This includes the automated filtration device AUTOFIM deployed on *Polarstern* for underway filtration, automated Remote Access water Samplers (RAS) and long-term sediment traps deployed on the FRAM moorings for year-round sampling.

Many zooplankton species are affected by the community composition at the base of the food web as they rely on it as food sources. However, which specific food sources are supporting the zooplankton biomass is relatively unclear due to the difficulties of tracing the carbon from those food sources to the tissues of organisms. Recent research has indicated that carbon isotopes of essential amino acids have potential to trace the proportional contribution of specific microalgae groups to zooplankton biomass (Vane et al. 2023) and during this expedition samples will be taken to refine and apply this approach. Similarly, the zooplankton community composition may shift due to the increasing inflow of warmer Atlantic water into the Fram Strait. Altered zooplankton trophic interactions and community compositions will have consequences for the carbon sequestration and flux. Most of our knowledge on zooplankton species composition and distribution has been derived from traditional multiple net samplers, which integrate depth intervals of up to several hundred meters. Nowadays, optical systems, such as the zooplankton recorder LOKI (Light frame On-sight Key species Investigations), continuously take pictures of the organisms during vertical casts from 1,000 m to the surface. Linked to each picture, hydrographical parameters are being recorded, i.e. salinity, temperature, oxygen concentration, and fluorescence. This will allow us to exactly identify distribution patterns of key taxa in relation to environmental conditions. We will also use the UVP5 (Underwater Vision Profiler which is mounted on the ship´s CTD/Rosette Water Sampler to also tackle zooplankton distribution patterns albeit with much less taxonomic resolution than with LOKI.

Moreover, we will also include research dedicated to protistan parasites. These are severely understudied in the marine realm although they are likely to affect the population dynamics of phytoplankton (including bloom timing and magnitude) and zooplankton. We will therefore conduct a baseline study of the diversity of different parasite groups and their association with potential hosts. This investigation will also form the basis for future biogeographic studies. The analyses will combine different microscopy techniques (LM, SEM, CFLM) as well as molecular data, the latter facilitating observation of parasitism even at times where easily discernible parasite life-cycle stages are absent.

In summary during PS136 the following detailed objectives were addressed:

- Monitoring plankton species composition and biomass distribution
- Determining autotrophic and heterotrophic microbial activities
- Monitoring biogeochemical parameters
- Investigating selected phyto- and zooplankton (including their parasites)
- Determining the composition of organic matter and gel particles
- Characterizing biogeographical patterns of marine microbes along a transect from the German Bight to the Fram Strait

- Assessing photosynthetic biomass and microbial community composition in sea-ice
- Exchanging sediment traps and Remote Access Samplers for year-round assessments of vertical flux and microbial community composition
- Collecting water-samples for chronobiological transcriptome-studies

Work at sea

Measurements and sample collections for a large variety of parameters were accomplished at 18 stations of the 'deep-sea long-term observatory HAUSGARTEN' during PS136, including the frontal zone separating the warm and cold-water masses originating from the West Spitsbergen Current and the East Greenland Current. Measurements and sampling comprised CTD casts, underway sampling with the automated filtration device AUTOFIM, net hauls and the deployment of RAMSES, LOKI and is summarised in tables.

Biogeochemistry

A diverse set of discrete seawater samples was collected during the cruise consisting of chemical and biological parameters which are associated with organic matter composition and microbial activity, to determine the processes affecting the turnover of organic matter in the arctic ocean. In total, 18 stations were sampled, utilizing a CTD/Rosette Water Sampler (Fig. 4.1).

Fig. 4.1: Deployment of the CTD with Rosette Water Sampler

The euphotic zone was sampled during a "shallow" cast (surface, Chl *a* max., below Chl *a* max., 50 m, and 100 m) at every station (Tab. 4.1). Additionally, samples were taken from a "deep" cast (200, 500, 750, 1,000 and 1,200 m) at selected stations to investigate the connectivity of surface and deep waters via the export of organic matter. Samples were taken for dissolved biogeochemical parameters, such as dissolved organic carbon (DOC/TDN) via filtration of

seawater through 0.45 µm GMF syringe filters into combusted glass vials, acidification with hydrochloric acid (Suprapur), and storage at 4°C until HPLC analysis. Dissolved amino acids (DAA) and combined carbohydrates (DCHO) were filtered over 0.45 µm Acrodisc filters into combusted glass vials and stored at -20°C. Samples for total alkalinity (TA) measurements were filtered through 0.45 µm Acrodisc filters and stored at 4°C. Dissolved inorganic carbon (DIC) samples were treated with mercury(II)chloride and also stored at 4°C. In addition, we collected seawater samples to determine the concentration (abundance and area) and the carbon content of transparent exopolymer particles (TEP) and Coomassie stainable particles (CSP) using 0.4 µm polycarbonate filters and the dyes Alcian Blue and Coomassie Brilliant Blue for staining, respectively. These filters were stored subsequently at -20°C until further microscopic and colorimetric analyses in the laboratory. Nutrient (NUT) samples were filtered through 0.4 µm cellulose acetate filters and stored at -20°C. Samples for lipid analysis were filtered over a 0.2 µm hydrophilic Durapore filter, flash-frozen in liquid nitrogen, and stored at -80°C. All samples will be shipped and analysed in the laboratories at GEOMAR in Kiel, Germany.

Furthermore, multiple methods were applied to determine the phytoplankton and bacterial abundances and growth rates. For bacterial (BA) and picophytoplankton (PA) abundance samples were fixed with GDA 25% and frozen at -80°C. Further analysis by flow cytometry will take place at GEOMAR. Phytoplankton primary production (PP) and bacterial biomass production (BBP) rates were determined on board using a radioactive tracer approach with ^{14}C-sodium bicarbonate and ^{3}H-leucine, respectively. Additionally, a FastOcean APD Profiling System (Chelsea Technologies, UK) was deployed to assess the *in situ* phytoplankton primary production. However, due to persistent technical software issues, the device was deployed only at one station (N4). To study the functional gene expression profiles of arctic bacterioplankton communities (RNAmetaT), additional samples were taken at all stations from surface, DCM, 50 and 100 m depth. These samples were preserved with RNALater, immediately flash-frozen, and stored at -80°C until further processing in the home laboratory.

Tab. 4.1: Biogeochemical parameters sampled from the CTD/Rosette Water Sampler. Abbreviations as follows: DOC - dissolved organic carbon; DCHO - dissolved carbohydrates; DAA - dissolved amino acids; DIC - dissolved inorganic carbon; TA - total alkalinity; NUT - inorganic nutrients; TEP - transparent exopolymer particles; CSP - Coomassie stainable particle; RNAmetaT - bacterial RNA for metatranscriptomic analysis; LIP - lipids; BA/PA - bacterial and picophytoplankton abundance; BBP - bacterial biomass production; PP - phytoplankton primary production.

Station	ID	DOC/ DCHO/ DAA	DIC/ TA	NUT	TEP/ CSP	RNA metaT	LIP	BA/ PA	BBP	PP
PS136_4-2	S3 deep	X		X	X			X		
PS136_4-9	S3 shallow	X	X	X	X	X	X	X	X	X
PS136_5-1	HG-IV shallow	X	X	X	X	X	X	X	X	X
PS136_7-1	HG-III shallow	X	X	X	X	X	X	X	X	X
PS136_8-1	HG-IV deep	X		X	X			X		

Station	ID	DOC/ DCHO/ DAA	DIC/ TA	NUT	TEP/ CSP	RNA metaT	LIP	BA/ PA	BBP	PP
PS136_10-1	HG-II shallow	X	X	X	X	X	X	X	X	X
PS136_11-1	HG-I deep	X		X	X			X		
PS136_11-12	HG-I shallow	X		X	X	X	X	X	X	
PS136_12-3	SV-IV shallow	X	X	X	X	X	X	X	X	X
PS136_14-1	SV-I shallow	X	X	X	X	X	X	X	X	X
PS136_17-1	N3 shallow	X	X	X	X	X	X	X	X	X
PS136_18-1	N4 shallow	X	X	X	X	X	X	X	X	X
PS136_18-11	N4 deep	X		X	X			X		
PS136_23-1	HG-V shallow	X	X	X	X	X	X	X	X	X
PS136_25-1	HG-VII shallow	X	X	X	X	X	X	X	X	X
PS136_27-1	HG-IX shallow	X	X	X	X	X		X	X	X
PS136_27-9	HG-IX deep	X		X	X			X		
PS136_28-1	HG-VIII shallow	X		X	X	X		X	X	
PS136_30-1	EG-IV shallow	X	X	X	X	X	X	X	X	X
PS136_31-1	EG-III shallow	X		X	X	X		X	X	
PS136_32-1	EG-II shallow	X		X	X	X		X	X	
PS136_33-1	EG-I shallow	X	X	X	X	X		X	X	X
PS136_33-9	EG-I deep	X		X	X			X		
PS136_35-1	HG-VI shallow	X		X	X	X		X	X	

Microbial Ecology

- Water-sampling:

Seawater samples were taken at 5 - 12 depths by a CTD/Rosette Water Sampler and aliquots were filtered for analysing biogeochemical parameters such as chlorophyll *a* (unfractionated, and fractionated on 3 µm and 0.4 µm), particulate organic carbon and nitrogen (POC and PN), and biogenic silica (PbSi), respectively (Fig. 4.2). At mooring stations, filtrations for seston

(TPM, total particulate matter) were carried out. Furthermore, unfiltered water samples were fixed with formalin (final concentration 0.5 - 1.0 %) for later quantitative assessment of the phytoplankton community by inverted microscopy. At each station oblique phytoplankton net hauls were carried out to a depth of ca 20 m study the species richness and distribution of live phytoplankton. In the onboard laboratory the net samples were analysed semi-quantitatively to provide species lists for each station. In addition, epifluorescence microscopy was used to screen the samples for zoospores of marine parasites.

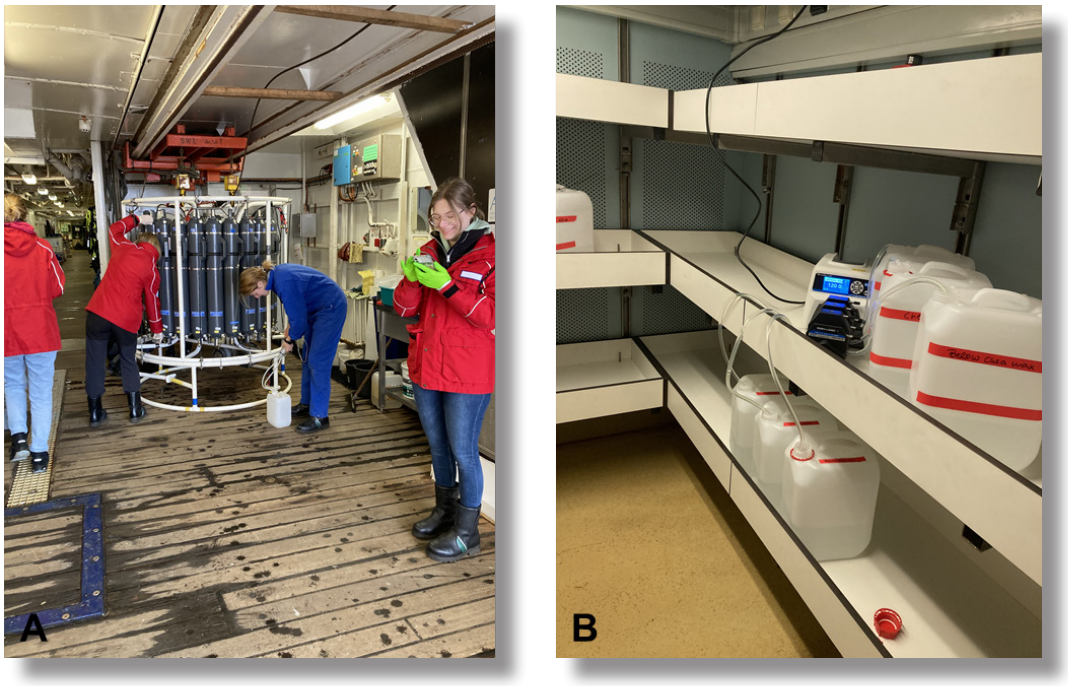

Fig. 4.2: Processing of CTD-samples (Left) Subsampling from the Niskin-bottles deployed on the CTD/Rosette Water Sampler (Right) Set-up filtration for eDNA via peristaltic pumps on Sterivex-filter with a pore-size of 0.22 µm

In the HAUSGARTEN area and on along latitudinal gradient from Bremerhaven to the Fram Strait we collected samples to characterize geographical differences in microbial community composition via eDNA analyses based on 16S/18S meta-barcoding (Tab. 4.2). In order to address horizontal and vertical differences we combined sampling using the CTD/Rosette Water Sampler and sampling via the underway sampling system AUTOFIM, permanently installed on board *Polarstern*. We used AUTOFIM to collect samples on a transect from Bremerhaven to the Fram Strait with a resolution of ~ 3 h (~ 33 nm) on a 0.4 µm filter and additional samples were collected from five depths via the CTD/Rosette Water Sampler from the top 100 m depth in the HAUSGARTEN area (Tab. 4.3). Samples obtained by sampling with the CTD/Rosette Water Sampler for 18S meta-barcoding analyses were fractionated by three filtrations on 10.0 µm, 3.0 µm, and 0.4 µm filters, while samples for prokaryotic community analyses were filtered directly on 0.22 µm filters. One additional archive sample was collected from every depth by filtration on 0.22 µm to provide a sample for future analyses methods. Samples for chronobiological transcriptome studies are listed in (Tab. 4.4).

Tab. 4.2: Overview of stations sampled for eDNA analyses and other parameters during PS136. DNA Euk and Prok: DNA of eukaryotes and prokaryotes; POC/N/bSI: particulate organic carbon, nitrogen and biogenic silica; total particulate organic matter (TPM); seston.

Station	DNA Euk and Prok	Archive Filter	POC/N, PbSi shallow	POC/N, PbSi, TPM deep	Seston	Hand net 20 µm	Utermöhl counting
HG-I	X	X	X			X	X
HG-II	X	X	X			X	X
HG-III	X	X	X			X	X
HG-IV	X	X	X	X	X	X	X
HG-V	X	X	X			X	X
HG-VI	X	X	X			X	X
HG-VII	X	X	X			X	
HG-VIII	X	X	X			X	X
HG-IX	X	X	X			X	X
N-4	X	X	X	X	X	X	X
N-3	X	X	X			X	X
EG-I	X	X	X			X	X
EG-III	X	X	X			X	
EG-IV	X	X	X	X	X	X	X
SV-IV	X	X	X			X	X
SV-I	X	X	X			X	X
S-3	X	X	X	X	X	X	X

Tab. 4.3: Overview underway sampling via AUTOFIM. Sampling for eDNA Analyses of geographical patterns along a transect from the German Bight to the Fram Strait.

Date	Time	Date	Time
22/05/2023	21:30	25/05/2023	08:20
23/05/2023	00:30	25/05/2023	10:00
23/05/2023	03:30	25/05/2023	19:30
23/05/2023	06:30	26/05/2023	09:30
23/05/2023	09:30	26/05/2023	15:00
23/05/2023	11:30	26/05/2023	18:30
23/05/2023	21:00	26/05/2023	21:30
24/05/2023	01:00	27/05/2023	08:35
24/05/2023	09:45	27/05/2023	12:30
24/05/2023	11:00	27/05/2023	15:30
24/05/2023	12:30	27/05/2023	18:30
24/05/2023	16:45	28/05/2023	09:00
24/05/2023	17:30	28/05/2023	12:25

Tab. 4.4: Sampling for chronobiological transcriptome studies.

Date	Time
30/05/2023	13:00
30/05/2023	16:00
30/05/2023	19:00
30/05/2023	22:00
31/05/2023	01:00
31/05/2023	03:00
31/05/2023	06:00
31/05/2023	09:00

Sea-ice sampling:

At five different stations in vicinity of the EGC, sea ice cores were collected for eDNA based characterization of microbial sea ice communities and quantification of Chl *a* biomass (Fig. 4.3; Tab. 4.5). Ice samples were melted at 4°C in defined volumes of filtered sea-water aboard *Polarstern* and particles were collected fractionally on filters with pore sizes of 10 µm, 3 µm, and 0.4 µm in analogy to water samples. All samples were preserved, refrigerated or frozen at -20°C or -80°C for storage until analyses in the home laboratory (AWI, Bremerhaven).

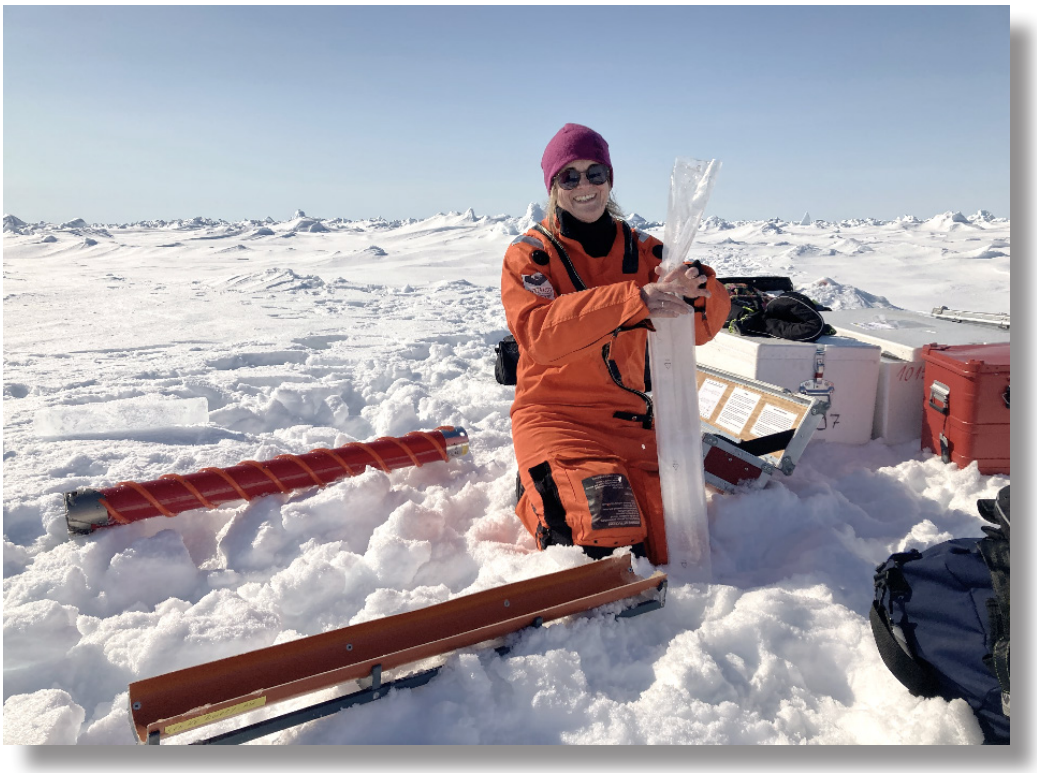

Fig. 4.3: Collecting sea ice-cores for eDNA analyses of eukaryotic microbial community composition and determinations of Chl a biomass

Tab. 4.5: Overview sea ice stations. Stations sampled for eDNA analyses and quantification of photosynthetic biomass in sea-ice.

Cruise	Station	Date	Latitude	Longitude
PS136	Floe 1	06/06/2023	79,794935°N	4,484816°E
PS136	Floe 2	08/06/2023	79,103223°N	3,494404°E
PS136	Floe 3	13/06/2023	78,947687°N	5,633781°W
PS136	Floe 4	14/06/2023	78,79826°N	1,822286°W

Exchange of moored autonomous sampling devices for biological and biogeochemical parameters

The PEBCAO-team accomplished the preparation and post-deployment processing of sediment traps, long-term bottom lander and automated water samplers (PPS and RAS) deployed on moorings at the stations HG-IV, SV-IV, and N4 (Tab. 4.6).

The Remote Access Sampler (RAS, McLane; Fig. 4.4) deployed during PS131 at station SV-IV in July 2022 to collect samples year-round for eDNA analyses and quantification of nutrient concentrations was recovered and redeployed as part of the mooring exchange, while the RAS at station EG-I could not be recovered due to heavy ice-conditions, though a new RAS was deployed. Sampling at SV-IV from July 2022 to June 2023 was very successful, as all RAS-bags contained water samples for the anticipated time-periods. The bags were filled with 500 ml seawater that were collected twice a month over the entire collection period with an interval of fourteen days. Samples are preserved with mercury chloride to avoid degradation of samples via biological processes and changes in microbial community composition. On board *Polarstern* the sample-tubes were detached from the device and stored in a box at 4°C until further processing in the laboratory in Bremerhaven. In general, we observed intense biofouling of the device after one year of deployment.

Tab. 4.6: Overview exchange of long-term installations.

Station	Latitude	Longitude	Device ID	Depth [m]	Deployment period
Recoveries of moored sediment traps					
HG-IV	78° 59.880‘ N	004° 18.819‘ E	FEVI-44 upper	197	21/07/2022 – 15/06/2023
HG-IV	78° 59.880‘ N	004° 18.819‘ E	FEVI-44 lower	2341	21/07/2022 – 15/06/2023
SV-IV	79° 00.472‘ N	006° 57.861‘ E	F4S-6 upper	202	21/07/2022 – 15/06/2023
SV-IV	79° 00.472‘ N	006° 57.861‘ E	F4S-6 lower	604	21/07/2022 – 15/06/2023
Deployments of sediment traps					
HG-IV	79° 00.015‘ N	004° 19.907‘ E	FEVI-46 upper	204	15/06/2023 – 31/05/2024
HG-IV	79° 00.015‘ N	004° 19.907‘ E	FEVI-46 lower	2348	15/06/2023 – 31/05/2024
EG-I	78° 58.721‘ N	005° 25.645‘ W	EGC-9	501	15/06/2023 – 31/05/2024

Station	Latitude	Longitude	Device ID	Depth [m]	Deployment period
SV-IV	79° 00.700‘ N	006° 57.720‘ E	F4S-7 (2023) upper	194	15/06/2023 – 31/05/2024
SV-IV	79° 00.700‘ N	006° 57.720‘ E	F4S-7 (2023) lower	604	15/06/2023 – 31/05/2024
Recovery Long-term Lander					
HG-IV	79° 01.464‘ N	004° 12.563‘ E		2590	19/06/2022 – 18/06/2023
Deployment Long-term Lander					
Long-term Lander	79° 01.848‘ N	004° 13.336‘ E		2516	17/06/2023 – 15/06/2024
Recovery BioOptical Platform (BOP)					
SV-IV	79° 00.732‘ N	007° 01.951‘ E	F4W-4	427	21/07/2022 – 15/06/2023
Deployment BioOptical Platform (BOP)					
SV-IV	79° 00.700‘ N	006° 57.720‘ E	F4S-7 (2023)	496	15/06/2023 – 31/05/2024

Phytoplankton community incubation experiments

At 9 stations the phytoplankton community was sampled with CTD Niskins at the chlorophyll *a* maximum (between 85 and 10 m). Two different incubations were performed at each of these stations using a silicic acid gradient (0, 2, 5, 10, 20 µm): 24 h incubations were performed to investigate carbon, nitrate and silicic acid uptake rates and 48 h incubations were performed to investigate silica incorporation. Initial samples were taken for HPLC, POC/PON, BSi, POP and DIC analysis. In separate bottles nutrients (nitrate, nitrite, phosphate, silicic acid) were added to create a silica gradient and avoid nutrient limitation during the incubations. To measure nutrient uptake rates, stable isotopes (13C, 15N, 30Si) were added to each 2 L bottle. Subsequently the bottles were incubated for 24 h at 4°C and under stable light conditions. After the incubation the water was filtered for subsequent POC/PON and BSi analysis allowing to assess changes in productivity and uptake rates. To investigate silica incorporation the phytoplankton community was first concentrated using reverse filtration and then incubated for 48 h in cell culture bottles with the silica stain PDMPO under the same silicic acid gradient. Afterwards the samples were fixed with formalin to subsequently assess differences in silica incorporation with an Amnis Imaging Flow Cytometer. To investigate the consequences of changing upwelling intensities on the phytoplankton communities, further incubations were conducted at two stations during transit to HAUSGARTEN using Arctic inflow waters (Tab. 4.7). Water was sampled with the CTD/Rosette Water Sampler from 1,000 m depth and from the Chl *a* max. The phytoplankton community was concentrated using reverse filtration and the remaining water was sterile-filtered and mixed to simulate different upwelling intensities (i.e. 0, 25, 50, 75, 100% deep water). Subsequent incubations to investigate productivity, nutrient uptake rates and silica incorporation were performed as described above.

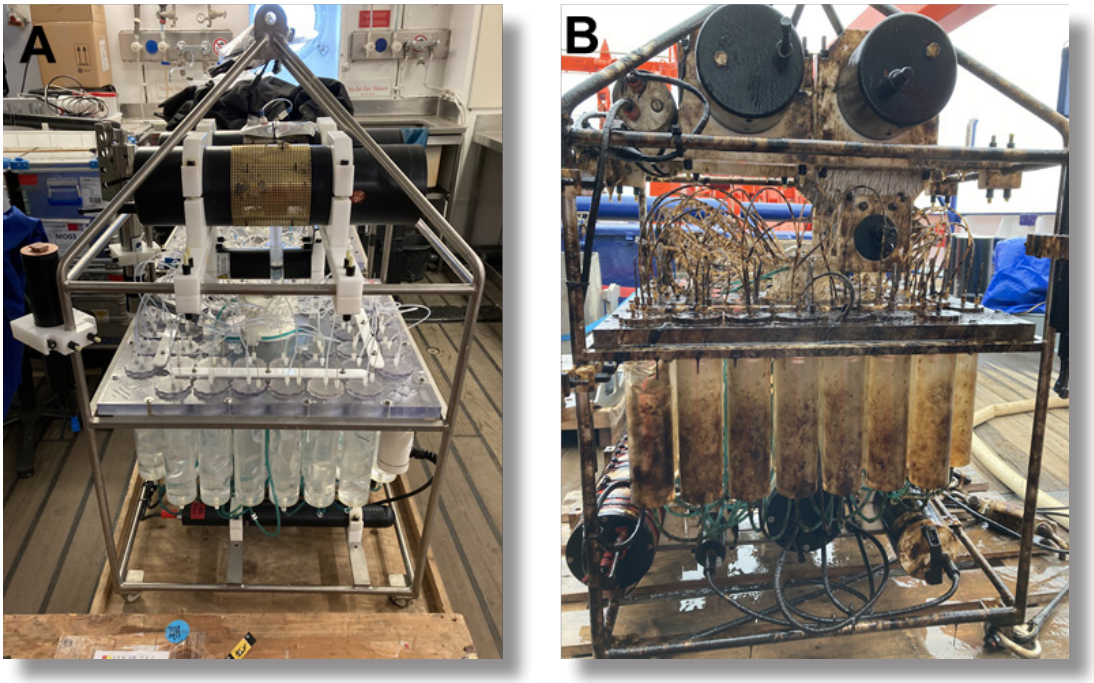

Fig. 4.4: Remote Access Samplers (RAS; McLane, USA); (A) RAS-sampler ready for deployment on a long-term mooring including a sensor set; (B) RAS-sampler recovered after one year of deployment at SV-IV in Atlantic Waters of the Fram Strait

In addition to the 24-hour incubations, at two stations (HG-I and HG-IV) the phytoplankton community was collected and incubated for 72 h in 2 L bottles, with the same added nutrients and silicate gradient as described above. After the incubation, four *Calanus finmarchicus* females were added to each bottle, attached to a plankton wheel in the dark and allowed feeding for 8 h. Afterwards, the copepods were removed and euthanised in 96% ethanol for later DNA analysis of their stomach contents. DNA samples, formalin preserved samples, and POC/PON filters of the phytoplankton community collected with the CTD/Rosette Water Sampler, after 72 h and 80 h (after copepod feeding) were taken to indicate the change in phytoplankton community and productivity after adding silicate and removal by the copepod feeding. The grazing experiment aimed to investigate the changes in phytoplankton community under different silicate concentrations as well as the dietary selection from the phytoplankton by the copepods.

Additionally, phytoplankton filtrates from the chlorophyll *a* maximum were collected at eight stations on GF/F filters. These were stored at -20°C and -80°C for compound specific carbon isotope analysis of amino acids and fatty acids, respectively.

Tab. 4.7: Overview phytoplankton community experiments. Phytoplankton community and biomarker filtrate sampling from the CTD/Rosette Water Sampler at the chlorophyll maximum.

Station name	Nutrient uptake	Silicification	Biomarker	Grazing
70°N	x (Upwelling exp.)	x (Upwelling exp.)	x	
75°N	x (Upwelling exp.)	x (Upwelling exp.)	x	

Station name	Nutrient uptake	Silicification	Biomarker	Grazing
HG-I	x	x	x	x
HG-III	x	x	x	
HG-IV			x	
HG-V	x	x	x	x
HG-IX	x	x	x	
N-3	x	x	x	
SV-I	x	x	x	
EG-I	x	x	x	
EG-IV	x	x	x	

Trophic transfer of biomolecules with biomarkers

Sourcing of biomolecules synthesised by specific phytoplankton clades to the biomass of Arctic copepod species (*Calanus finmarchicus*, *C. glacialis* and *C. hyperboreus*) was investigated by collecting the copepods from distinct areas in the Fram Strait. Four multi-nets fitted with five nets of 150 µm mesh size were deployed vertically at stations S3, HG-IV, N3 and N4 to five depth layers 0-50, 50-200, 200-500, 500-1,000, and 1,000-1,500 m. In addition, copepods were sampled in the 0-50 meter with six Bongo nets at HG-VII, HG-IX, SV-I, SV-II, EG-I, and EG-IV. Sampled copepods were primarily preserved at -20°C for compound specific carbon isotope analysis of amino acids. At locations, where respective copepod species were abundant in the catch, additional individuals were preserved at -20°C for bulk isotope analysis and -80°C for fatty acid analysis. For confirmation of species identification, some individuals of *C. finmarchicus* and *C. glacialis* were preserved in 96% ethanol.

In combination with specific phytoplankton species cultivated in the laboratory and the biomarker filtrates, the proportional contribution of amino acids synthesized specific phytoplankton clades to the copepod biomass will be inferred. This proportional inference will be done according to the principles and approach outlined by Vane et al. (2023).

Seaweed sinking to understand its fate in the deep sea

To understand the potential of seaweed for carbon dioxide removal and long-term storage for climate mitigation we wanted to investigate the fate of sunken seaweed and land biomass in the deep sea (4,000 m water depth). To do this, three packages of dead/frozen seaweed (*Sargassum fluitans* and *S. natans, Ulva lactuca, Saccharina latissima*) and one with land biomass (1) were deployed north of HAUSGARTEN site HG-VII (Fig. 4.5). The biomass was wrapped in a net and attached to concrete holders. The package with land biomass was equipped with a beacon to enable their location after one year. In 2024, a Remotely Operated Vehicle (ROV) will be sent down to retrieve subsamples of the packages and make a gradient analysis of the meiofauna and the oxygen consumption in the sediment around and below the packages to assess the environmental impact and fate of sunken biomass in the deep sea.

Fig. 4.5: Deployment of the seaweed bales

Zooplankton

The mesozooplankton community composition and depth distribution were investigated at six HAUSGARTEN stations and two stations in the East Greenland Current (Tab. 4.8). To analyse the large-scale zooplankton distribution in the upper 1500 m of the water column, we used a Multi-net midi (Hydrobios, Kiel Germany) equipped with five nets of 150 µm mesh size (Fig. 4.6A). The net was towed vertically at HAUSGARTEN sites S3, HG-I, HG-IV, HG-IX, N4, EG-I, and EG-IV to sample five depths layers (i.e. 1,500, 1,000, 500, 200, 50, 0 m). At HG-I and EG-I, the bottom depth was shallower than 1,500 m, and here the depth intervals were adjusted, yielding a higher resolution of the upper water column. Due to technical difficulties, the cast at station HG-I at first did not yield any samples, but was repeated later during the cruise. All samples were immediately preserved in 4% formalin buffered with hexamethylenetetramine. In the laboratories at AWI, these samples will be digitized, and the organisms on the images will be determined to the lowest taxonomical level possible via the internet application EcoTaxa. From these data, together with the data from the flowmeter attached to the net opening, we will determine zooplankton species composition and abundance. EcoTaxa also automatically provides the sizes of the organisms, and they will be used to calculate biomasses according to Cornils et al. (2022).

Tab. 4.8: Overview Multi-net and LOKI casts during PS136 to study zooplankton abundance, depth distribution and community composition. LOKI was always deployed to 1,000 m depth, for the Multi-net, the maximum depth is given.

Station	Date	time	MN cast	MN depth max	LOKI
PS136_04	29/05/23	06:45	x	1500	x
PS136_05	30/05/23	14:20	x	1500	x
PS136_11	02/06/23	18:20	x	no samples	x
PS136_16	04/06/23	23:52	x	1200	-
PS136_18	06/06/23	00:25	x	1500	x

Station	Date	time	MN cast	MN depth max	LOKI
PS136_27	09/06/23	16:55	x	1500	x
PS136_28	10/06/23	14:18	x	1500	x
PS136_29	11/06/23	14:35	x	1500	x
PS136_33	13/06/23	14:34	x	980	x

One RAS was deployed close to the surface (~ 25 m) in mooring F4-S7. Two RAS were deployed in mooring EGC-9; one at ~ 50 m and another at ~ 200 m. RAS close to the surface were equipped with biogeochemical sensors (SUNA-nitrate, PAR, pH, CDOM, backscatter, Chl *a*, and pCO_2) and a CTD-O_2 and the deeper RAS was equipped with a CTD-O_2. A SUNA nitrate sensor was deployed alongside 32 CTD cast to obtain high-resolution nitrate profiles down to max. 1,500 m (Tab. 5.2). The Suna data is processed following Sakamoto et al. (2009), using the CTD's temperature and salinity data. Further quality control will be conducted by comparison to the CTD's Niskin bottle nitrate data.

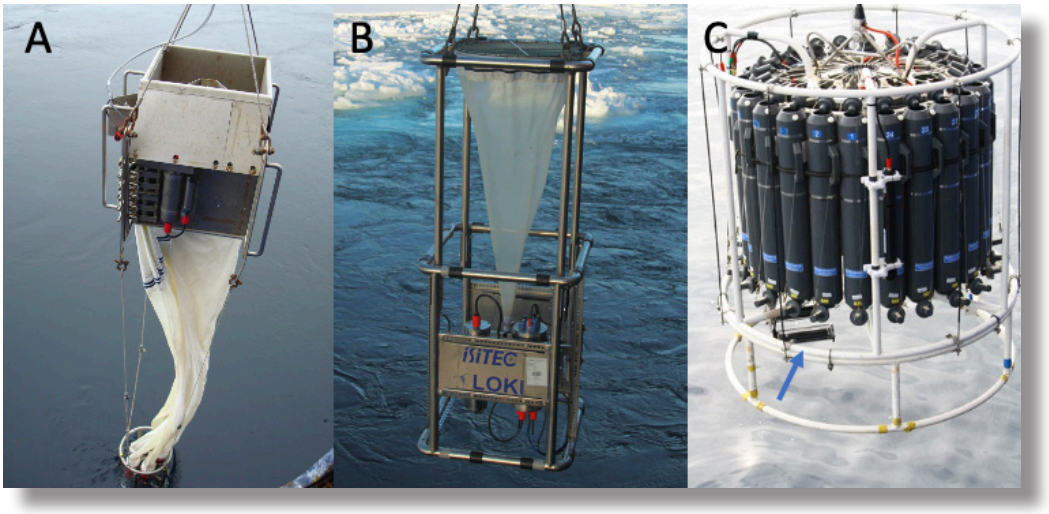

Fig. 4.6: Deployment of gear to address community composition and biomass of zooplankton. The Multi-net midi (A), the LOKI (Light frame On-sight Key species Investigations) system (B) and the UVP (Underwater Vision Profiler) attached to bottom of the CTD/Rosette Water Sampler (blue arrow) to study zooplankton biodiversity and depth distribution in the Fram Strait

To analyse the vertical distribution of zooplankton species in the upper 1,000 m of the water column with high spatial resolution, the optical system LOKI (Light frame On-sight Key species Investigations; Fig. 4.6 B) was deployed at the same stations as the Multi-net. LOKI was equipped with a 150 µm plankton net and took images of zooplankton organisms and particles at a rate of approx. 20 frames sec-1 while being towed vertically through the water column. Simultaneously, depth, temperature, oxygen content and fluorescence were recorded to relate the zooplankton abundance to the environmental conditions. LOKI captures the dominating copepods, ostracods and chaetognaths very well, however, fragile zooplankton such as gelatinous plankton is often destroyed by the net. Therefore, we mounted an Underwater Vision Profiler (UVP) on the frame of the CTD/Rosette Water Sampler (Fig. 4.6 C) and activated it for every CTD cast. The UVP takes images directly into the water and therefore delicate organisms remain intact, however, the resolution of the images is lower than those obtained by

LOKI, and do not allow to determine genera. All images will be analysed, as the images from preserved samples, via EcoTaxa.

Preliminary (expected) results

Biogeochemistry

Bacterial biomass production and phytoplankton primary production were determined on board via radioisotope incubations (Fig. 4.7). Preliminary results on bacterial biomass production (BBP) suggest the highest heterotrophic activity at the central HAUSGARTEN stations, restricted to the upper 25 m of the water column, which is consistent with previous cruises (e.g. PS126). However, phytoplankton primary production (PP), at the moment calculated with previously determined DIC values, showed the highest activity around 7°E corresponding to station SV-IV and coinciding with a phytoplankton bloom event by e.g. *Phaeocystis* (Fig. 4.7).

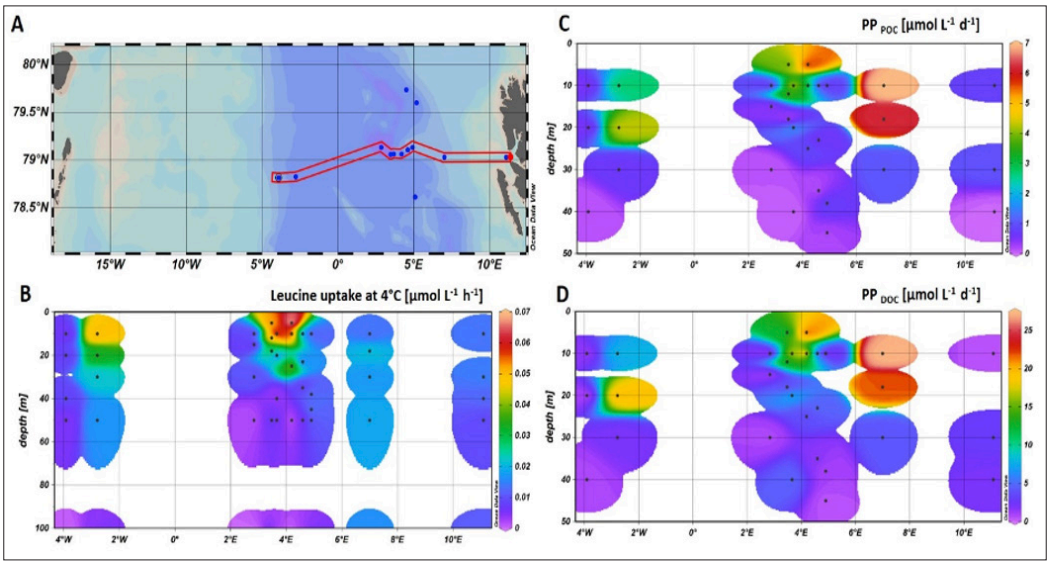

Fig. 4.7: Phytoplankton primary production (PP) and bacterial biomass production (BBP) along a West-East transect from EG-I to SV-I: West-East transect marked in red (A), BBP expressed as leucine uptake at 4°C in the upper 100 m (B), phytoplankton primary production in the upper 50 m split into particulate organic carbon (PPPOC) (C) and dissolved organic carbon (PPDOC) (D). Actual depths from where discrete seawater samples were obtained are marked with black dots

Phytoplankton

The preliminary on-board analyses of the live net samples revealed 108 taxa in total of which 50 were identified to species level. The taxon distribution was rather patchy. *Phaeocystis pouchetii* for instance was very abundant in some sites but completely absent or represented only by a small number of cells in others (Fig. 4.8). While Svalbard and differed the most in terms of species composition, there was no clear species gradient on a north-west or south-west trajectory. Several of the samples also contained protistan parasites (Fig. 4.9). An unknown species of *Miracula*, an oomycete genus with a wide geographical distribution was found at Station EG-I.

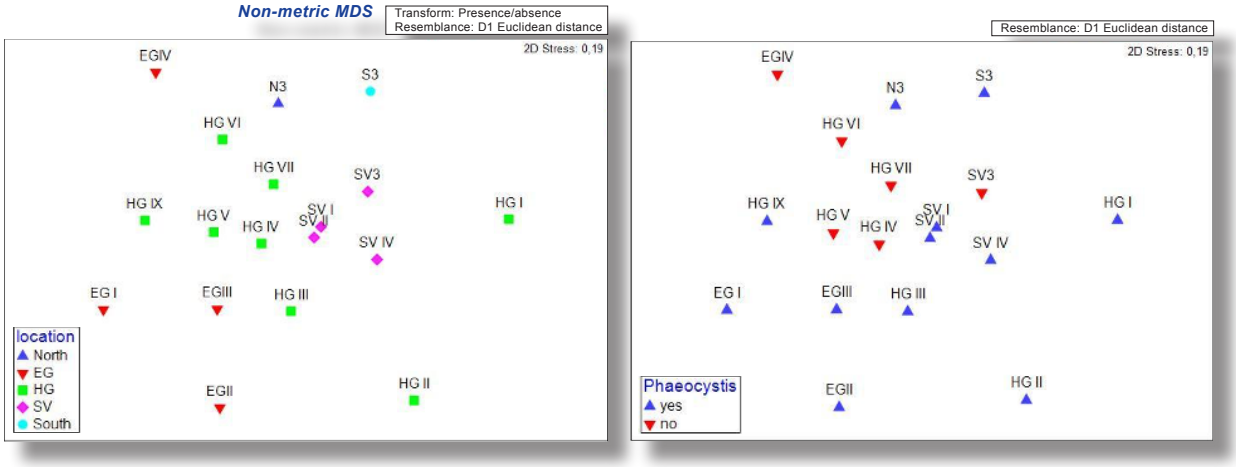

Fig. 4.8: nMDS plots of the preliminary net phytoplankton analyses

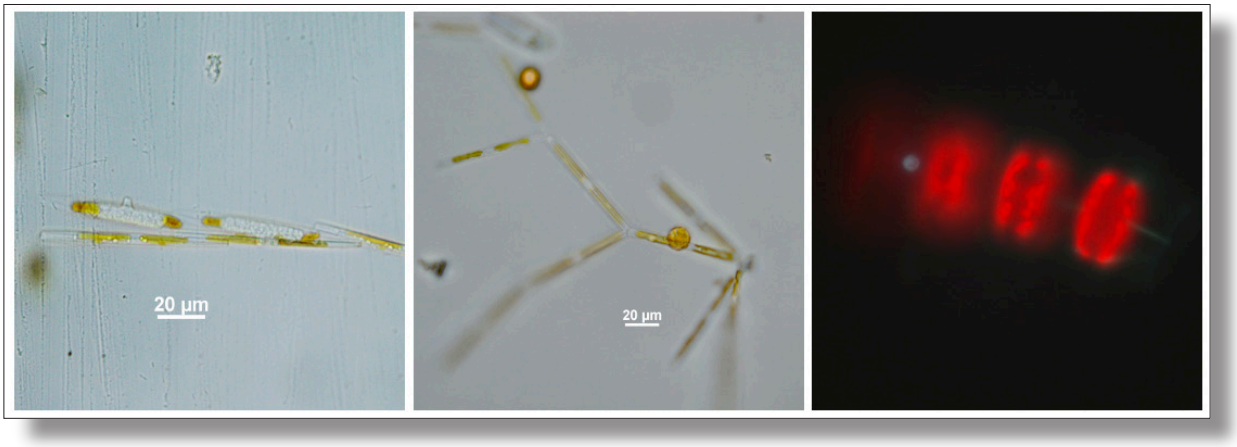

Fig. 4.9: Left: an unidentified Miracula species infecting two cells of the diatom Pseudo-nitzschia. Centre: A possible parasite zoospore attached to cells of the diatom Nitzschia frigida, Right: zoospore attached to a centric diatom chain

Zooplankton

As to be expected, copepods clearly dominated the zooplankton community at all stations. The other taxa found were Amphipoda, Hydrozoa, Polychaeta, Ostracoda, and Chaetognatha (Fig. 4.10). In general, samples from stations in the West Spitsbergen Current and in the centre of the Fram Strait (HG I-IX, S3, N4) contained more zooplankton than samples from East Greenland Current. The highest abundances were found in the surface layer (MN: 0 – 50 m) with the herbivorous copepod genus *Calanus* being the most abundant species in terms of body mass. In deeper intervals, *Metridia longa*, an omnivorous copepod, and the carnivorous chaetognaths (arrow worms) were frequent. However, detailed analyses of both, samples and image data sets will only be possible in the laboratories at AWI. Here, semi-automatic image analyses will yield detailed information on biodiversity, geographic distribution and size structure of the zooplankton communities in relation to environmental conditions (depth, temperature, salinity, chlorophyll *a* concentration) and the data will continue our time series, started in 2011, on zooplankton biomass and abundance.

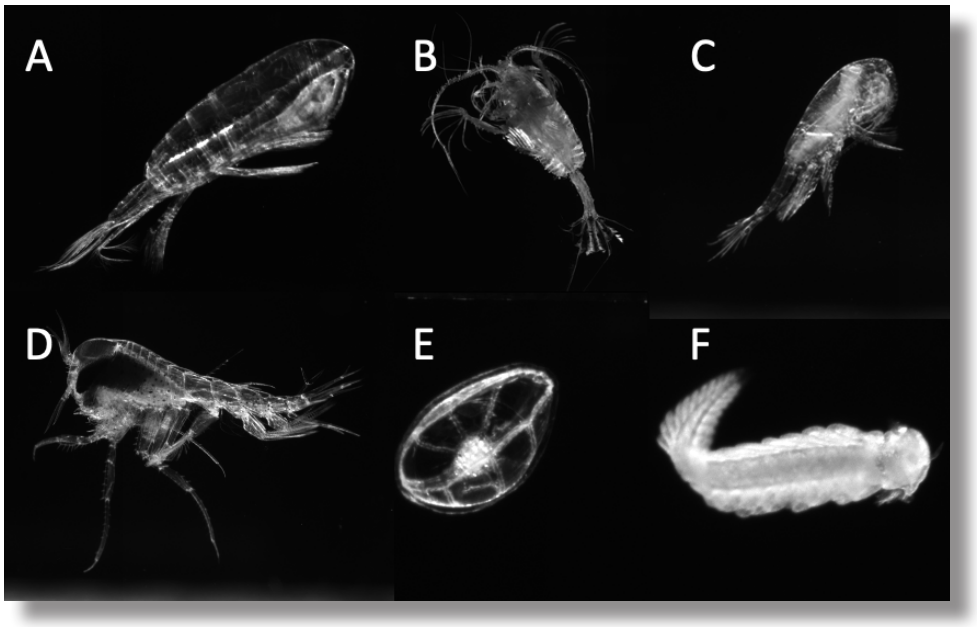

Fig. 4.10: Zooplankton in the Fram Strait Examples from the optical system LOKI (Light frame On-sight Key species Investigations). A: Calanus finmarchicus (Copepoda), B: Paraeuchaeta sp. (Copepoda), C: Metridia longa (Copepoda), D: Themisto sp. (Amphipoda), E: Hydrozoa, F: Polychaeta

Data management

During our cruises, we sample a large variety of interrelated parameters. Many of the samples (i.e. Chl, 16S/18S eDNA, phytoplankton and zooplankton biodiversity etc.) will be analysed at AWI or GEOMAR within approximately one year after the cruise. We plan that the full data set will be available at the latest about two years after the cruise. Samples taken for microscopical and molecular analyses, which cannot be analysed within two years after the cruise, will be stored at the AWI for at least ten years and available upon request to other scientists.

Data will be archived, published and disseminated according to international standards by the World Data Center PANGAEA Data Publisher for Earth & Environmental Science (www.pangaea.de) within two years after the end of the expedition at the latest. By default, the CC-BY license will be applied. Molecular data (DNA and RNA data) will be archived, published and disseminated within one of the repositories of the International Nucleotide Sequence Data Collaboration (INSDC, www.insdc.org) comprising of EMBL-EBI/ENA, GenBank and DDBJ). Images from the zooplankton net samples as well as from both *in situ* optical recorders LOKI and UVP will be uploaded to the website EcoTaxa where they will not only be taxonomically analysed but also archived. The resulting tables presenting abundances and, in case of preserved organisms, also biomasses will be archived in PANGAEA. Any other data will be submitted to an appropriate long-term archive that provides unique and stable identifiers for the datasets and allows open online access to the data. Analysis of BOP and SWIPS-Particle-Camera is quite time consuming and will therefore be done in the home laboratories at AWI-Bremerhaven and MARUM.

This expedition was supported by the Helmholtz Research Programme “Changing Earth – Sustaining our Future” Topic 6, Subtopic 6.1.

In all publications based on this expedition, the Grant No. **AWI_PS136_02** will be quoted and the following publication will be cited:

Alfred-Wegener-Institut Helmholtz-Zentrum für Polar- und Meeresforschung (2017) Polar Research and Supply Vessel POLARSTERN Operated by the Alfred-Wegener-Institute. Journal of large-scale research facilities, 3, A119. http://dx.doi.org/10.17815/jlsrf-3-163.

References

Bachy C, Sudek L, Choi CJ, Eckmann CA, Nöthig EM, Metfies K, Worden AZ (2022) Phytoplankton Surveys in the Arctic Fram Strait Demonstrate the Tiny Eukaryotic Alga *Micromonas* and Other Picoprasinophytes Contribute to Deep Sea Export. Microorganisms, 10(5):961. https://doi.org/10.3390/microorganisms10050961

Bauerfeind E, Nöthig EM, Pauls B, Kraft A, Beszczynska-Möller A (2014) Variability in pteropod sedimentation and corresponding aragonite flux at the Arctic deep-sea long-term observatory HAUSGARTEN in the eastern Fram Strait from 2000 to 2009. Journal of Marine Systems, 132:95–105.

Busch K, Bauerfeind E, Nöthig EM (2015) Pteropod sedimentation patterns in different water depths observed with moored sediment traps over a 4 year period at the LTER station HAUSGARTEN in eastern Fram Strait. Polar Biology, 38:845–859. https://doi.org/10.1007/s00300-015-1644-9

Cornils A, Thomisch K, Hase J, Hildebrandt N, Auel H, Niehoff B (2022) Testing the usefulness of optical data for zooplankton long-term monitoring: Taxonomic composition, abundance, biomass, and size spectra from ZooScan image analysis. Limnology and Oceanography: Methods 20(7):428–450. https://doi.org/10.1002/lom3.10495

Engel A, Piontek J, Metfies K, Endres S, Peeken I, Gäbler-Schwarz S, Nöthig EM (2017) Inter-annual variability of transparent exopolymer particles in the Arctic Ocean reveals high sensitivity to ecosystem changes. Scientific Reports, 7:4129.

Engel A, Bracher A, Dinter T, Endres S, Grosse J, Metfies K, Peeken I, Piontek J, Salter I, Nöthig E-M (2019) Inter-Annual Variability of Organic Carbon Concentration in the Eastern Fram Strait During Summer (2009–2017). Frontiers in Marine Science, 6:187. https://doi.org/10.3389/fmars.2019.00187

Fadeev E, Rogge A, Ramondenc S, Nöthig E-M, Wekerle C, Bienhold C, Salter I, Waite A, Hehemann L, Boetius A, Iversen M (2021) Sea ice presence is linked to higher carbon export and vertical microbial connectivity in the Eurasian Arctic Ocean. Communications Biology, 4:1255. https://doi.org/10.1038/s42003-021-02776-w

Hátún H, Azetsu-Scott K, Somavilla R, et al. (2017) The subpolar gyre regulates silicate concentrations in the North Atlantic. Scientific Reports, 7:14576. https://doi.org/10.1038/s41598-017-14837-4

Kraft A, Nöthig EM, Bauerfeind E, Wildish DJ, Pohle GW, Bathmann UV, Beszczynska-Möller A, Klages M. (2013) First evidence of reproductive success in a southern invader indicates possible community shifts among Arctic zooplankton. Marine Ecological Progress Series, 493:291-296.

Krause JW, Schulz IK, Rowe KA, et al. (2019) Silicic acid limitation drives bloom termination and potential carbon sequestration in an Arctic bloom. Scientific Reports, 9:8149. https://doi.org/10.1038/s41598-019-44587-4

Lalande C, Nöthig E-M, Fortier L (2019) Algal Export in the Arctic Ocean in Times of Global Warming Geophysical Research Letters. https://doi.org//10.1029/2019GL083167

Lalande C, Nöthig EM, Bauerfeind E, Hardge K, Beszczynska-Möller A, Fahl K (2016) Lateral supply and downward export of particulate matter from upper waters to the seafloor in the deep eastern fram strait. Deep Sea Res. Part I Oceanogr. Res. Pap. 114, 78-89. https://doi.org/10.1016/j.dsr.2016.04.014

Metfies K, von Appen WJ, Kilias E, Nicolaus A, Nöthig EM (2016) Biogeography and photosynthetic biomass of Arctic marine pico-eukaryotes during summer of the record sea ice minimum 2012. PLoS One 11. https://doi.org/10.1371/journal.pone.0148512

Nöthig E-M, Bracher A, Engel A, Metfies K, Niehoff B, Peeken I, et al. (2015) Summertime plankton ecology in Fram Strait - a compilation of long- and short-term observations. Polar Research, 34:23349. https://doi.org/10.3402/polar.v34.23349

Nöthig E-M, Ramondenc S, Haas A, Hehemann L, Walter A, Bracher A, Lalande C, Metfies K, Peeken I, Bauerfeind E and Boetius A (2020) Summertime Chlorophyll a and Particulate Organic Carbon Standing Stocks in Surface Waters of the Fram Strait and the Arctic. Frontiers in Marine Science, 19: 7. https://doi.org/10.3389/fmars.2020.00350

Ramondenc S, Nöthig EM, Hufnagel L, Bauerfeind E, Busch K, Knüppel N et al. (2022) Effects of atlantification and changing sea-ice dynamics on zooplankton community structure and carbon flux between 2000 and 2016 in the eastern Fram Strait. Limnol. Oceanogr. https://doi.org/10.1002/lno.12192

Vane K, Cobain MRD, Trueman CN, et al. (2023) Tracing basal resource use across sea-ice, pelagic, and benthic habitats in the early Arctic spring food web with essential amino acid carbon isotopes. Limnology and Oceanography, 68(4):862–877. https://doi.org/10.1002/lno.12315

von Appen WJ, Waite AM, Bergmann M, Bienhold C, Boebel O, Bracher A, Cisewski B, Hagemann J, Hoppema M, Iversen MH, Konrad C, Krumpen T, Lochthofen N, Metfies K, Niehoff B, Nöthig EM, Purser A, Salter I, Schaber M, Scholz D, Soltwedel T, Torres-Valdes S, Wekerle C, Wenzhöfer F, Wietz M, Boetius A (2021) Sea-ice derived meltwater stratification slows the biological carbon pump: results from continuous observation,Nature Communications, 12 (1), p. 7309

von Jackowski A, Becker KW, Wietz M, Bienhold C, Zäncker B, Nöthig EM, Engel A (2022) Variations of microbial communities and substrate regimes in the eastern Fram Strait between summer and fall" Environmental Microbiology, 24(9):4124–4136. https://doi.org/10.1111/1462-2920.16036

von Jackowski A, Grosse J, Nöthig EM, Engel A (2020) Dynamics of organic matter and bacterial activity in the Fram Strait during summer and autumn. Philosophical Transactions of the Royal Society A, 378:2181. https://doi.org/10.1098/rsta.2019.0366

Wietz M, Bienhold C, Metfies K, Torres-Valdes S, von Appen WJ, Salter I, Boetius A (2021) The polar night shift: seasonal dynamics an drivers of Arctic Ocean microbiomes revealed by autonomous sampling. ISME Communications, 1:76.

5. PELAGIC BIOGEOCHEMISTRY – NUTRIENTS AND NET COMMUNITY PRODUCTION

Jennifer Freer[1], Linda Rehder[2], Daniel Scholz[2], Sinhué Torres-Valdés[2]; not on board: Sebastian Rokitta[2], Adrian Martin[3], Pete Brown[3]

[1]UK.BAS
[2]DE.AWI
[3]UK.NOC

Grant-No. AWI_PS136_03

Part I: Nutrients

Objectives

Beginning in 2018 during PS114, we have been deploying Remote Access Samplers (RAS) equipped with several sensors (SUNA nitrate, pH, pCO2, CTD-O2, PAR and Eco-triplet) in the Fram Strait as part of the FRAM/HAUSGARTEN LTO activities. Whenever possible we have deployed four of these biogeochemical packages in two moorings (EGC, F4S and/or F4W-1), targeting sub-surface and core waters of the East Greenland Current and West Spitsbergen Current. Deployments (and eventual recoveries) in this configuration have then been taken place during PS121 in 2019 and PS126 in 2021. In 2022, during PS131, only two biogeochemical packages were deployed in subsurface waters as the other two RAS were deployed elsewhere as part of the ATWICE expedition. With the RAS we typically collect 48 seawater samples at roughly weekly intervals, for later analysis of dissolved inorganic and organic nutrients. Additionally, we also collect water samples from CTD/Rosette Water Sampler casts for nutrient analyses onboard. Our aim is to use data from sensors and RAS deployments, in combination with data from CTD casts to assess temporal variability of biogeochemical variables associated with inflowing and outflowing water masses in the Fram Strait. This will allow us to evaluate the role of water property exchange in the deepest gateway of the Arctic, within the context of Arctic Ocean nutrient budgets. As in previous expeditions, we carry out these deployments in collaboration with colleagues within the FRAM community; the Microbial Observatory (Katja Metfies, Christina Bienhold, Anja Nicolaus, Matthias Wietz), Physical Oceanography of Polar Oceans (Wilken von-Appen, Mario Hoppmann, Matthias Monsees, Torsten Kanzow) and Deep-Sea Ecology and Technology (Normen Lochthofen, Janine Ludszuweit). For PS136, we started a new collaboration with colleagues (Adrian Martin, Peter Brown) from the National Oceanography Centre (NOC), Southampton (UK) as part of their BIOPOLE programme (https://biopole.ac.uk/). They provided an extra RAS to complement our work in the Fram Strait.

Work at sea

Nutrients

In order to address our objectives as described in the expedition programme (Soltwedel 2023), during PS136 we collected seawater samples from CTD/Rosette Water Sampler casts (Tab. 5.1) for the analyses onboard of dissolved oxygen and dissolved nutrients (nitrate + nitrite, nitrite, ammonium, total dissolved nitrogen, phosphate, total dissolved phosphorus, and

silicate). In collaboration with colleagues from Polar Biological Oceanography and Deep-Sea Ecology and Technology, we deployed two AWI RAS and one RAS from colleagues of the NOC (UK).

Tab. 5.1: Events sampled for the collection and analysis of dissolved nutrients and dissolved oxygen (DO) during PS136. Sample collection included two random duplicates per cast.

Event	Nutrients	DO	Deepest sample	# depths	# samples
PS136_4-2	x	x	1200 m	10	12
PS136_4-9	x	x	100 m	5	7
PS136_5-1	x	x	100 m	5	7
PS136_7-1	x	x	100 m	6	8
PS136_8-1	x	x	2570 m	13	15
PS136_9-1	x	x	800 m	15	17
PS136_1-1	x	x	100 m	5	7
PS136_11-1	x	x	1200 m	10	12
PS136_11-2	x	x	100 m	5	7
PS136_12-3	x	x	100 m	5	7
PS136_13-1	x	x	751 m	11	13
PS136_14-1	x	x	100 m	6	8
PS136_14-5	x	x	250 m	9	11
PS136_17-1	x	x	100 m	6	8
PS136_17-8	x	x	800 m	14	16
PS136_18-1	x	x	100 m	6	8
PS136_18-11	x	x	1200 m	11	13
PS136_23-1	x	x	100 m	6	8
PS136_24-1	x	x	800 m	13	15
PS136_25-1	x	x	100 m	6	8
PS136_27-1	x	x	100 m	6	8
PS136_27-9	x	x	1200 m	10	12
PS136_28-1	x	x	100 m	5	7
PS136_3-1	x	x	100 m	6	8
PS136_3-7	x	x	800 m	12	14
PS136_31-1	x	x	100 m	6	8
PS136_31-7	x	x	800 m	13	15
PS136_32-1	x	x	100 m	6	8
PS136_33-1	x	x	100 m	6	8
PS136_33-9	x	x	900 m	10	12

One RAS was deployed close to the surface (~ 25 m) in mooring F4-S7. Two RAS were deployed in mooring EGC-9; one at ~ 50 m and another at ~ 200 m. RAS close to the surface were equipped with biogeochemical sensors (SUNA-nitrate, PAR, pH, CDOM, backscatter, Chl a, and pCO2) and a CTD-O2 and the deeper RAS was equipped with a CTD-O2. A SUNA nitrate sensor was deployed alongside 32 CTD cast to obtain high-resolution nitrate profiles down to max. 1,500 m (Tab. 5.2). The Suna data is processed following Sakamoto et al. (2009), using the CTD's temperature and salinity data. Further quality control will be conducted by comparison to the CTD's Niskin bottle nitrate data.

Tab. 5.2: Summary of Suna nitrate profiles.

Event	Profile depth [m]
PS136_02_001	994
PS136_03_001	1000
PS136_04_002	1500
PS136_04_009	100
PS136_05_001	101
PS136_09_001	800
PS136_10_001	100
PS136_11_001	1240
PS136_11_012	100
PS136_12_003	100
PS136_13_001	751
PS136_14_001	100
PS136_14_005	270
PS136_17_001	100
PS136_17_008	800
PS136_18_001	100
PS136_18_011	1500
PS136_23_001	100
PS136_23_005	10
PS136_24_001	800
PS136_25_001	100
PS136_27_001	101
PS136_27_009	1511
PS136_28_001	100
PS136_30_001	100
PS136_30_007	1500
PS136_31_001	100
PS136_31_007	800
PS136_32_001	100
PS136_33_001	100
PS136_33_009	933
PS136_35_001	1000

Dissolved oxygen

Dissolved oxygen was determined following the amperometric Winkler titration method as described by Langdon (2010), adopting GO-SHIP best practice recommendations. Soon after laboratory set up, 1 L of thiosulphate solution (titrant) was prepared (50 g/L) and let to stabilise for about two days. Thiosulphate calibrations were carried out using 1.667 mM OSIL Scientific

certified Iodate Standards; first, five blanks (involving 2 x 1 mL additions of iodate standard, each titrated one at a time) were measured followed by five standards (each with 10 mL of iodate standard). A first calibration was carried two days after the thiosulphate solution was prepared and a second calibration was carried out the following day in order to confirm the solution was stable and results from calibrations were consistent. There on, calibrations were carried out approximately every 4-7 days, with a total of five calibrations carried out during PS136. Seawater samples were collected using a tygon tube attached to the spigot of the Niskin bottles and placed directly into volume-calibrated borosilicate glass bottles with narrow necks. Care was taken to avoid bubbles inside the sampling tube and the sampling bottles. Water was left to spill over approximately three or more times the volume of the sampling bottle before the sample was drawn. A hand-held thermometer was used to measure the temperature of the seawater at the time of sample collection (i.e. fixing temperature) using a relatively fast-response temperature probe. Samples were immediately fixed by dispensing 1 mL of manganese chloride, followed by 1 mL of alkaline iodide, and then mixed thoroughly. Bottle lids were then secured in place using steel clips. When sampling was completed, the precipitate of the sample was let to settle to about a third of the volume (> 1 hour). Samples were then mixed thoroughly for a second time and the precipitate let to settle for a further hour or until analysis. Analysis was carried out using a Metrohm Ti-Touch titration unit set up with the amperometric end point detection. Before analysis 1 mL of 5 M sulphuric acid was added to a sample for titration. Analysis took place within 24 h after sample collection. In all casts, two randomly selected depths were sampled in duplicate. Due to time constrains data was not processed onboard, but will be processed within six months following the expedition and then passed on to the Physical Oceanography team in order to calibrate the O_2 sensors mounted on the CTD frame.

Nutrient analysis

During PS136, we used a 7-channel Seal Analytical AA-500 autoanalyzer set up in Dry Lab 3 on *Polarstern* (Fig. 5.1) for the analysis of micro-molar concentrations of 1) dissolved inorganic nutrients; nitrate plus nitrite (NO_3^- + NO_2^-), nitrite (NO_2^-), ammonium (NH_4^+), silicate ($Si(OH)_4$), and phosphate (PO_4^{3-}), and 2) total nutrients; total phosphorus (TP) and total nitrogen (TN). The nutrient analyser was controlled by the Seal Analytical Software AACE version 8.03 Beta15, which allows for automated and simultaneous analysis of up to 7 channels. Following analyser set up, analytical reagents (stock and working solutions), standards (stock solutions and calibrants) and lab-made quality control solutions were prepared. ‘Stocks’ are concentrated solutions from which ‘working’ reagents/standards are prepared as required by solution stability or usage. Analyses were carried out following current Seal Analytical Methods, which are based on standard and widely used colorimetric and fluorometric techniques for the analysis of nutrients in water and seawater. Here we list the methods used during PS136 as provided by the manufacturers:

1. Total dissolved nitrogen in seawater No. G-218-98 revision 13 (MT23)
2. Nitrate and nitrite in water and seawater No. A-044-19 revision 5 (MT519A)
3. Nitrite in water and seawater No. A-003-18 revision 3 (MT518)
4. Total dissolved phosphorus in seawater No. A-009-19 revision 3 (MT533)
5. Phosphate in water and seawater No. A-004-18 revision 4 (MT518)
6. Silicate in water and seawater No. A-006-19 revision 3 (MT519)
7. Ammonium in water and seawater No. G-327-05 revision 8

Fig. 5.1: Chemistry lab set up in Dry Lab 3 on Polarstern during PS136; the image shows a titration unit for the measurement of dissolved oxygen (left-hand side) and a nutrient autoanalyzer set up on the main bench of the lab.

We adopted best practices procedures for the analyses of nutrients in seawater following GO-SHIP recommendations, as described in Hydes et al. (2010) and Becker et al. (2020). Calibration standards for the analysis were prepared using 1,000 mg/L NO_3^-, NO_2^-, PO_4^{3-} and Si MERCK solutions. An intermediate standard containing 4.032, 0.152, 3.560, and 0.947 µmol/mL of nitrate, nitrite, silicate and phosphate was prepared in Milli-Q water using a 100 mL volumetric flask. Although working calibration standards are typically prepared in a saline solution or 'artificial seawater' (35 g NaCl in 1 L of Milli-Q water), which is also used as a matrix for the analysis, in later years the so called "ultra clean or analytical grade reagents" have been found to be contaminated with a given nutrient (usually phosphate, nitrate and organic nitrogen, and even silicate). In our case, the analytical grade NaCl was found to be contaminated with nitrate and organic nitrogen. Therefore, standards and the analysis matrix were based on Milli-Q water instead. From the intermediate standards, five calibration standards were prepared regularly using 500 mL flasks to yield the target concentrations shown in Table 5.3. These values were then input into an analysis template file in the AACE software, from which all consecutive runs are then built. For each analysis, standards were measured in triplicate, with the first measurement intended as preconditioning and thus ignored as calibrant. It is good practice to adapt calibration concentration ranges for the particular system being measured, in this case, the Arctic Ocean. Here though, we used a rather high range for phosphate. This was determined/imposed by the method to measure TP, which is designed to work efficiently with a top standard of 5 µmol L^{-1}. A calibration range with a top standard lower than this is likely to yield high noise in the signal. However, the phosphate and TP channels were stable and linear throughout the expedition, with calibration slopes being typically 1.

Tab. 5.3: Set of calibration standards (*Std*) used for dissolved inorganic nutrient analysis. Concentration units are µmol L^{-1}. Concentrations in the first column are the sum of NO_3^- and NO_2^-, hence NO_3^- + NO_2^-. Note that the concentration of TN calibration standards is the sum of inorganic nitrogen species (i.e. NO_3^-, NO_2^-, and NH_4^+).

	NO_3^- + NO_2^-	**NO_2^-**	**$Si(OH)_4$**	**PO_4^{3-} & TP**	**TN**	**NH_4^+**
Std 1	0.469	0.017	0.399	0.106	0.528	0.059
Std 2	6.209	0.226	5.284	1.406	6.991	0.782
Std 3	11.950	0.435	10.169	2.707	13.254	1.504
Std 4	17.961	0.643	15.054	4.007	19.917	2.227
Std 5	23.431	0.852	19.939	5.307	26.381	2.949

Several quality controls were implemented in the analysis in order to secure data quality: Low nutrient seawater (LNSW) from OSIL Scientific can have multiple uses. It can be used as a saline matrix, as a low concentration standard or, as in our case, to determine whether contamination with any given nutrient occurred during sample collection or preparation of reagents. It is expected that the signal produced is close to the baseline (i.e. blank) or above, and remain constant throughout analyses.

Recovery Standards (Cadmium coil and column reduction efficiency). The measurement of some nutrients such as NO_3^-+NO_2^- and TN require continuous monitoring of the reduction efficiency of the Cadmium (Cd) coil, in the former, and Cd column in the latter. The colorimetric method upon which the measurement of these two nutrients is based, relies on the chemical reaction between reagents and NO_2^-. Thus, in order to measure NO_3^-, this has to be reduced to NO_2^- (the Cd is oxidised and the NO_3^- is reduced). In the case of TN, the reaction is slightly more complicated, as all dissolved nitrogen present in the water first needs to be oxidised to NO_3^- + NO_2^- and then reduced to NO_2^-. For TN there is thus an extra step to monitor; the oxidation efficiency, which is dealt with in the next subsection. In order to monitor the reduction efficiency, two lab-made standards containing only NO_2^- and only NO_3^- were prepared, both at a concentration of 23.31 µmol L^{-1}. The concentration yielded by measuring both recovery standards should be equal within the precision of the analyses. The reduction efficiency is the ratio of the NO_3^- standard to the NO_2^- standard in percentage. As per best practice recommendations, the Cd coil or column were reactivated or replaced when the reduction efficiency was less than 95%.

Recovery Standards (TN oxidation efficiency). As mentioned above, the measurement of TN requires the oxidation of all nitrogenous compounds present in the sample. There are no certified reference materials available in the market to test the oxidation efficiency and the accuracy of the method. However, there are steps that can be taken. During for PS136, we used an OSIL Scientific 10 mmol L^{-1} ammonium (NH_4^+) certified standard, from which we prepared a 15 **µmol-**NH_4^+ L^{-1} solution. This standard was measured in duplicate in every run. Although this standard is not an organic compound, it is most useful as the NH_4^+ first needs to be oxidised to NO_3^-+NO_2^- and then reduced to NO_2^-.

Certified reference materials (KANSO and OSIL Scientific). In order to assess the accuracy and consistency of the methods employed, we used two types of certified reference materials (CRMs); 1) KANSO Technos Co., LTD, Japan, lots CL, CO, CP and CR, and 2) OSIL Scientific, UK, nutrient standards. KANSO are so called 'RMNS or reference materials for the measurement of nutrients in seawater'. These are made from natural seawater, typically by combining deep and surface water from selected ocean regions to yield target concentrations, plus further processing (e.g. sterilisation). Table 5.4 shows the certified concentration of the CRM lots used during PS136. When data is processed, these values will be used to assess the accuracy of the analysis and corrections will be applied to results would this be deemed necessary. OSIL Scientific standards are concentrated solutions distilled-water-based and certified to 100 µmol-PO_4^{3-} L^{-1}, 100 µmol-NO_2^- L^{-1}, 1,000 µmol-NO_3^- L^{-1} and 1,000 µmol-Si L^{-1}. These concentrated solutions were used to prepare a quality control standard with concentrations equal to our second top calibration standard (*STD* 4 in Tab. 5.3), so as to have another independent standard to assess the consistency of the analysis.

Tab. 5.4: RMNS certified nutrient concentrations (in µmol kg^{-1} and µmol L^{-1}) and salinity

RMNS lot (units)	NO_3^-	NO_2^-	$Si(OH)_4$	PO_4^{3-}
CL (µmol kg^{-1})	5.47 ± 0.15	0.015 ± 0.006	13.80 ± 0.30	0.425 ± 0.019
CL (µmol L^{-1})	5.60 ± 0.15	0.015 ± 0.006	14.13 ± 0.03	0.435 ± 0.019
CL Salinity (psu)	34.685			
CO (µmol kg^{-1})	15.86 ± 0.15	0.04 ± 0.04	34.72 ± 0.16	1.177 ± 0.014
CO (µmol L^{-1})	16.58 ± 0.2	0.04 ± 0.04	35.54 ± 0.16	1.204 ± 0.014
CO Salinity (psu)	34.282			
CR (µmol kg^{-1})	5.46 ± 0.16	0.97 ± 0.07	14.0 ± 0.30	0.394 ± 0.014
CR (µmol L^{-1})	5.59 ± 0.16	0.993 ± 0.071	14.33 ± 0.30	0.403 ± 0.014
CR Salinity (psu)	34.619			
CP (µmol kg^{-1})	24.80 ± 0.30	0.31 ± 0.07	61.1 ± 0.30	1.753 ± 0.018
CP (µmol L^{-1})	25.39 ± 0.3	0.317 ± 0.071	62.5 ± 0.30	1.794 ± 0.018
CP Salinity (psu)	34.398			

Sample collection and analysis

40 mL-samples were collected directly into 50 mL sterile Falcon tubes for the analysis of nutrients. Tubes were rinsed three times with seawater before the sample was drawn. Two duplicate samples were randomly collected from each cast. In order to optimise lab work (e.g. number of samples analysed per run) and reduce the amount chemical waste produced, analyses were carried out when a minimum of two or more CTD casts worth of samples were available. When required samples were stored in the fridge and were analysed within 24 hours of sample collection. Analyses took place daily once station work began and consisted of 2-3 CTD casts worth of samples, 15 to 20 samples from our colleagues Antonia Thielecke and Natasha Bryan (SIDE Effects project), and 15-20 samples from RAS recovered in previous *Polarstern* expeditions (PS121, PS126, and PS131). All samples were analysed in duplicate. Due to time constrains and workload, data was not processed onboard. Data processing will take place within six months of the expedition.

During lab set up and preparation stages, it was found that one of the main reagents for the analysis of silicate, oxalic acid, did not dissolved and instead precipitated. We have in recent years encountered issues with reagents, which are sometimes contaminated with one or more of the nutrients of interest. This was a new case, not previously encountered. The product used (oxalic acid) was brand new, of analytical grade and exactly the same CAS number used for previous expeditions. Given that reagents are pre-weighed as described by the respective method, we did not have the means to reduce the weight accurately. What we did was to homogenise the oxalic acid crystals in one litre of Milli-Q water using a 1 L volumetric flask. 500 mL were then transferred into another 1 L volumetric flask using a measuring cylinder and then topped up to 1 L. This amount of oxalic acid (50%) did dissolve and was used for the analysis. Having carried out lab tests in preparation for station work, we found that the oxalic acid reagent was yielding expected results, which we also assessed using certified reference materials.

Another problem encountered was the fact that the software that controls the nutrient analysis started generating corrupted files. This resulted in some data not being exported to a usable format as the software crashed the moment raw data was edited (e.g. to correct peak markers that were not placed correctly by the software). We reinstalled the software a couple of times, but this did not improve the situation. We also installed a newer version of the software, which made the computer slower and crashed in the middle of an analysis run. We revert to the old

version of the software and discovered that corrupted files were generated when using one of the software options, by which one can copy a previous analysis template. Typically, this saves time as we do not need to type in calibration standards labels, quality control labels and sample IDs. That is, we can edit a previous template, thereby saving time and avoiding typing mistakes. In a previous expedition, we used this option every run for almost two months with no problems. This time however, it did not work. What we did in the end, was to generate new templates from scratch on every analysis run. This did not produce corrupted files. However, there are still some raw data files from which the results of the analyses have not yet been retrieved. We will contact the manufacturers and will ask assistance in retrieving the data.

Preliminary (expected) results

Upon mooring recovery, data retrieval, processing and quality control of sensor data will take up to six months. Nitrate SUNA sensor data will take longer as it requires measurements of nitrate from RAS samples for the final step of calibration. RAW sensor data will be submitted to PANGAEA soon after the expedition together with mooring raw data and metadata from other groups. Analysis of nutrients from RAS samples will take up to 1 year and will likely be analysed during the next FRAM/HAUSGARTEN expedition. Data from analysis was not processed onboard as on previous occasions, in part due to time constrains given we dedicated extra time to help with the analysis of samples for our colleagues from the SideEffects project and in part due to the problems encountered with the software. However, we aim to have the data from the analyses carried out onboard ready within 6-8 months after the expedition.

In Figures 5.2 to 5.4 we show preliminary results from our full sensor set up, as deployed in mooring F4-S6 (West Spitsbergen Current, 23 m water depth), deployed in 2022 and recovered in 2023 during PS136. Data show the annual cycle of nitrate (SUNA sensor), dissolved oxygen, fluorescence chlorophyll *a*, CDOM, PAR, backscatter, pH, pCO_2, temperature, salinity, and depth (from pressure). Low nitrate concentrations are observed in Aug-Sep 2022, associated with high chlorophyll, likely following or during a late summer phytoplankton bloom (consistent with low light availability, and declining dissolved oxygen concentrations). Some spikes in nitrate concentration are visible, which are more consistent with deeper waters (i.e. pressure increases), likely due to the mooring being knocked down by ocean currents and thus measuring deeper waters with higher nitrate levels. As temperature decreases towards the winter months, nitrate replenishes due to convection. Some spikes of low salinity and temperature, with higher oxygen, suggest fresh water flowing by. Increases in pressure during winter months do not result in changes in nitrate concentration as the water column is well mixed. As light becomes gradually available towards the end of the cycle, chlorophyll spikes are visible again and so the backscatter signal increases, suggesting more biogenic particles in the water. pH and pCO_2 reflect biological activity as well, but these variables are also influenced by sensors being in contact with deeper waters as the mooring is knocked down.

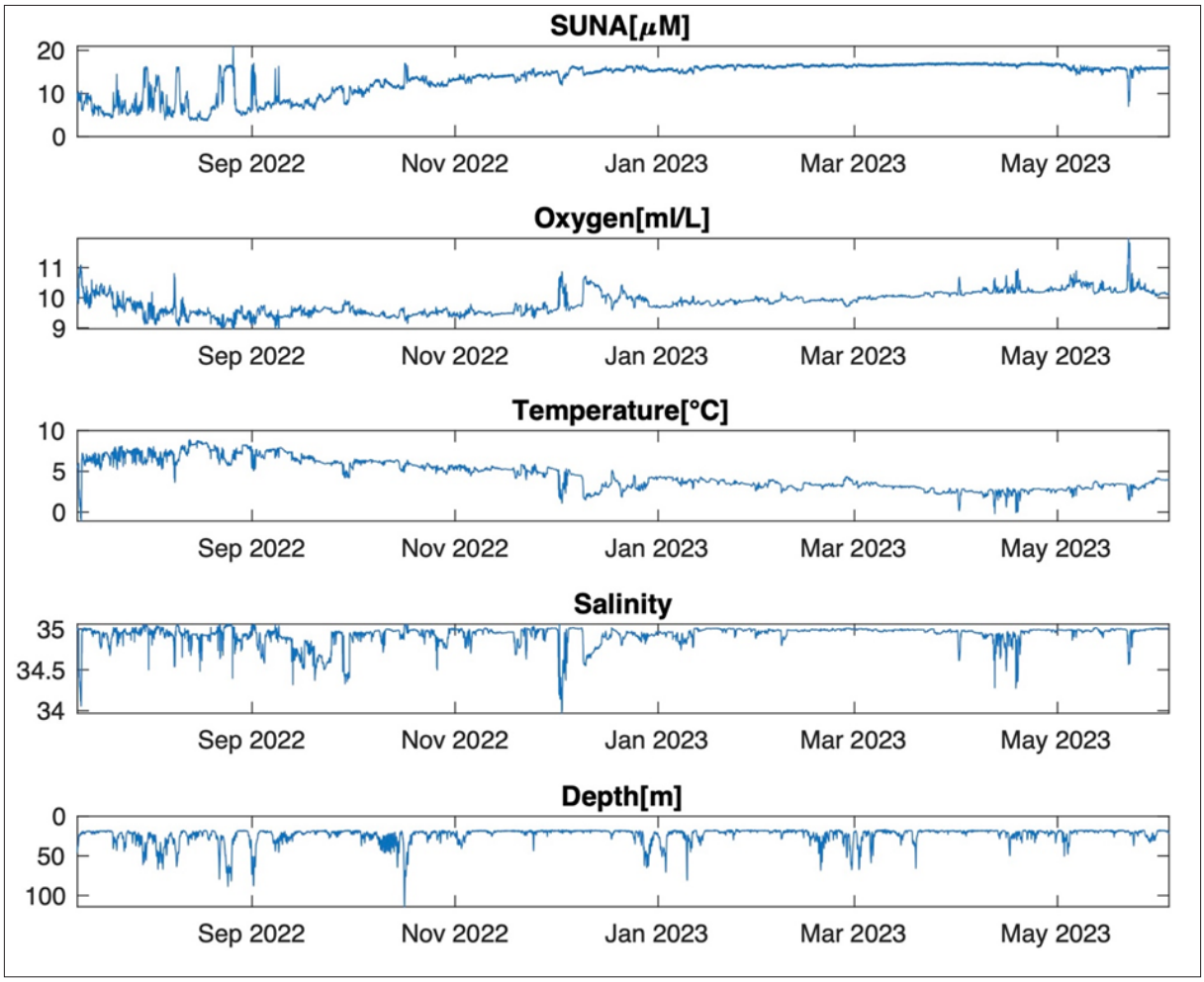

Fig. 5.2: Time series of nitrate (SUNA sensor), dissolved oxygen, temperature, salinity and depth (from pressure); data from sensors deployed in mooring F4-S6 recovered on PS136

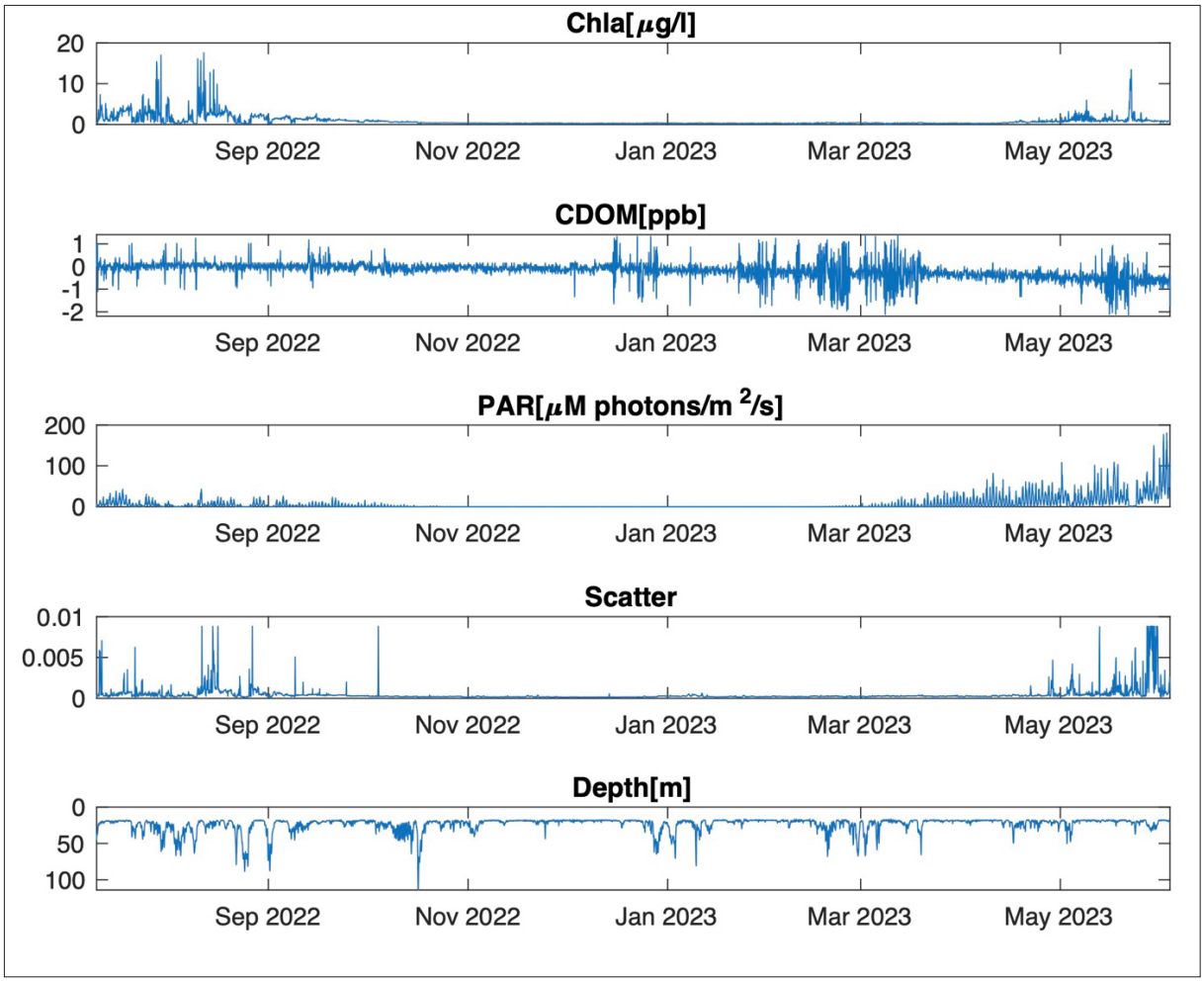

Fig. 5.3: Time series of chlorophyll a, CDOM, PAR and backscatter; depth is shown again as reference. Data from sensors deployed in mooring F4-S6 recovered on PS136

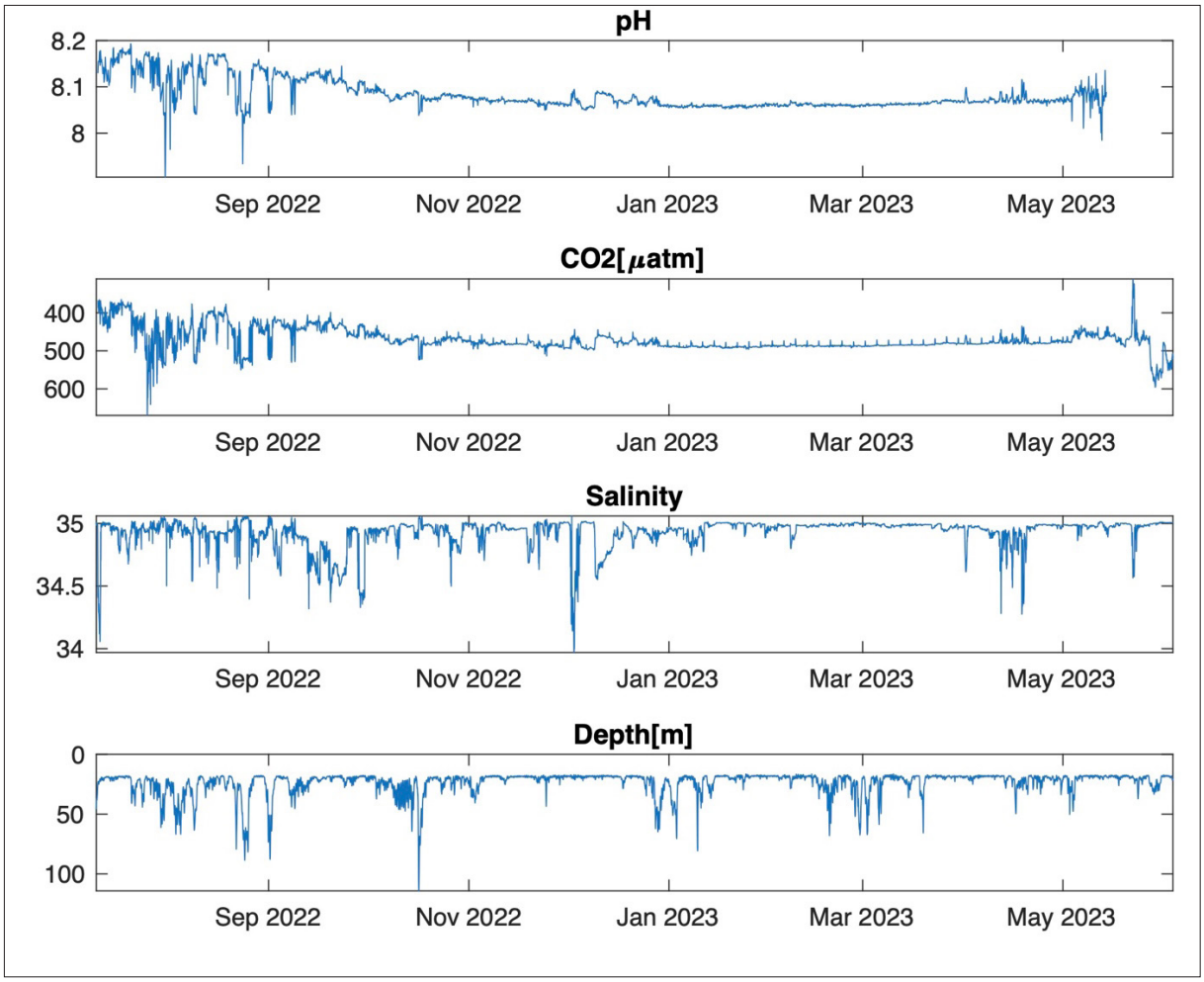

Fig. 5.4: Time series of pH and pCO_2, with salinity and depth as reference; data from sensors deployed in mooring F4-S6 recovered on PS136

Part II: Phytoplankton incubation experiment

Objectives

Phytoplankton plays a fundamental role in marine biochemical cycling, provides the basis of the marine food web system and contributes about 50% of the global oxygen budget (Field et al. 1998; Falkowski et al. 2000). Arctic phytoplankton is prone to Climate Change, especially to global warming due to a 4-times faster increase in sea surface temperatures in comparison to other oceans (Cooley et al. 2022). Along this long-term warming trend, phytoplankton also experiences short-term extreme events such as heatwaves which increase in their frequency, duration and intensity (Hobday et al. 2016). Temperature as a universal driver effects phytoplankton in various manners: Increasing average sea surface temperatures are expected to result in a shift of species composition with a tendency of *Phaeocystis* dominated blooms (Ahme et al. 2023). Also, cellular metabolism and thus net O_2 production as well as net C-fixation likely change due to altered thermodynamics in their physiological processes. This together likely results in changed physiological performance of a phytoplankton community. To better understand and project the consequences of temperature on Arctic phytoplankton communities, it was anticipated to conduct an incubation experiment with a natural Arctic spring bloom community acclimated to present day and two IPCC projections of future temperatures.

Work at Sea

In order to set up the experiment, sea water containing phytoplankton (~ 1.5 mg Chl *a* L^{-1}) was collected from the Teflon inflow system (11 m water depth). Water was sampled at the central HAUSGARTEN site HG-IV (Fig. 3.1), which was covered with drifting one-year sea ice (temperature: -1.6°C). Sea water was pre-filtered through 150 µm nylon mesh to exclude zooplankton, diluted with sterile filtered sea water (0.2 µm pore size) and enriched with nutrients and trace metals according to F/2 medium (Guillard and Ryther 1962). Cultures were incubated in triplicates at 2°C, 6°C and 9°C in 5 L Schott bottles with a Chl *a* concentration of ~ 0.5 mg L^{-1}. Irradiance was set at 30 µmol photons m^{-2} s^{-1} in a 24 h light:dark cycle and bottles were placed in aquaria to optimize temperature treatment control. To avoid sedimentation of phytoplankton and to keep carbonate chemistry stable, cultures were continuously aerated with fresh air from outside the ship (tube inflow outside the work shop on E-deck). Cultures were incubated in a cooling container (Fig. 5.5) at the respective acclimation temperatures for 14 days with a dilution at day 7.

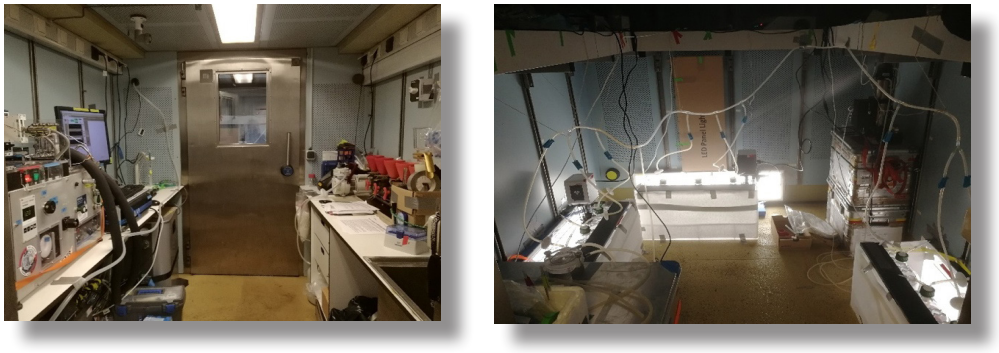

Fig. 5.5: Lab set-up in the cooling container. Left: The front part (9°C) was used for the placement of the MIMS system (including cryostat and two compressors for a provision of 4 mbar compressed air), filtration and fluorometrically Chl a determination. Right: The back part (0°C) was used for the incubation set-up including three aquaria equipped with thermostats, FRRF measurements as well as concentration of algae suspension as MIMS preparation.

Growth rates were assessed on a daily basis via Chl *a* concentrations and nutrient uptake (nitrate and silicate). Chl *a* samples were filtered on GF filters (Whatmann, 0.7 µm pore size). One replicate per culture bottle was extracted (90% acetone) and measured on board fluorometrically (Turner trilogy, Chl *a*-acidification method; Knap et al. 1996), the other replicate per culture bottle was stored at -80°C and will be analysed on land. Nutrient samples were sterile filtered (0.45 µm pore size) and stored at -20°C. Measurements for nitrate, nitrite, phosphate and silicate will be done at AWI.

At the start of the experiment (T0), before the dilution and at the final harvest, various parameters were measured. For the determination of the species composition, DNA samples (0.2 µm pore size, stored at -20°C), microscopy samples (fixed with lugol, stored at 4°C) and flow cytometry samples (fixed with formaldehyde, stored at -80°C) were collected. Also, Chl *a* samples and samples for particulate organic carbon (POC) and nitrogen (PON) were collected on GF Filters (Whatmann, 0.7 µm pore size). POC and PON samples were collected on pre-combusted filters and stored at -20°C.

Additionally, physiological *in vivo* assays were performed. Variable Chl *a* – based fluorescence was measured using Fast Repetition Rate Fluorometry (FRRF). Photo-chemical parameters such as Fv/Fm, relative maximum electron transport rates (rETRmax), light saturation index (Ik), absorption cross section of PSII (sigma), re-opening time of PSII (tau) and regulated and unregulated non-photochemical quenching (NPQ) were assessed during *in situ* acclimation temperature in photosynthesis-irradiance (PI)-curves. For the final harvest, the photo-chemical assays were performed at *in situ* acclimation temperature and additionally at abruptly shifted temperatures. Therefore, triplicate samples from each temperature treatment were incubated for 1 h at the other two acclimation temperatures (2°C → 6°C →9°C, 6°C → 9°C, 9°C → 6°C → 2°C) and measured in the FRRF directly afterwards to assess both, the acclimated state of the cultures as well as the direct thermodynamic effects on physiology.

Membrane-inlet-mass-spectrometry (MIMS) was used to measure O_2 production during light phases and O_2 consumption during dark phases to measure net and gross photosynthesis as well as dark respiration of the phytoplankton communities. For the MIMS measurements, cells were concentrated over a 3 µm polycarbonate filter in a reverse filtration unit and resuspended in 50 mM HEPES sea water medium of pH 8.0 to ensure a stabilized carbonate chemistry during measurement. Measurements were performed in PI-curves of increasing irradiance (0 – 140 µmol photons m^{-2} s^{-1}). At T0, one sample was measured at 2°C. Before the dilution, one pooled sample of each temperature treatment was measured. At the final harvest, each replicate was measured individually at the *in situ* acclimation temperature and directly after an abrupt temperature shift, similar to the photo-chemical assay (2°C → 6°C →9°C, 6°C → 9°C, 9°C → 6°C → 2°C).

Preliminary results

The entire experiment was successful. The incubation set-up of 5 L Schott bottles in temperature-controlled aquaria worked well and could withstand *Polarstern* driving through first-year sea ice including ramming and maximum 1.5 m waves. Also, aerating bottles with fresh air from outside the ship could be installed successfully.

All temperature treatments were kept stable and all phytoplankton cultures showed positive growth rates based on Chl *a* concentration. During the first days, cultures at 6°C acclimation temperature grew the fastest, whereas after the dilution at day 7, the 9°C acclimated cultures grew the fastest. All cultures were dominated by *Phaeocystis pouchetii* at the start of the experiment, whereas the community shifted towards a diatom dominated bloom in all temperature treatments. This trend was faster at higher temperatures and at 2°C *P. pouchetii* was still present at the harvest day.

Photo-chemical assays were not successful at 9°C at the harvest day due to instrument failure. Differences in most photo-chemical parameters between acclimation temperatures as well as abruptly shifted temperatures were apparent.

MIMS assays worked well. For the first time, the instrument itself was used successfully with the cuvette system to measure physiological rates based on O_2 fluxes. First pre-results show a surprisingly stable ratio of gross photosynthesis:respiration (gross PS:Resp) along the three different temperature treatments, even though communities differed between treatments. However, the abrupt temperature shifts showed thermodynamic effects on the gross PS:Resp ratio with a clear stimulation in net PS from 2°C to 6°C and inhibition from 9°C to 6°C and 2°C. The unchanged gross PS:Resp ratio in acclimated cultures irrespective of the actual temperature, however, demonstrates the high potential of phytoplankton to regulate and adjust their physiology to a very similar installation irrespective of acclimation temperature or community composition.

All other parameters will be analysed during the upcoming month in the labs at AWI.

Data management

Environmental data will be archived, published and disseminated according to international standards by the World Data Center PANGAEA Data Publisher for Earth & Environmental Science (https://www.pangaea.de) within two years after the end of the cruise at the latest. By default, the CC-BY license will be applied.

Any other data will be submitted to an appropriate long-term archive that provides unique and stable identifiers for the datasets and allows open online access to the data.

This expedition was supported by the Helmholtz Research Programme “Changing Earth – Sustaining our Future” Topic 6, Subtopic 6.2 and 6.3, Topic 2, Subtopic 2.1.

In all publications based on this expedition, the Grant No. **AWI_PS136_03** will be quoted and the following publication will be cited:

Alfred-Wegener-Institut Helmholtz-Zentrum für Polar- und Meeresforschung (2017) Polar Research and Supply Vessel POLARSTERN Operated by the Alfred-Wegener-Institute. Journal of large-scale research facilities, 3, A119. http://dx.doi.org/10.17815/jlsrf-3-163.

References

Ahme A, von Jackowski A, McPherson RA, Wolf KKE, Hoppmann M, Neuhaus S, John U (2023) Winners and Losers of Atlantification: The Degree of Ocean Warming Affects the Structure of Arctic Microbial Communities. Genes, 14 (3), 623.

Becker S, Aoyama M, Woodward EMS, Bakker K, Coverly S, Mahaffey C, Tanhua T (2020) GO-SHIP Repeat Hydrography Nutrient Manual: The precise and accurate determination of dissolved inorganic nutrients in seawater, using continuous flow analysis methods. Frontiers in Marine Science, 7, 581790. https://doi.org/10.3389/fmars.2020.581790

Cooley S, Schoeman D, Bopp L, Boyd P, Donner S, Ito S, Kiessling W, Martinetto P, Ojea E, Racault MF (2022) Oceans and coastal ecosystems and their services. IPCC AR6 WGII: Cambridge University Press.

Falkowski P, Scholes RJ, Boyle E, Canadell J, Canfield D, Elser J, Gruber N, Hibbard K, Högberg P, Linder S, et al. (2000) The Global Carbon Cycle: A Test of Our Knowledge of Earth as a System. Science, 290 (5490), 291-296.

Field CB, Behrenfeld MJ, Randerson JT, Falkowski P. (1998) Primary Production of the Biosphere: Integrating Terrestrial and Oceanic Components. Science, 281 (5374), 237-240.

Guillard R, Ryther J (1962) f/2 medium: Retrieved from National Center for Marine Algae and Microbiota (NCMA)

Hobday AJ, Alexander LV, Perkins SE, Smale DA, Straub SC, Oliver EC, Benthuysen JA, Burrows MT, Donat MG, Feng M. (2016) A hierarchical approach to defining marine heatwaves. Progress in Oceanography, 141, 227-238.

Hydes DJ, Aoyama M, Aminot A, Bakker K, Becker S, Coverly S, Daniel A, Dickson AG, Grosso O, Kerouel R, van Ooijen J, Sato K, Tanhua T, Woodward EMS, Zhang JZ (2010) Determination of dissolved nutrients (N, P, Si) in seawater with high precision and inter-comparability using gas-segmented continuous flow analysers. GO-SHIP Repeat Hydrography Manual: A collection of expert reports and guidelines. IOCCP report #14, ICPO Publications series no. 134, Version 1.

Knap A, Michaels A, Close A, Ducklow H, Dickson A (1996) Protocols for the joint global ocean flux study (JGOFS) core measurements. JGOFS, Reprint of the IOC Manuals and Guides No. 29, UNESCO 1994 19.

Langdon C (2010) Determination of dissolved oxygen in seawater by Winkler titration using the amperometric technique. GO-SHIP Repeat Hydrography Manual: A collection of expert reports and guidelines. IOCCP report #14, ICPO Publications series no. 134, Version 1.

Sakamoto CM, Johnson KS, Coletti LJ (2009) Improved Algorithm for the Computation of Nitrate Concentrations in Seawater using an in situ Ultraviolet Spectrophotometer. Limnology and Oceanography: Methods, 7, 132-143

6. PHYSICAL OCEANOGRAPHY

Rebecca McPherson[1], Emelie Breunig[2];
not on board: Wilken-Jon von Appen[1]

[1]DE.AWI
[2]DE.Uni Hamburg

Grant No. AWI_PS136_04

Objectives

The physical conditions which lead to enhanced primary and export production in the Arctic Ocean remain unclear. And with both rapid increases in ocean temperatures amplified in the Arctic region and sea ice retreat of the past two decades, the connection between these physical changes and the effects on polar marine ecosystem only increases in importance.

The recirculation of Atlantic Water (AW) in the Fram Strait controls how much of the warm nutrient-rich AW flowing northward in the West Spitsbergen Current (WSC) enters the Arctic Ocean. This determines the oceanic heat input and therefore the extent of the partially ice-free halocline formation area north of Svalbard. The inflow also impacts the light and nutrient distribution in the Arctic and therefore habitat distribution and biogeography in the Arctic Ocean as well as their future evolution. The monitoring programme of the AW inflow into the Arctic via the West Spitsbergen Current started in 1997. Expedition PS136 contributed to maintaining this long- standing time series observatory, as the AW inflow conditions drive the changing physical (and also biogeochemical and biological) properties of the Arctic Ocean.

The intermittent presence of sea-ice and meltwater impacts both the physical and biochemical vertical structure of the water column but also limits *in situ* observations to summer months, when the ice has retreated. The effects of changes in the environmental conditions on the polar marine biodiversity can only be detected through long-term observation of the species and processes. The Frontiers in Arctic Marine Monitoring (FRAM) Helmholtz infrastructure initiative has increased the ability to observe the temporal evolution of the coupled physical-chemical-biological system in the upper water column and throughout the water column to the seafloor.

The HAUSGARTEN observatory includes CTD/Rosette Water Sampler stations in the Atlantic-influenced West Spitsbergen Current towards the East of the Fram Strait, in the Arctic-influenced East Greenland Current to the West, and in the transition regions in the central and northern parts of the region. The FRAM observatory includes moored year-round observations for sensor data and sample collection in representative stations of those contrasting water masses. These observations span the whole water column with an emphasis on the upper euphotic zone. Continuing these interdisciplinary time series allows for the evaluation of interannual variations in addition to shorter-term interactions on mesoscale to seasonal timescales. The large range and combination of sensors that the moorings are equipped with (details below) enable these temporal changes to be related to the observed changes in physical, chemical and biological structure in the Fram Strait.

Two main multidisciplinary time series locations were pursued in the framework of FRAM and its continuation: the F4 site at 1,000 m water depth in the inflowing Atlantic Water boundary current (WSC) and the EG-I site at 1,000 m water depth in the outflowing Polar Water boundary current (East Greenland Current) (Fig. 6.1). By being embedded in very different water masses

representing end points of Arctic conditions, they allow for a better prediction of what conditions and changes are to be expected in the future Arctic Ocean.

Work at sea

The cruise covered a large number of working areas over the duration of PS136 (Fig. 6.1).

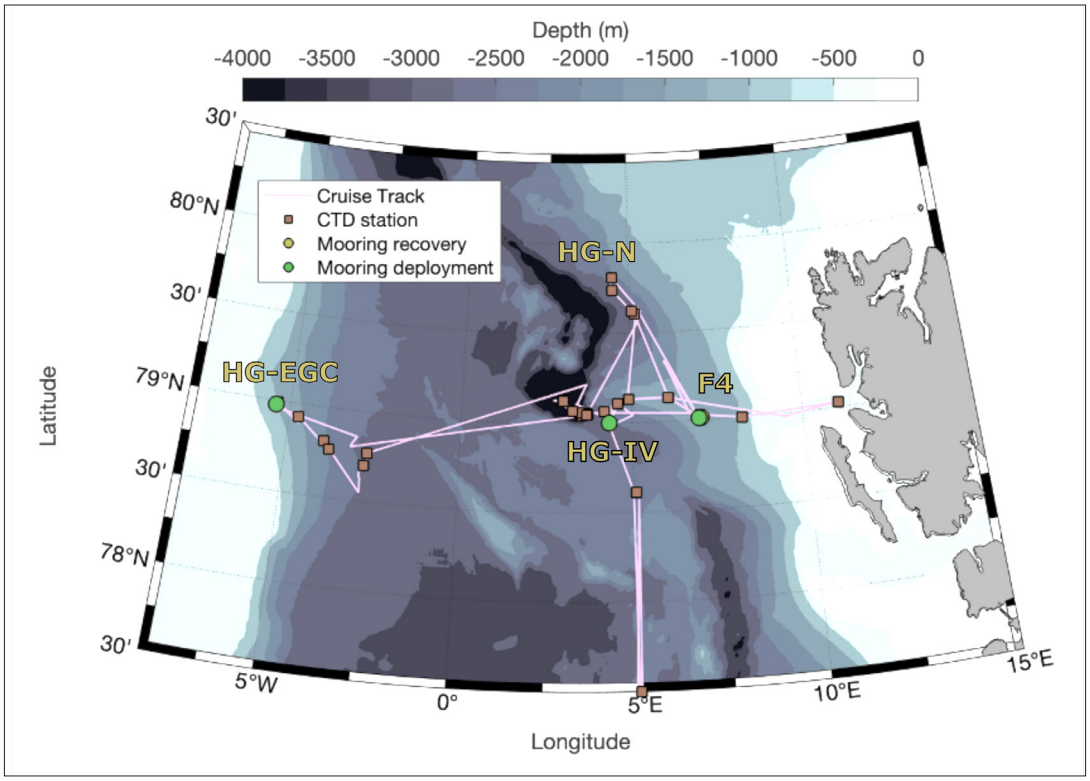

Fig. 6.1: Map of the Fram Strait and HAUSGARTEN region with ship track (pink), CTD stations (orange), mooring recoveries (yellow) and deployments (green) from PS136. Names of each cluster of the repeat stations are in yellow.

CTD

Hydrographic measurements during the *Polarstern* cruise PS136 were conducted using a CTD (conductivity, temperature, and depth sensor, Fig. 6.2 c). The sensors and a Rosette Water Sampler were provided by the physical oceanography group from DE.AWI ("OZE rosette"). The standard sensor configuration of the CTD system throughout the cruise consisted of two temperature sensors, two conductivity cells, a pressure sensor, two oxygen sensors, one fluorescence sensor, a transmissometer, and a photosynthetically active radiation (PAR) sensor, see Table 6.2 for more details.

A total of 34 CTD profiles were conducted in the Fram Strait (Fig. 6.1) at the standard LTER HAUSGARTEN stations. Details of each are provided in Table 6.1. These included both full water column profiles and profiles of solely the upper 100 m to focus on the physical and biogeochemical processes found there. A SUNA which measured nitrogen was also mounted to the frame of the CTD for shallow casts (< 2,000 m water depth), and an attached Underwater Vision Profiler (UVP) operated during all casts.

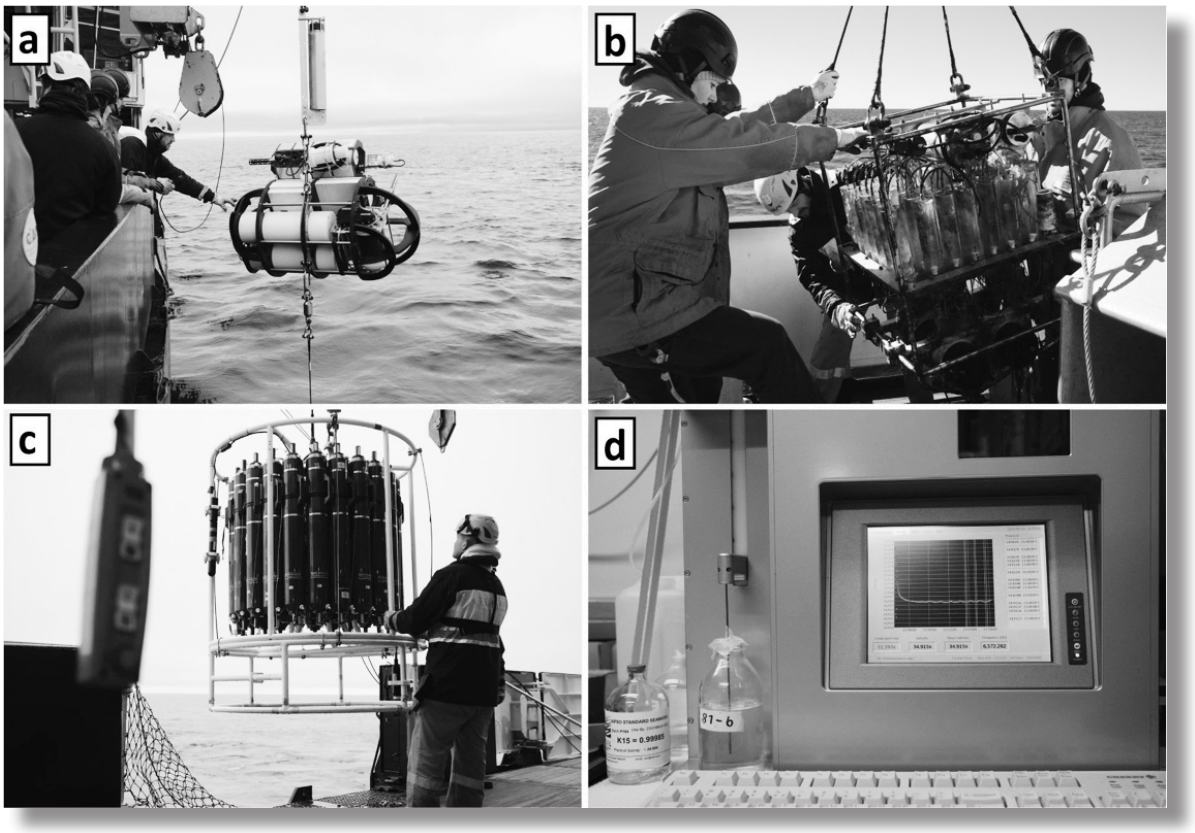

Fig. 6.2: Photographs showing (a) the deployment of the winch atop mooring F4-W3 from PS126, (b) the recovery of a RAS from mooring F4S-6, (c) the deployment of the CTD and (d) the Salinometer which was used to measure the salinity of water collected by the CTD and thus calibrate the instrument's conductivity sensors (photo credit: Mario Hoppmann)

The CTD sonde was mounted in a Rosette Water Sampler with 24 bottles (12 litres each) for water sampling (Fig. 6.2 c). Water samples were taken during all scientific profiles. The Niskin bottles were fired on the upcast, after waiting for 60 s at each target depth for both, sampling the 'true' ambient water mass, and also allowing for lagging sensors to adjust. The resulting water samples were mainly used for filtrations and chemical measurements, and for calibrating the salinity and oxygen observations. Results from on-board salinometry are presented in the subsequent section.

One Niskin bottle (#4) did not fire after the third CTD cast for the remainder of the cruise, though there were no other issues with any of the other bottles. The central release mechanism that controls the firing of the bottles was removed and replaced from the other CTD/Rosette Water Sampler on board, though the issue remained (though now bottle #10 did not close). The first release mechanism was then cleaned and greased thoroughly, and remounted. This appeared to solve the problem and all bottles fired successfully after three test runs.

Tab. 6.1: List of CTD stations during PS136 and details of each station.

Station	Date (DD/MM/YY)	Time (UTC)	Latitude	Longitude	CTD depth [m]	Water depth [m]
PS136_2-1	27/05/2023	02:32	69° 59.958’ N	003° 48.698’ E	994	3252
PS136_3-1	28/05/2023	05:31	75° 00.191’ N	005° 06.158’ E	1000	3162
PS136_4-2	29/05/2023	01:48	78° 36.586’ N	005° 04.084’ E	1500	2325
PS136_4-9	29/05/2023	10:00	78° 36.673’ N	005° 04.576’ E	100	2326
PS136_5-1	30/05/2023	09:07	79° 03.850’ N	004° 11.548’ E	101	2447
PS136_7-1	31/05/2023	21:25	79° 06.414’ N	004° 35.843’ E	100	1894
PS136_8-1	01/06/2023	02:54	79° 59.555’ N	004° 18.625’ E	2571	2618
PS136_9-1	01/06/2023	19:24	79° 06.496’ N	004° 35,408’ E	800	1828
PS136_1-1	01/06/2023	23:25	79° 07.835’ N	004° 55,110’ E	100	1523
PS136_11-1	02/06/2023	09:25	79° 08.053’ N	006° 05.610’ E	1240	1273
PS136_11-12	03/06/2023	04:25	79° 08.036’ N	006° 05.231’ E	100	1272
PS136_12-3	03/06/2023	14:35	79° 01.750’ N	006° 59.858’ E	100	1296
PS136_13-1	03/06/2023	20:55	79° 00.005’ N	008° 13.516’ E	750	916
PS136_14-1	04/06/2023	06:30	79° 01.670’ N	011° 04,656’ E	100	286
PS136_14-5	04/06/2023	08:18	79° 01.690’ N	011° 04.662’ E	270	287
PS136_17-1	05/06/2023	02:33	79° 36.402’ N	005° 09.106’ E	100	2775
PS136_17-8	05/06/2023	12:29	79° 37.391’ N	005° 04.470’ E	800	2792
PS136_18-1	05/06/2023	16:12	79° 44.328’ N	004° 28.300’ E	100	2613
PS136_18-11	06/06/2023	06:27	79° 48.595’ N	004° 28,168’ E	1500	2280
PS136_23-1	07/06/2023	22:10	79° 03.448’ N	003° 39.848’ E	100	2147
PS136_23-5	07/06/2023	23:37	79° 02.942’ N	003° 42.089’ E	10	2866
PS136_24-1	08/06/2023	05:32	79° 02.531’ N	003° 32.773’ E	800	3581
PS136_25-1	08/06/2023	14:52	79° 03.598’ N	003° 26.645’ E	100	4091
PS136_27-1	09/08/2023	09:50	79° 07,693’ N	002° 57,958’ E	101	5521
PS136_27-9	09/06/2023	16:14	79° 07,363’ N	002° 58,261’ E	1500	5510
PS136_28-1	10/06/2023	10:15	79° 04,064’ N	003° 15,480’ E	100	5177
PS136_30-1	11/06/2023	07:48	78° 46,267’ N	002° 38,722’ W	100	2618
PS136_30-7	11/06/2023	13:33	78° 42,595’ N	002° 41,155’ W	1500	2620
PS136_31-1	12/06/2023	06:16	78° 48,754’ N	003° 54,922’ W	100	1963
PS136_31-7	12/06/2023	11:32	78° 46,344’ N	003° 45,516’ W	800	2047
PS136_32-1	12/06/2023	22:56	78° 55,672’ N	004° 43,492’ W	100	1476
PS136_33-1	13/06/2023	08:36	78° 59,422’ N	005° 23,248’ W	100	1021
PS136_33-9	13/06/2023	16:50	78° 58,412’ N	005° 25,492’ W	932	938
PS136_35-1	15/06/2023	02:34	79° 02,716’ N	003° 40,912’ E	1000	2897

While no sensors were changed throughout the cruise, it was noted in the first week that the fluorometer entered into the default configuration setup was the wrong sensor. The serial numbers between the instrument mounted on the CTD frame and that in the software did not match. This was discovered after an unusual fluorometer profile was obtained during the initial test cast. The calibration coefficients for the correct sensor were obtained and the configuration updated after the second cast. The wrong sensor serial number was 7239, and the correct sensor was 1670. All other sensor serial numbers were double checked after this and there were no further issues. This was noted in the protocol.

After the configuration change, the CTD/Rosette Water Sampler was operated with the same sensor configuration throughout the entire duration of the expedition (Tab. 6.2). No major problems with any of the sensors were encountered. During the final CTD cast, an offset in oxygen was observed on the upcast after a calibration stop at 800 m water depth. After flushing the sensors afterwards, the sensor offset returned to near-zero. The behaviour of the temperature and salinity sensors was monitored by taking differences between the values of primary and secondary sensors (secondary minus primary). In general, both temperature and conductivity sensor pairs performed well.

Tab. 6.2: CTD/Rosette Water Sampler configuration. This includes only the correct serial number for the Fluorometer.

	Type	**Serial Number**
CTD sonde	SBE9+	SN 0485
CTD sensors:		
Temperature	SBE3+	Primary sensor: SN 2460
		Secondary sensor: SN 2417
Conductivity	SBE4	Primary sensor: SN 2055
		Secondary sensor: SN 2054
Altimeter	Benthos PSA-916	SN 1228
Oxygen	SBE43	Primary sensor: SN 0880
		Secondary sensor: SN 4016
Transmissiometer	WET Labs C-Star	SN 814
Fluorometer	WET Labs ECO-AFL/FL	SN 1670

Optimare Precision Salinometer measurements

In order to evaluate the drift and offset of the conductivity measurements using the CTD, a total of 24 water samples were collected from the Niskin bottles attached to the CTD. These samples were analysed using an Optimare Precision Salinometer (OPS) (Fig. 6.2 d). Table 6.3 displays the results of the conductivity measurements using the OPS (SalOPS) along with a comparison to the values obtained by both the primary and secondary CTD oxygen sensors (Sal 00 and Sal 01, respectively; Tab. 6.3). The mean difference and standard deviation between the OPS measurements and the CTD oxygen sensors is also calculated.

Tab. 6.3: Salinity samples overview. Displayed are the CTD station number, the number of the Niskin bottle from which the water was sampled, both CTD sensors and OPS measurements, and the calculated differences between the CTD and OPS measurements are also included.

Station	Date	Niskin #	Depth [m]	Sal00	Sal01	SalOPS	Sal00 - SalOPS	Sal01 - SalOPS
PS136_4-2	29/05/2023	7	810	349.049	349.065	349.056	-0.0007	0.0009
PS136_4-2	29/05/2023	7	810	349.049	349.065	349.051	-0.0002	0.0014
PS136_4-2	29/05/2023	1	1215	349.067	349.081	349.070	-0.0003	0.0011
PS136_4-2	29/05/2023	1	1215	349.067	349.081	349.064	0.0003	0.0017
PS136_8-1	01/06/2023	1	2614	349.205	349.214	349.195	0.0010	0.0019
PS136_8-1	01/06/2023	1	2614	349.205	349.214	349.195	0.0010	0.0019
PS136_8-1	01/06/2023	2	1216	349.092	349.109	349.084	0.0008	0.0025
PS136_8-1	01/06/2023	2	1216	349.092	349.109	34.9089	0.0003	0.0002
PS136_8-1	01/06/2023	9	810	349.045	349.064	349.046	-0.0001	0.0018
PS136_8-1	01/06/2023	9	810	349.045	349.064	349.048	-0.0003	0.0016
PS136_11-1	02/06/2023	1	1216	349.061	349.072	349.060	0.0001	0.0012
PS136_11-1	02/06/2023	1	1216	349.061	349.072	349.063	-0.0002	0.0009
PS136_11-1	02/06/2023	2	1012	349.052	349.065	349.052	0.0000	0.0013
PS136_11-1	02/06/2023	2	1012	349.052	349.065	349.045	0.0007	0.0020
PS136_18-11	06/06/2023	3	1216	349.077	349.088	349.068	0.0009	0.0020
PS136_18-11	06/06/2023	3	1216	349.077	349.088	349.065	0.0012	0.0023
PS136_18-11	06/06/2023	8	810	349.038	349.046	348.984	0.0054	0.0062
PS136_18-11	06/06/2023	8	810	349.038	349.046	349.007	0.0031	0.0039
PS136_33-9	13/06/2023	5	810	348.740	348.748	347.137	0.1603	0.1611
PS136_33-9	13/06/2023	5	810	348.740	348.748	347.112	0.1628	0.1636
PS136_33-9	13/06/2023	1	912	348.796	348.799	347.223	0.1573	0.1576
PS136_33-9	13/06/2023	1	912	348.796	348.799	347.169	0.1627	0.1630
PS136_33-9	13/06/2023	9	606	348.623	348.631	347.002	0.1621	0.1629
PS136_33-9	13/06/2023	9	606	348.623	348.631	346.973	0.1650	0.1658
						mean	0.0410	0.0420
						std	0.0712	0.0710

Underway measurements

During PS136, standard oceanographic underway measurements by means of a thermosalinograph (TSG) with a double sensor configuration, as well as a vessel-mounted ADCP (VMADCP), were continuously recorded. The TSG data were validated using water samples taken from the keel water inlet, which were later analysed using the OPS lab salinometer.

Moorings

- Recoveries:

During expedition PS136, a total of three moorings were recovered in the central HAUSGARTEN area (Fig. 6.1; Tab. 6.4). All of these moorings were deployed in summer 2022 during PS131 so were in the water and sampling for one year. A total of 34 instruments (hydrographic and biological) were recovered without major complications or instrument loss. There was little to no sea ice at the three central HAUSGARTEN mooring stations and the sea state was generally very calm. Thus, the conditions were ideal for mooring recovery.

A fourth mooring (HG-EGC-8) was planned to be recovered during PS136. However, due to thick (over 2 m) and dense sea ice cover at the western station, this recovery was not possible. A helicopter surveyed the surrounding area and found there to be no nearby gaps in the sea ice that could be used for the recovery. This mooring shall be recovered next year during PS143, if conditions allow. There are no foreseen problems to the instrumentation with leaving it in the water for another year, as the acoustic releasers have a minimum of a 3-year battery life.

Upon recovery, there were some line entanglements towards the bottom of the mooring HG-IV-FEVI44. This was due to little wind which kept the ship and floats relatively stationary and allowed the loose line to rise into itself. This did not damage the instruments, merely slowed down the recovery process.

The winch and profiler on mooring F4-W4 (Fig. 6.1 a) were recovered by Zodiac, having been released separately to the bottom part of the mooring. The second part, on which the BioOptical Platform was mounted, was recovered the usual way over the side of the ship. The recovered winch system on mooring F4-W4 did not appear to have worked over the 1-year deployment. It appears that the release mechanism of the profiler had stuck and the winch mechanism itself, upon sensing the excess loose line in the water, had automatically stopped. This, however, remains speculation at this moment. Further tests need to be conducted to determine the exact reason.

All hydrographic instrumentation and the ADCP that were downloaded onboard after recovery appeared to have sampled continuously over the 1-year deployment period. There were no problems detected with battery life or programming.

- Deployments:

A total of three moorings were redeployed on PS136 (Tab. 6.4) with generally minor modifications in the placement of sensors, particularly in the upper 50 m to better resolve the physical and biological structure of the upper water column.

Though mooring HG-EGC-8 was not recovered, the mooring HG-EGC-9 was still deployed. A new position was determined after consultation with relevant colleagues who concluded a slightly more westerly position would still capture the water masses of interest. A large enough hole in the ice was found approximately half a nautical mile west of the HG-EGC-8 coordinates, and the new mooring, HG-EGC-9, was successfully deployed (Tab. 6.4).

Pre-deployment, some technical issues were identified with the software of the winch and profiler system that were to be deployed on mooring F4W-5. These problems could not easily be resolved onboard thus it was decided not to deploy this mooring. The BioOptical Platform that was to be deployed on mooring F4W-5 was then inserted into mooring F4S-7 at the relevant depth, i.e. F4S-7 and F4W-5 were merged as one mooring (Fig. 6.3). Minor modifications were required to ensure the other instrumentation on mooring F4S-7 remained at the designated depths, and the deployment went smoothly. The sea state was generally very calm throughout the deployments and, apart from the thick ice cover at mooring site HG-EGC, there was little to no sea ice at each station.

Tab. 6.4: List of moorings recovered and deployed during PS136

For further information see the end of the chapter.

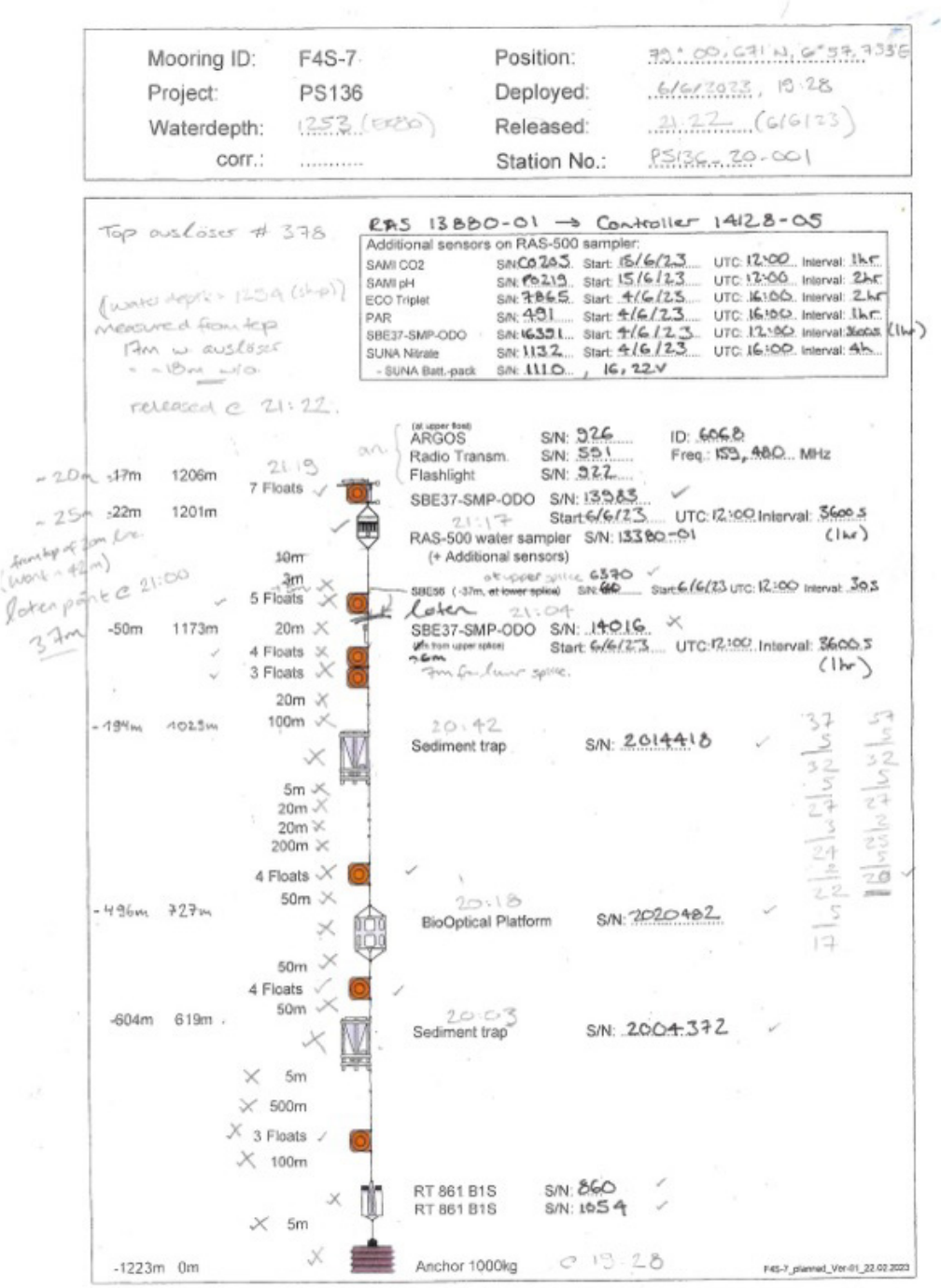

Fig. 6.3: The mooring diagram and protocol for the deployed mooring F4S-7; this shows the inclusion of the BioOptical Platform that was inserted from FSW-5

Preliminary (expected) results

CTD

The CTD casts sampled the different water masses in the central Fram Strait (Fig. 6.4 a). To the East of the strait, the warm and saline Atlantic Water flows northwards as the West Spitzbergen Current (Fig. 6.4 b, c). Maximum near-surface temperatures of over 4°C are found along the continental shelf break of Svalbard (Fig. 6.4 b). Moving westwards towards Greenland, this warm Atlantic water is then found below the cold (< 0°C) and fresh surface Polar Water that flows southwards from the Central Arctic Ocean.

In the upper 100 m of the water column, a layer of peak chlorophyll was found at 20 m towards the Greenland continental shelf (Fig. 6.4. d). These peaks generally occurred when sea-ice was present in the region, in the marginal ice zone. Surface-intensified chlorophyll was also found at the central HAUSGARTEN stations. These peaks of chlorophyll generally coincided with areas of increased oxygen (Fig. 6.4 e). Oxygen levels were surface-intensified, with higher values found in the western part of the Fram Strait where the Polar Water was identified.

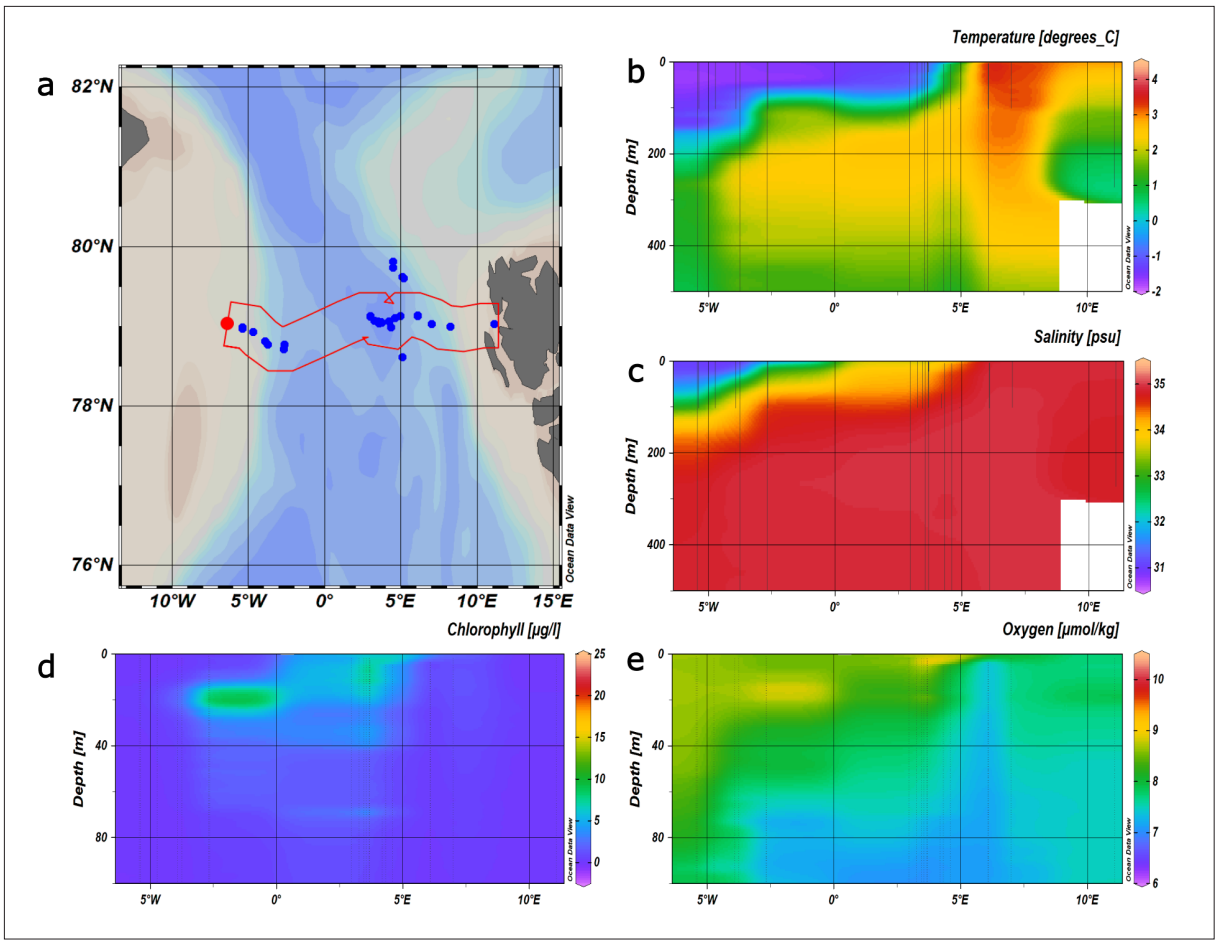

Fig. 6.4: A transect of hydrographic properties in the upper water column across the Fram Strait. (a) The CTD stations (blue) and the longitudinal transect (red), (b) temperature, (c) salinity, (d) chlorophyll, (e) oxygen. Note that (d) and (e) have a different vertical scale to (b) and (c). The properties have been interpolated between each profile across the transect

Salinometer

The conductivity measurements using the OPS salinometer were carried out with the water sampled from the CTD/Rosette Water Sampler. The analysis generally proceeded without any major complications.

A mean difference between the OPS and the primary and secondary CTD conductivity sensors was calculated as 0.0410 and 0.0420, respectively (Tab. 6.3). This difference resulted primarily from the last eight measurements when the OPS measurements started to deviate more strongly from the CTD salinity sample values. The deviations were likely a result of a particle stuck in the OPS system and the instrument was flushed several times to mediate this. By excluding the last eight measurements, the difference between the OPS and the primary conductivity sensor reduces to 0.00028 and 0.0017 for the secondary sensor.

The last eight measurements are therefore excluded from the following analysis. A linear regression between the CTD salinity sensors and the OPS measurements was performed and shown in Figure 6.5. Both CTD sensors showed a high agreement with the OPS values with $R^2 > 0.99$, though the secondary CTD salinity sensor features slightly smaller deviations from the OPS measurements.

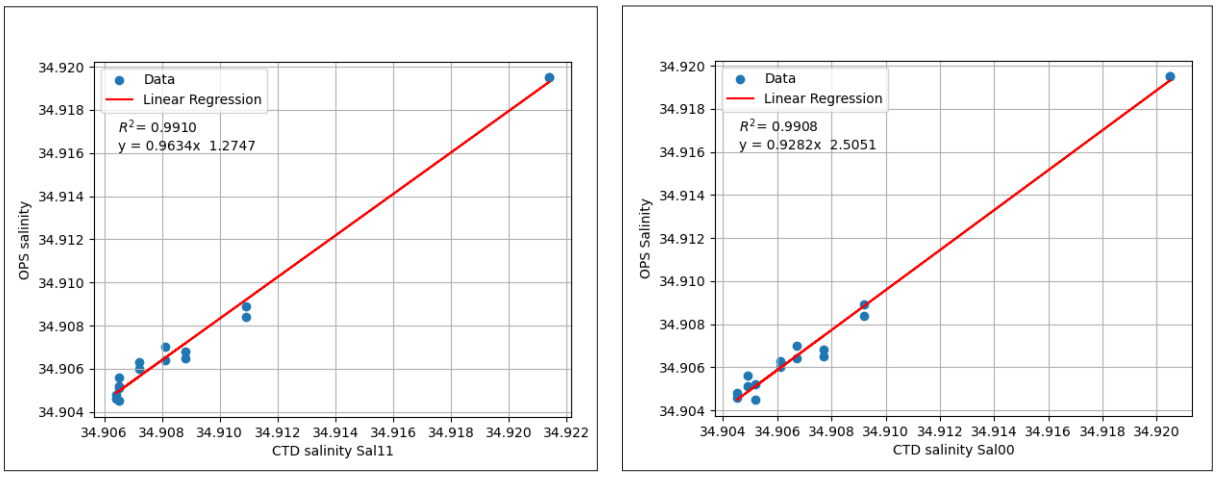

Fig. 6.5: Linear regression fit between OPS lab measurements and primary (left), secondary (right) CTD sensor data excluding the last eight measurements, which featured major deviations

Moorings

The physical sensors on the moorings all performed as planned, but they have not been analysed in detail and put into the interannual context.

A long-term timeseries of near-surface temperatures in the West Spitzbergen Current can be determined using the upper instruments of the F3 and F4 moorings. The timeseries from 1997 to 2023 shows the seasonal, interannual and decadal changes in the Atlantic Water temperatures (Fig. 6.6). This preliminary analysis highlights the strong seasonal cycle observed in the WSC with peak temperatures in summer, and pronounced interannual variability. Further analysis will examine the changes in the mixed layer, and link the variability of the stratification to the primary production in the region.

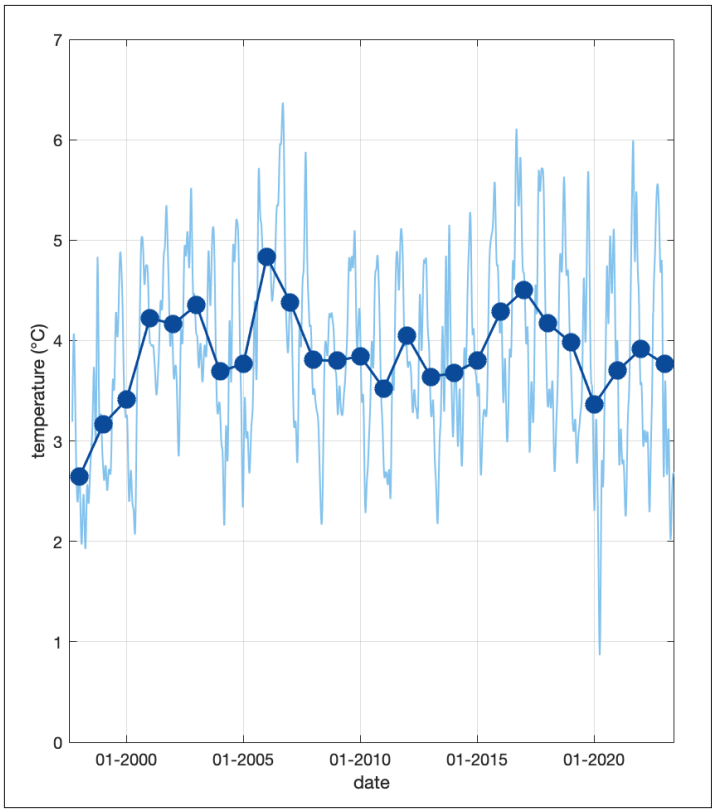

Fig. 6.6: Near-surface temperatures of the West Spitsbergen Current from 1997 to 2023. The thin lines are monthly means and the dots are the yearly mean (defined from June – July of the following year). Temperatures are taken from mooring locations F3 and F4 (Fig. 6.1)

Data management

Upon return to shore, the raw data collected on PS136 will be archived at the World Data Center PANGAEA Data Publisher for Earth & Environmental Science (https://www.pangaea.de). The CTD casts will be processed within a year and the processed data set of full casts and measurements at the bottle stops will be archived at PANGAEA. The physical measurements on the moorings (temperature, salinity, velocity) will be processed within a year and then archived at PANGAEA.

This expedition was supported by the Helmholtz Research Programme “Changing Earth – Sustaining our Future” Topic 2, Subtopic 2.3.

In all publications based on this expedition, the Grant No. **AWI_PS136_03** will be quoted andthe following publication will be cited:

Alfred-Wegener-Institut Helmholtz-Zentrum für Polar- und Meeresforschung (2017) Polar Research and Supply Vessel POLARSTERN Operated by the Alfred-Wegener-Institute. Journal of large-scale research facilities, 3, A119. http://dx.doi.org/10.17815/jlsrf-3-163.

Tab. 6.4: List of moorings

Name	Longitude			Latitude			Depth	Top	Deployment time (UTC)						Recovery time (UTC)						Deployment Station	Recovery Station
	Degrees	Minutes		Degrees	Minutes		Meters	Meters	Year	Month	Day	Hour	Minute		Year	Month	Day	Hour	Minute			
Recoveries																						
FEVI-44	4	19.94	E	78	59.99	N	2568	38	2022	7	9	15	26		2023	5	31	10	30		PS131_3-1	PS136_6-3
F4-S-6	6	57.76	E	79	0.67	N	1231	16	2022	7	10	8	13		2023	6	3	12	19		PS131_34-1	PS136_13-2
F4-W-4	7	1,95	E	79	0.73	N	1249	132	2022	7	7	12	9		2023	6	3	10	52		PS131_16-1	PS136_12-1
Deployments																						
F4-S-7	6	57.75	E	79	00.67	N	1253	20	2023	6	6	21	22								PS136_2-1	
FEVI-46	4	19.77	E	78	59,95	N	2599	39	2023	6	1	9	20								PS136_8-2	
HG-EGC-9	5	25,09	W	78	59.34	N	979	48	2023	6	13	16	4								PS136_33-7	

7. PHYTOOPTICS

Hongyan Xi[1], Gianluca Volpe[2];
not on board: Astrid Bracher[1,3,]
Sonja Wiegmann[1], Zhiyong Xie[4]

[1]DE.AWI
[2]IT.ISMAR
[3]DE.UNI-HB
[4]DE.HZH

Grant-No. AWI_PS136_04

Outline

Ocean colour remote sensing allows for estimating the overall phytoplankton biomass (indicated by chlorophyll *a* concentration, Chl *a*), distinctive major groups (abbreviated as phytoplankton functional types, PFT), and coloured dissolved organic matter (CDOM) at global and high temporal (daily) scales not met by discrete sampling during the expedition. However, at high latitudes, ocean colour satellite data has sparse coverage due to the presence of sea ice, clouds and low sun elevation. To complement remote sensing data, underway spectrophotometry and hyperspectral radiometry enables to obtain attenuation and absorption data which can be further processed to Chl *a* and marker pigment concentrations, PFT Chl *a* and CDOM (Liu et al. 2018, 2019; Bracher et al. 2020) at high sampling resolution for the surface waters crossed during the entire cruise and for the underwater light profile at the CTD stations. However, the derivation of these final biogeochemical products requires the verification with direct analysis of these parameters on regularly sampled discrete water in order to quantify the potential and limitations in terms of uncertainties of these optically derived biogeochemical parameters. In conjunction with satellite data (e.g. products from Losa et al. 2017; Xi et al. 2020, 2021; Oelker et al. 2022) these discrete and continuously sampled data sets are of high value to upscale biogeochemical or phytoplankton quantities at higher resolution and better coverage. In addition, these data serve for validating ocean colour products from the Sentinel-3 OLCI and the Sentinel-5P TROPOMI sensors. The groups of A. Bracher and G. Volpe are part of the Sentinel-3 Validation Team and PIs of the ESA study Sentinel-5P Ocean Colour. Overall, data collected during *Polarstern* cruise PS136 provides a fundamental contribution for further development of hyper- and multispectral ocean colour satellite retrievals focusing on fluorescence and absorption signals.

The main focus is to process these different optical data sets by verification with phytoplankton group data derived from collocated HPLC measurements to determine the amount and composition of phytoplankton throughout the water column along the cruise transect. In addition, also the absorption by other particles and coloured dissolved organic matter (CDOM), the reflectance and diffuse attenuation of the underwater light from the UV to the NIR are determined. The data sets will be used to develop, improve further and validate ocean colour retrievals and data products from the two Copernicus satellite missions Sentinel-3 and -5. These data sets are used to assess trends and variability of phytoplankton and its composition over the last 25 years (e.g. Xi et al. 2023). Our long-term observations have already revealed important patterns of spatio-temporal distributional patterns and changes in plankton diversity. Our results clearly indicate, for instance, that Chl *a* values increase in summer in the eastern but not in the western Fram Strait (Nöthig et al. 2015, 2020; Engel et al. 2019). This is in

accordance with the increasing contributions of nanoflagellates to the summer phytoplankton community (see also Xi et al. 2023). The optical expedition data set is further used to upscale information of these components on three-dimensional scale resolved for the cruise transect timing and area.

Objectives

During *Polarstern* expedition PS136, we focused to broaden our sampling frequency of information on phytoplankton, particulate and chromophoric dissolved organic matter (CDOM) abundance and composition by taking continuous optical measurements which directly give information on inherent and apparent optical properties (IOPs and AOPs, respectively). Specific objectives were to

- to collect a high spatial and temporal resolved data set on phytoplankton (total and composition) and its degradation products at the surface and at selected stations for the full euphotic zone using continuous optical observations during the cruise and from ocean colour remote sensing calibrated with discrete water sample measurements,
- to develop and validate (global and regional) algorithms and associated radiative transfer models in accordance to the previous objective by using discrete water samples for pigment analysis and absorption measurement,
- to obtain a big data set for ground-truthing ocean colour satellite data, specifically from the new Sentinel-3 (A and B) OLCI and the Sentinel-5-Precursor TROPOMI sensors,
- to obtain a spectral characterisation of the underwater light field and its interplay with optical constituents, such as phytoplankton and CDOM abundance and composition.

Work at sea

Measurements and sample collections for a large variety of parameters were accomplished in accordance to the PEBCAO-team at 19 stations of the LTER observatory HAUSGARTEN during PS136, including the frontal zone separating the warm and cold-water masses originating from the West Spitsbergen Current and the East Greenland Current. Measurements and sampling comprised CTD/Rosette Water Sampler casts, underway spectrophotometry and backscattering with AC-s and eco-VSF, respectively, and the deployment of the optical package with RAMSES, AC-s, and eco-VSF (Tabs 7.1-3).

Phytoplankton pigments, particulate matter absorption (PAB) and coloured dissolved organic matter (CDOM)

At the HAUSGARTEN permanent sampling sites we deployed our optical profiler (profiling system to measure the optical properties vertically) integrated with an *in situ* spectrophotometer (AC-S; WETlabs), TRIOS RAMSES sensors (for light downwelling irradiance, Ed, and upwelling radiance, Lu), a pressure sensor, a datalogger and battery (Fig. 7.1). They were operated out of the shade mostly just before or after (shallow) CTD stations (see Chapter 4; Tab. 4.1). The frame was lowered to maximal 150 m with a continuous speed of 0.1 m/s or during daylight with additionally stops at 2, 5, 8, 10, 15, 20, 25, and 30 m to allow a better collection of radiometric data. On the monkey deck another RAMSES Ed sensor for irradiance in the air was also mounted and measured during the stations. The Apparent Optical Properties of water (AOPs) (mostly light attenuation through the water column) was estimated based on downwelling and upwelling irradiance measurements in the surface water profile (down to the 0.1% light depth) from the radiometers calibrated for the incident sunlight with measurements of a radiometer on deck and directly from the radiance and irradiance above water radiometry.

The AC-S measured the inherent optical properties (IOPs: total attenuation, scattering and absorption) in the water profile.

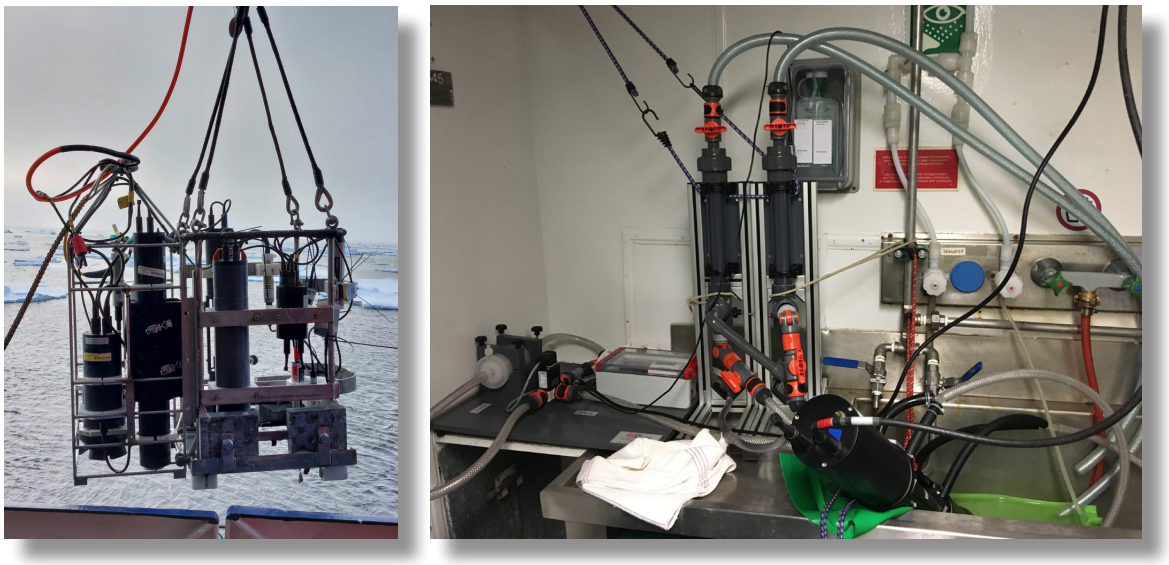

Fig. 7.1: Left: Underwater light field measurements with TRIOS RAMSES radiometers detecting the hyperspectral up- and downwelling radiation, WETLABS AC-s (including pressure sensor, data logger and battery) measuring extinction and absorption and eco-VSF (incl. own CTD and connected via cable) measuring the backscattering at four wavelengths within the surface water profile.

Right: Continuous measurements of the extinction and absorption of light in Arctic surface waters using a WETLABS AC-s mounted to the Polarstern surface seawater pump system. From those measurements directly, the absorption and scattering of particles and CDOM is determined for the whole spectrum in the visible resolved with about 3 nm resolution. This data then can be decomposed various specific algorithms to determine the particle size distribution and the various phytoplankton pigment composition.

In addition, we sampled arctic seawater with the CTD/Rosette Water Sampler at the main HAUSGARTEN stations at five depths from surface to 100 m for further filtration in the laboratory to have HPLC samples and measured the filters and filtered sea water samples to obtain the absorption spectra of total particulates, phytoplankton and CDOM (Tabs 7.1-3, details below).

Laboratory work on board

- Continuous optical measurements:

Continuous inherent optical properties (IOPs) with a hyperspectral spectrophotometer: For the continuous underway surface sampling another AC-S was operated in flow-through mode to obtain total and particulate matter attenuation and absorption of surface water. The instrument is mounted to a seawater supply taking surface ocean water (Fig. 7.1). A flow-control with a time-programmed filter is mounted to the AC-S to allow alternating measurements of the total and the CDOM inherent optical properties of the seawater. Flow-control and debubbler-system ensure that water flows through the instrument with no air bubbles.

- Discrete surface seawater sampling (underway surface sampling):

Surface waters were sampled from the seawater pump on *Polarstern* with an interval of three hours to have a full coverage of the surface water samples along the whole cruise track. Water samples from both CTD stations (Tab. 7.1) and underway stations (Tab. 7.2) were filtered in the laboratory to take the following samples and measurement: (1) HPLC phytoplankton pigment samples (pore size 0.7 µm filtered pads were immediately stored onboard in the -80°C freezer); (2) particle and phytoplankton absorption spectra (ap, ad, and aph) obtained by measuring a second set of filtered pads for each sample; and (3) CDOM absorption spectra obtained by measuring the filtered water samples with 0.2 µm pore size filters.

Tab. 7.1: List of date, time, sample depth of the Phytooptics Group discrete water samples at CTD Stations (*unclear station numbers) and corresponding light stations during PS136.

FRAM name	CTD-Station	Corresponding light Station	UTC Date	Time (at max depth)	Sampled Depth [m]
HG-I	PS136_11-1*	PS136_11-2	03/06/2023	04:22:00	10,17,25,50,100
HG-II	PS136_10-2	PS136_10-3	01/06/2023	23:25:59	10,38,45,50,100
HG-III	PS136_4-1	PS136_9-2	31/05/2023	21:24:34	10,23,35,50,100
HG-IV	PS136_5-1	PS136_5-3	30/05/2023	09:07:03	5,10,25,50,100
HG-V	PS136_23-1	PS136_23-4	07/06/2023	22:09:02	5,20,40,50,100
HG-VI	PS136_24-1	PS136_24-3	08/06/2023	05:31:08	10,20,35,50,75
HG-VII	PS136_25-1	PS136_25-4	07/06/2023	22:09:02	3,12,25,50,100
HG-VIII	PS136_26-8*	PS136_26-1	10/06/2023	10:15:23	10,15,25,50,100
HG-IX	PS136_27-1	PS136_27-4	09/06/2023	09:49:41	10,15,30,50,100
S3	PS136_4-9	PS136_4-8	29/05/2023	10:00:41	10,25,34,50,100
N3	PS136_17-1	PS136_17-2	05/06/2023	02:33:13	5,16,25,50,100
N4	PS136_18-3	PS136_18-1	05/06/2023	16:08:26	10,30,40,50,100
SV-I	PS136_14-3	PS136_14-4	04/06/2023	06:30:30	10,30,40,50,100
SV-II	UW65	PS136_15-2	08/06/2023	00:27:45	10,25,40,50,100
SV-III	PS136_13-1	PS136_13-5	03/06/2023	20:53:34	5,15,22,50,100
SV-IV	PS136_12-3	PS136_12-6	03/06/2023	14:33:54	10,18,30,50,100
EG-I	PS136_33-1	PS136_33-4	13/06/2023	08:34:44	10,20,40,50,100
EG-II	PS136_32-1*	None	12/06/2023	22:54:09	10,25,35,50,100
EG-III	PS136_31-1	PS136_31-4	12/06/2023	06:14:43	10,40,50,100
EG-IV	PS136_30-1	PS136_30-2	11/06/2023	07:48:10	10,20,30,50,100

Tab. 7.2: List of the Phytooptics Group discrete water sample analysis for phytoplankton pigments (analysed at AWI with HPLC), determination of CDOM (analysed with LWCC on board), particulate and phytoplankton absorption (analysed with QFT-ICAM on board) at underway stations (sampled from seawater supply pumped from 9 m depth) at given date, time, latitude and longitude during PS136.

Sample ID	Date UTC	Time UTC Start	Time UTC End	Latitude [°]	Longitude [°]
1	23/05/2023	14:59:50	15:04:00	56.96	5.52
2	23/05/2023	17:05:20	17:08:00	57.27	5.32
3	23/05/2023	19:59:50	20:01:25	57.69	5.04
4	23/05/2023	23:03:10	23:04:53	58.16	4.73
5	24/05/2023	02:00:15	02:02:03	58.51	4.45
6	24/05/2023	05:27:50	05:30:00	59.02	4.20
7	24/05/2023	08:02:00	08:06:50	59.42	4.17
8	24/05/2023	12:00:00	12:02:15	59.98	4.17
9	24/05/2023	14:02:00	14:04:30	60.28	4.17
10	24/05/2023	17:01:40	17:03:05	60.73	4.11
11	24/05/2023	19:41:00	19:42:50	61.14	4.08
12	24/05/2023	22:55:00	22:56:54	61.64	4.14
13	25/05/2023	01:54:10	01:55:55	62.08	4.17
14	25/05/2023	05:51:20	05:53:10	62.68	4.17
15	25/05/2023	08:08:40	08:12:40	63.04	4.30
16	25/05/2023	13:13:30	13:16:00	63.77	4.24
17	25/05/2023	15:09:00	15:10:30	64.03	4.18
18	25/05/2023	16:56:00	16:57:30	64.31	4.10
19	25/05/2023	19:59:05	20:01:00	64.75	3.99
20	25/05/2023	22:50:00	22:52:00	65.20	3.86
21	26/05/2023	02:03:10	02:04:48	65.72	3.72
22	26/05/2023	05:07:25	05:08:45	66.18	3.59
23	26/05/2023	08:00:50	08:02:35	66.65	3.51
24	26/05/2023	11:01:00	11:03:00	67.23	3.57
25	26/05/2023	14:30:40	14:32:10	67.87	3.64
26	26/05/2023	17:06:20	17:08:00	68.34	3.67
27	26/05/2023	19:56:03	19:58:00	68.87	3.73
28	26/05/2023	22:53:00	22:54:40	69.41	3.77
29	27/05/2023	02:10:03	02:11:36	70.00	3.83
30	27/05/2023	04:56:40	04:58:20	70.15	3.83
31	27/05/2023	08:05:26	08:07:20	70.79	3.92
32	27/05/2023	11:02:40	11:04:30	71.38	4.00
33	27/05/2023	13:56:00	13:58:27	71.75	4.06
34	27/05/2023	16:56:36	16:58:20	72.37	4.22
35	27/05/2023	19:48:40	19:52:00	72.98	4.41
36	27/05/2023	22:53:28	22:55:15	73.63	4.61

Sample ID	Date UTC	Time UTC Start	Time UTC End	Latitude [°]	Longitude [°]
37	28/05/2023	02:02:23	02:03:45	74.29	4.84
38	28/05/2023	05:17:20	05:19:00	75.00	5.10
39	28/05/2023	07:53:20	07:54:25	75.23	5.10
40	28/05/2023	11:12:52	11:14:20	75.87	5.10
41	28/05/2023	14:04:05	14:06:00	76.44	5.09
42	28/05/2023	17:12:15	17:14:10	77.06	5.08
43	28/05/2023	19:57:20	19:59:23	77.60	5.08
44	28/05/2023	23:01:56	23:03:50	78.21	5.07
45	29/05/2023	02:00:28	02:02:01	78.61	5.07
46	29/05/2023	05:17:38	05:19:50	78.61	5.07
47	29/05/2023	08:07:50	08:09:20	78.61	5.07
48	29/05/2023	16:59:01	17:00:10	78.62	5.13
49	29/05/2023	22:57:38	22:59:00	78.62	5.14
50	30/05/2023	05:14:34	05:16:06	78.61	4.98
51	30/05/2023	07:53:00	07:54:26	79.00	4.34
52	30/05/2023	14:12:40	14:14:00	79.08	4.25
53	30/05/2023	23:33:18	23:34:30	79.07	4.16
54	31/05/2023	05:36:54	05:38:30	79.03	4.30
55	31/05/2023	14:02:50	14:02:20	79.05	4.22
56	31/05/2023	20:53:50	20:55:00	79.09	4.56
57	01/07/2023	05:20:14	05:21:48	78.99	4.31
58	01/07/2023	13:06:02	13:07:35	79.03	4.33
59	01/07/2023	18:44:30	18:47:55	79.08	4.39
60	01/07/2023	23:24:25	23:27:00	79.13	4.92
61	02/06/2023	08:03:30	08:07:00	79.05	5.14
62	02/06/2023	13:20:00	13:22:00	79.14	6.08
63	03/06/2023	08:20:10	08:22:47	79.10	6.38
64	03/06/2023	20:15:58	20:18:20	79.00	7.90
65	04/06/2023	15:51:25	15:53:41	78.98	9.51
66	04/06/2023	23:03:19	23:06:20	79.17	6.04
67	05/06/2023	15:27:00	15:31:00	79.73	4.56
68	05/06/2023	23:02:07	23:05:07	79.76	4.43
69	06/06/2023	11:11:54	11:14:25	79.63	5.33
70	06/06/2023	15:56:55	15:59:15	79.47	5.59
71	06/06/2023	22:59:06	23:02:00	79.23	6.25
72	07/06/2023	06:53:05	06:55:55	79.02	6.78
73	07/06/2023	11:09:00	11:11:40	79.02	6.82
74	07/06/2023	15:34:25	15:36:40	79.25	6.22
75	07/06/2023	21:02:35	21:05:00	79.09	4.07
76	08/06/2023	12:58:12	13:02:00	79.03	3.57
77	08/06/2023	23:04:03	23:07:00	79.04	3.52

Sample ID	Date UTC	Time UTC Start	Time UTC End	Latitude [°]	Longitude [°]
78	09/06/2023	04:41:20	04:45:00	79.07	3.32
79	09/06/2023	17:02:45	17:05:10	79.12	2.99
80	09/06/2023	22:51:40	22:54:30	79.13	2.94
81	10/06/2023	08:23:11	08:25:25	79.12	2.82
82	10/06/2023	14:15:30	14:18:30	79.10	3.39
83	10/06/2023	17:18:40	17:21:10	79.11	3.21
84	10/06/2023	22:36:10	22:38:20	78.87	1.32
85	11/06/2023	01:59:05	02:01:05	78.87	-0.51
86	11/06/2023	06:05:30	06:07:00	78.82	-2.55
87	11/06/2023	17:34:25	17:37:00	78.66	-2.82
88	11/06/2023	22:55:25	22:58:18	78.58	-2.76
89	12/06/2023	02:09:59	02:12:37	78.68	-2.90
90	12/06/2023	13:58:00	14:01:10	78.86	-3.37
91	12/06/2023	21:05:35	21:09:00	79.00	-4.13
92	13/06/2023	05:10:10	05:13:20	78.94	-5.04
93	13/06/2023	20:03:35	20:08:00	78.96	-5.42
94	13/06/2023	22:56:27	22:59:16	78.95	-4.93
95	14/06/2023	01:49:53	01:53:14	78.93	-3.90
96	14/06/2023	05:21:00	05:23:40	78.85	-3.00
97	14/06/2023	11:16:50	11:20:20	78.79	-2.80
98	14/06/2023	15:08:40	15:11:30	78.83	-1.88
99	14/06/2023	17:31:00	17:33:40	78.82	-0.77
100	14/06/2023	21:05:10	21:09:00	78.78	0.84
101	14/06/2023	22:47:35	22:50:10	78.82	1.59
102	15/06/2023	01:56:47	01:59:28	79.02	3.60
103	15/06/2023	06:23:15	06:25:50	79.14	4.52
104	15/06/2023	08:50:30	08:52:55	79.30	5.29
105	15/06/2023	12:08:45	12:11:10	79.57	5.26
106	15/06/2023	18:03:30	18:05:58	79.43	5.04
107	15/06/2023	20:22:25	20:24:30	79.22	5.02
108	15/06/2023	23:58:40	23:01:55	79.05	4.28
109	16/06/2023	01:56:46	01:59:17	79.11	3.61
110	16/06/2023	08:26:45	08:29:00	79.10	3.43
111	16/06/2023	11:28:00	11:31:02	79.15	3.96
112	16/06/2023	14:18:55	14:20:20	79.18	5.45
113	16/06/2023	17:04:35	17:08:00	78.79	6.51
114	16/06/2023	20:14:40	20:17:15	78.15	6.23
115	16/06/2023	22:50:06	22:52:36	77.61	6.45
116	17/06/2023	02:00:00	02:02:31	76.95	6.85
117	17/06/2023	06:00:35	06:03:15	76.17	7.28
118	17/06/2023	10:15:45	10:19:30	75.90	7.91

Preliminary results

Phytoplankton pigments, particulate matter absorption (PAB) and coloured dissolved organic matter (CDOM)

The continuously measured optical data are used via using semi-analytical techniques to determine the spectrally resolved underwater light attenuation and the concentration of optical constituents, such as Chl *a* concentration, CDOM absorption and particle backscattering, but also for validating satellite ocean colour retrievals following formerly established procedures for HAUSGARTEN cruises PS93.2, PS99, and PS107 (see Liu et al. 2018; 2019). We expect this new data set for our long-term measurements to elucidate further changes in the Fram Strait pelagic environment due to Global Change and/or other environmental shifts.

So far, we have obtained the following measurements/data (see Table 7.3):

- Underway flow-through measurements:
  - 26-day (23rd May – 17th June 2023) non-stop total and particulate absorption/attenuation measurements of surface water from AC-S during ship transect
- Discrete samples (underway samples):
  - HPLC pigments: 94 samples from CTDs, 118 samples from Underway (will be analysed at AWI)
  - Particulate, CDOM and phytoplankton absorption: 94 samples from CTDs,
  - 118 samples from underway
- Station work from RAMSES + ACS + eco-ESF profiler mostly down to 150 m (HG-VI, HG-VII, and HG-VIII only down to 50 m, EG-III and EG-IV only down to 30 m):
  - 19 valid RAMSES underwater hyperspectral radiance and irradiance profiles
  - 19 valid ACS profiles for the total absorption
  - 16 eco-VSF (with own CTD) profiles for the back-scattering coefficient at four wavelengths. First seven stations (only four successful deployments) after RAMSES + ACS profiler, last 12 stations with RAMSES + ACS profiler on the same frame

Tab. 7.3: Bio-optical parameters sampled at PS136 stations. HPLC: Phytoplankton pigments by High Pressure Liquid Chromatography; CDOM: Coloured Dissolved Organic Matter absorption by LWCC; PAB: Particulate and phytoplankton absorption; RAMSES: hyperspectral upwelling and downwelling radiation in the water; ACS: hyperspectral total absorption and attenuation in the water (* only surface water sample was taken).

FRAM name	HPLC	PAB	CDOM	ACS-profile	RAMSES	Eco-VSF-profile
HG-I	x	x	x	x	x	x
HG-II	x	x	x	x	x	x
HG-III	x	x	x	x	x	x
HG-IV	x	x	x	x	x	x
HG-V	x	x	x	x	x	x
HG-VI	x	x	x	x	x	x
HG-VII	x	x	x	x	x	x

FRAM name	HPLC	PAB	CDOM	ACS-profile	RAMSES	Eco-VSF-profile
HG-VIII	UW78*	UW78*	UW78*	x	x	x
HG-IX	x	x	x	x	x	x
S3	x	x	x	x	x	x
N3	x	x	x	x	x	x
N4	x	x	x	x	x	x
SV-I	x	x	x	x	x	x
SV-II	x	x	x	x	x	x
SV-III	x	x	x	x	x	x
SV-IV	x	x	x	x	x	x
EG-I	x	x	x	x	x	x
EG-II	x	x	x			
EG-III	x	x	x	x	x	x
EG-IV	x	x	x	x	x	x

On board we were able to already analyse the ICAM data. We have obtained some first results on the Chl *a* concentration (Fig. 7.2) for the underway surface water and the CTD samples. Results show that for most of the HAUSGARTEN stations the highest Chl *a* concentrations were found in the first 30 to 50 m and then decreased with the depth. Highest Chl *a* concentrations (3.7 - 4.7 mg Chl *a* m^{-3}) were found for stations HG-IV, SV-IV, N4, and EG-IV as compared to the other stations. The underway Chl *a* concentrations (Fig. 7.3) show that along the cruise track we see well the extension of the central HAUSGARTEN area surface water phytoplankton bloom (max. ~ 5 mg Chl *a* m^{-3}) extending to the area around the N stations (max. ~ 7 mg m^{-3}), and another bloom at the western part of the East Greenland (max. ~ 4 mg m^{-3}) current probably as well in the zone of the marginal ice zone. Chl *a* was probably have encountered a few phytoplankton bloom areas around 65°N, the central Fram Strait and also between 77-78°N. In addition, we show the results of underway CDOM absorption at 440 nm which is a good indicator of DOM in the Arctic Ocean (see Chapter 4; Fig. 4.12). It shows that the CDOM concentrations were abundant in the North Sea and then decreased when the latitude is above 66°N. In the eastern Fram Strait the CDOM was at low to moderate level but was high in the western Fram Strait where the Arctic current dominates, indicating that Arctic waters contain more DOM compared to north Atlantic waters. These results are comparable to the historical data collected in the same season, and can be used to investigate seasonality and time series change in optical properties, CDOM, and phytoplankton composition structure by combining the data from previous Fram Strait cruises.

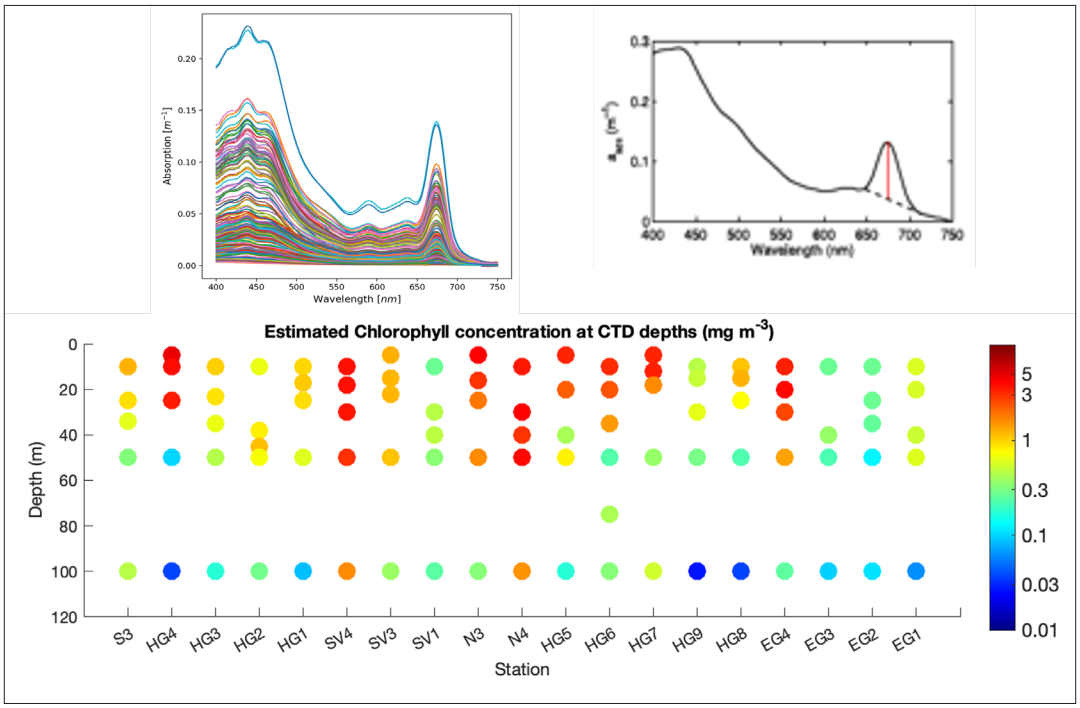

Fig. 7.2: Chl a concentrations in the upper 100 m of the water column at PS136 CTD stations (lower panel) estimated using the absorption peak line height method (Roesler and Barnard 2013; Liu et al. 2018; upper panel right) from the QFT-ICAM measured particulate absorption spectra (upper panel left)

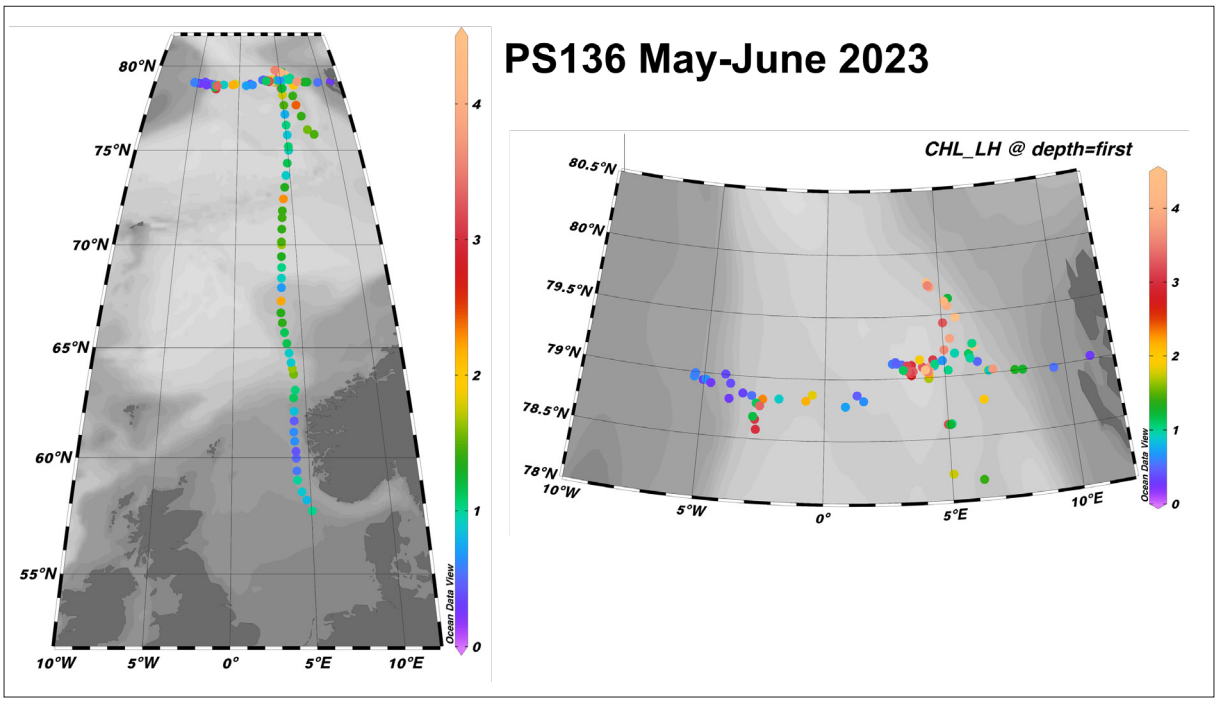

Fig. 7.3: Surface Chl a concentrations (mg/m³) from PS136 underway particulate absorption data measured by the QFT-ICAM on board on water samples using the absorption peak line height method (Roesler and Barnard 2013; Liu et al. 2018).
Left: results for the entire expedition transect, right: detailed map of Fram Strait region

Data management

Many of the samples will be processed and further analysed at AWI within approximately one year after the cruise. We plan that the full data set will be available at latest about 2-3 years after the cruise. Data will be made available to the public via PANGAEA (https://www.pangaea.de) in accordance with current institute data policies. AC-S data are foreseen to be uploaded to the FRAM data portal as raw data immediately after the cruise and as calibrated data set after carefully executing quality controls and calibrations with discrete water sample measurements.

This expedition was supported by the Helmholtz Research Programme “Changing Earth–Sustaining our Future” Topic 6, Subtopic 6.3 and additional funding by Copernicus Marine Service GLOPHYTS project.

In all publications, based on this cruise, the Grant No. **AWI_PS136_04** will be quoted and the following *Polarstern* article will be cited:

Alfred-Wegener-Institut Helmholtz-Zentrum für Polar- und Meeresforschung. (2017). Polar Research and Supply Vessel POLARSTERN Operated by the Alfred-Wegener-Institute. Journal of large-scale research facilities, 3, A119. http://dx.doi.org/10.17815/jlsrf-3-163.

References

Bracher A, Xi H, Dinter T, Mangin A, Strass VH, von Appen WJ, Wiegmann S (2020) High resolution water column phytoplankton composition across the Atlantic Ocean from ship-towed vertical undulating radiometry. Frontiers in Marine Science, 7, 235.

Engel A, Bracher A, Dinter T, Endres S, Grosse J, Metfies K, Peeken I, Piontek J, Salter I, Nöthig E.-M (2019) Inter-annual variability of organic carbon concentrations across the Fram Strait (Arctic Ocean) during summer 2009 -2017. Frontiers in Marine Science, 6, 187.

Liu Y, Roettgers R, Ramírez-Pérez M, Dinter T, Steinmetz F, Noethig EM, Hellmann S, Wiegmann S, Bracher A (2018) Underway spectrophotometry in the Fram Strait (European Arctic Ocean): a highly resolved chlorophyll *a* data source for complementing satellite ocean color. Optics Express, 26 (14), A678-A698.

Liu Y, Boss E, Chase AP, Xi H, Zhang X, Röttgers R, Pan Y, Bracher A (2019) Retrieval of phytoplankton pigments from underway spectrophotometry in the Fram Strait. Remote Sensing, 11, 318.

Losa S, Soppa MA, Dinter T, Wolanin A, Brewin RJW, Bricaud A, Oelker J, Peeken I, Gentili B, Rozanov VV, Bracher A (2017) Synergistic exploitation of hyper- and multispectral precursor Sentinel measurements to determine Phytoplankton Functional Types at best spatial and temporal resolution (SynSenPFT). Frontiers in Marine Science, 4, 203.

Nöthig EM, Bracher A, Engel A, Metfies K, Niehoff B, Peeken I, et al. (2015) Summertime plankton ecology in Fram Strait - a compilation of long- and short-term observations. Polar Research, 34. https://doi.org/10.3402/polar.v34.23349

Nöthig EM, Ramondenc S, Haas A, Hehemann L, Walter A, Bracher A, et al. (2020) Summertime chlorophyll a and particulate organic carbon standing stocks in surface waters of the Fram Strait and the Arctic Ocean (1991–2015). Front. Mar. Sci., 7, 350. https://doi.org/10.3389/fmars.2020.00350

Oelker J, Losa SN, Richter A, Bracher A (2022) TROPOMI-retrieved underwater light attenuation in three spectral regions in the ultraviolet to blue. Frontiers in Marine Science, 9, 787992. https://doi.org/10.3389/fmars.2022.787992

Roesler S, Barnard AH (2013) Optical proxy for phytoplankton biomass in the absence of photophysiology: Rethinking the absorption line height, Methods in Oceanography, 7, 79-94.

Xi H, Losa SN, Mangin A, Soppa MA, Garnesson P, Demaria J, Liu Y, Fanton d'Andon O, Bracher A (2020) Global retrieval of phytoplankton functional types based on empirical orthogonal functions using CMEMS GlobColour merged products and further extension to OLCI data. Remote Sensing of Environment, 240, 111704.

Xi H, Losa SN, Mangin A, Garnesson P, Bretagnon M, Demaria J, Soppa MA, Fanton d'Andon O, Bracher A (2021) Global chlorophyll a concentrations of phytoplankton functional types with detailed uncertainty assessment using multisensor ocean color and sea surface temperature satellite products. Journal of Geophysical Research: Oceans, 126, e2020JC017127.

Xi H, Bretagnon M, Losa SN, Brotas V, Gomes M, Peeken I, Alvarado LMA, Mangin A, Bracher A (2023) Two-decade satellite monitoring of surface phytoplankton functional types in the Atlantic Ocean, State of the Planet, accepted.

8. FRAM POLLUTION OBSERVATORY – MONITORING LITTER AND MICROPLASTIC AT HAUSGARTEN

Alexandra Aves[1];
not on board: Deonie Allen[1], Melanie Bergmann[2], Steve Allen[3],

[1]NZ.UCANT
[2]DE.AWI
[3]UK.STRATH

Grant-No. AWI_PS136_01

Outline

Marine litter or marine debris has long been on the political and public agenda as it has been recognized as a rising pollution problem affecting all oceans and coastal areas of the world and more than 1,300 species (Bergmann et al. 2017a). Over time, larger plastic litter items fragment into smaller particles termed “microplastics” (< 5 mm), which have recently received increasing attention (Ryan 2015) as they can be taken up more readily by a wider range of biota and humans.

Analysis of seafloor photographs (Fig. 8.1) taken for the epibenthic megafauna time series at three stations of the HAUSGARTEN observatory indicate that litter increased almost 30-fold between 2004 and 2017 at the northernmost station and reached densities similar to those reported from a canyon near the Portuguese capital Lisbon (Parga Martínez et al. 2020). This increase has prompted a focused study on litter and microplastic pollution in different ecosystem compartments and repeated sampling campaigns to observe temporal trends.

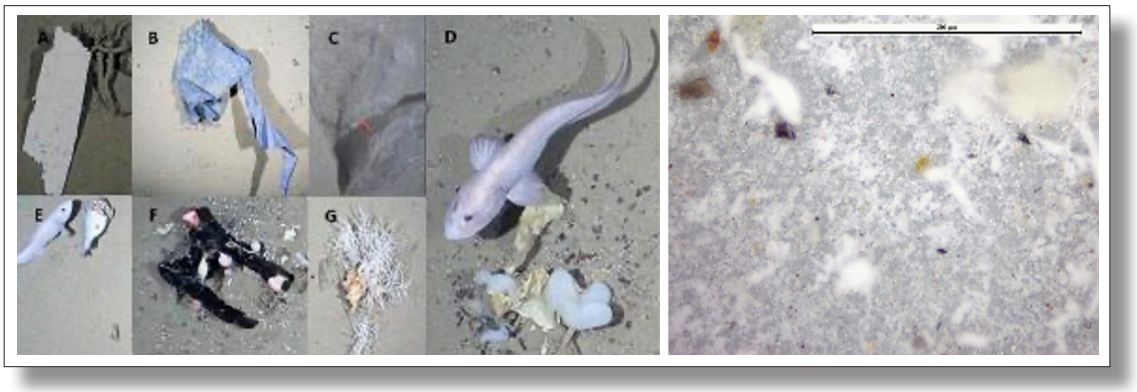

Fig. 8.1: Examples of marine litter and faunal interactions photographed by OFOS at HAUSGARTEN observatory (from Parga-Martinez et al. 2020) and atmospheric microplastics (from Allen et al. 2019)

This research has highlighted that Arctic sea ice, sea surface, water column; and deep-sea sediments harbour high levels of microplastic pollution, especially the seafloor, with up to ~ 13,000 microplastics per kg sediment at the northernmost station (Bergmann et al. 2017b; Peeken et al. 2018; Tekman et al. 2020). Plastic has also invaded the Arctic food web (Trevail

et al. 2015; Kühn et al. 2018) including sea ice-associated zooplankton (Botterell et al. 2022). Significant quantities of microplastic in Arctic snow samples indicate that atmospheric transport plays an important role (Bergmann et al. 2019). Recent data even suggest that the sea surface acts as a source of airborne microplastic (Allen et al. 2020). Still, on the whole, the role and processes of atmospheric transport of microplastics have not yet received the merited scientific attention although they are considered to play a key role (Zhang et al. 2020).

Objectives

Two active air sampling devices were fitted to the crow's nest to quantify airborne microplastic pollution. A low-volume air sampler which directly filters onto a glass fibre filter was run for 3-day time steps, alongside a nano-tank sampling device which was used to trap smaller nano-sized microplastics in an ethanol/MilliQ solution and run for 24-hour time steps. The transit from Bremerhaven to the HAUSGARTEN area is of particular interest to delineate large-scale pollution patterns and transport processes. In addition, passive air deposition samples were collected daily (24-hour time steps) throughout the transit and stationary periods of the *Polarstern* voyage. The passive samples were collected using 200 mL MilliQ/ethanol solution placed into a NILU Atmospheric Microplastic Collector System. This was taken to the on-board laboratory of *Polarstern* and filtered through appropriate pre-cleaned filters using glass vacuum filtration devices and the samples (on filter material) will be retained for chemical analysis.

Laboratory work was conducted during periods when no other researchers were in the laboratory to ensure minimum background contamination of the samples. There is very limited marine air sampling published to date (Liu et al. 2019; Wang et al. 2020; Allen et al. 2020, 2022), and this survey will follow the *Polarstern* air sampling campaign on from 2021. In addition, snow, ice, seawater and melt pond samples were gathered during helicopter flights to ice floes to assess atmospheric fallout and general environmental presence of microplastics. This will enable a comprehensive understanding of Arctic microplastics from the atmosphere to the deep sea. The data will complement previous measurements (Bergmann et al. 2019; Bergmann et al. 2023) and will support the ongoing atmospheric transport analysis of microplastic in the high latitude and Arctic marine environment.

Work at sea

Airborne microplastic monitoring

Three collection methods were used for airborne microplastic monitoring: passive deposition, nano-tank sampler and low-volume air sampler (Fig. 8.2). All three samplers were set up on the crow's nest at the top of *Polarstern*, 29 m above sea level. They were visited daily for sample changeover and collection and if anyone else was present the pumps were turned off and the deposition bucket covered until no other movement occurred near samplers. This sampling location also had the most direct and open access to marine air. To account for contamination from the ship, wind direction and ship direction will be considered for each sampling period to note any influences.

The deposition bucket was left uncovered for each 24-hour sampling period, with 200 mL of ethanol/MilliQ solution being placed inside the bucket after sample change over and cleaning. The liquid ensures passive deposition remains inside the bucket without being resuspended. The nano-tank sampler contained 500 mL of ethanol/MilliQ solution, with a pump intake attachment passing air through a liquid to trap smaller nano sized particles. The nano-tank sampler was changed over every 24 hours with an intake of ~ 10 L of air per minute. The low-volume air sampler filtered air directly onto a 47 mm glass fibre filter at ~ 20 L of air per minute and was only changed every three days. These sampling periods are based off

previous, currently unpublished, research. At the end of each sampling period, the nano-tank and deposition contents were filtered onto separate 27 mm glass fibre filters and stored in aluminium tins. The low-volume air sample filters were transferred directly into aluminium storage tins.

Fig. 8.2: Atmospheric sampling setup on the crow's nest of the Polarstern, including low volume air sampler, nano-tank sampler and deposition sampler (from left to right) (photo credit: Alex Aves)

Due to bad weather steaming from the departure of Bremerhaven to the stations and access to the crow's nest, we were unable to set up the monitoring equipment until a week into the cruise. Once the equipment was safely and successfully setup, air pumps were turned on and the deposition tank was opened beginning on 29/05/23. These three sample collection devices ran for 19 days, with 24-hour collection periods, finishing on 17/06/23.

For the duration of the expedition weather and location data were collected from the ship's record, which includes wind velocity and direction as well as ship course and navigational points. This data will enable the calculation of periods of air sampling that arrived at the sample site from the forward quarter of the ship (i.e. uncontaminated by ship or stack activities due to wind direction and strength) as well as information to complete modelling of potential transportation routes of air masses to the sample site.

In total, 19 days of air samples were collected: 19 deposition samples, 19 nano-tank samples and seven low-volume air samples (45 total). Blanks were also collected on three days throughout the sampling period, with nine 9 blanks covering the three collection types taken.

Microplastic ice station monitoring

To develop an understanding of microplastic concentrations in the Arctic; snow, ice core, melt pond and sea water samples were collected from five ice stations (Fig. 8.3). Each station was accessed via helicopter and chosen based on its suitability for sample collection and safety for scientists and landing. Accessing via helicopter ensured contamination was limited from the ship. Snow samples were collected using a metal scoop, funnel and 2 L stainless steel wide mouth bottle, from four sites on each ice floe. Two melt pond samples in 2 L stainless steel wide mouth bottles, and two seawater samples in 2 L stainless steel wide mouth bottles, tied together on a hemp rope, were collected from each ice floe. Ice cores were taken using a 9-cm diameter corer (Kovacs Enterprise, Roseburg, USA), labelled accordingly, and stored in LDPE bags. Two ice cores were taken from each ice floe and have been stored at -20°C until processing back on land. From each ice floe, four snow samples, two seawater, two melt pond and two ice cores were collected (with some exceptions). All floe samples (excl. ice cores) were melted and filtered onto pre-cleaned 47 mm glass fibre filters back in the on-board laboratory and were then stored in aluminium tins at 4°C. In total, ten ice cores were collected (plus one extra for comparison of merged ice) along with 25 snow, melt and seawater samples from the ice floes and 12 blanks to monitor for contamination throughout sampling and filtration.

Fig. 8.3: Snow sampling being undertaken on Arctic ice floe in the HAUSGARTEN area (photo credit: Jack Harding)

Assessment of microplastics in deep-sea organisms

Working with colleagues from the “Senckenberg am Meer” team on board (see Chapter 3), a selection of collected organisms were set aside and stored for microplastic analysis to help understand the potential for microplastic presence in deep-sea organisms, with a focus on filter feeders (Fig. 8.4). Epibenthic Sledge (EBS) hauls were conducted at a total of six sites,

with samples for microplastics being taken at each station from water depths between 1,254 m to 5,414 m. Positioning and CTD measurements were recorded during the trawl. Once the EBS was returned to the surface, contents were sorted into different sample types (epi, epi-U and supra) and then live sorted in a cold room laboratory using a 300 µm sieve. Individual specimens for microplastic research were sorted to phylum level, imaged using a digital camera and then rinsed in a glass petri dish with milli-q before being stored in glass Eppendorf tubes which were placed in a -20°C freezer. Blanks to check for contamination were taken by placing two pre-baked 47 mm glass fibre filters in pre-cleaned aluminium tins, opening them inside the imagery and sorting lab and soaking with milli-q. Echinodermata, Crustacea, Annelida, Chelicerata, Mollusca, Cnidaria, Porifera, Chaetognatha, and vertebrata phyla were all collected, with 105 samples in total collected for microplastic research.

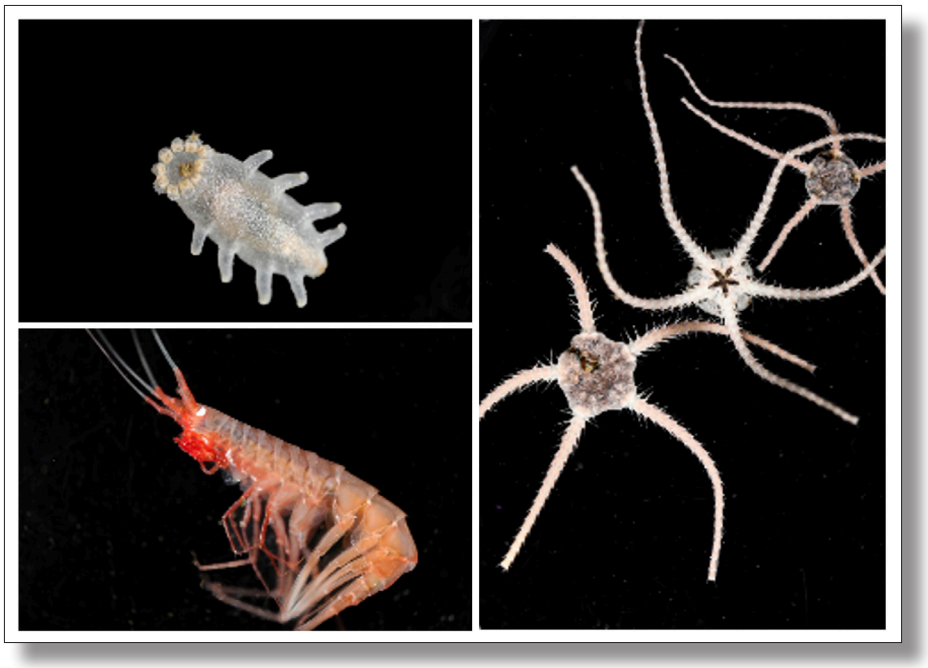

Fig. 8.4: Deep-sea organisms collected from the epibenthic sledge in the HAUSGARTEN (photo credit: Lydia Schmidt)

Preliminary (expected) results

Samples were successfully collected from the Arctic air, water, ice, snow, meltwater and deep sea for microplastic research. As well as the collection of samples onboard, preparation for analysis was also completed, with air, water, snow and meltwater samples filtered and stored ready for chemical identification of particles to understand the microplastic presence in this region. Ice core samples will be processed prior to analysis by shaving off the outside layer of the ice cores to reduce contamination, before being melted down into sections of the core and filtered for chemical analysis. A chemical digestion and analysis method for deep sea organism samples will need to be developed prior to analysis.

Chemical analysis of samples was not able to be completed onboard and planning for analysis of collected samples is underway based on current method developments. Depending on the findings from method development work and the sample type, analysis of samples will either be completed using mass-based quantification or spectroscopic identification. Once microplastic concentrations have been quantified across all environmental samples, modelling to understand the movement of microplastics throughout the environment will be undertaken.

Going forward, our aim is to gain quantitative polymer characterization across the whole range of environmental samples, allowing us to gain detailed insight to the movement, spatial variability, and role microplastics have in the Arctic.

Data management

Environmental data and imagery will be archived, published and disseminated according to international standards by the World Data Center PANGAEA Data Publisher for Earth & Environmental Science (https://www.pangaea.de) within two years after the end of the cruise at the latest. Any other data will be submitted to an appropriate long-term archive that provides unique and stable identifiers for the datasets and allows open online access to the data.

This expedition was supported by the Helmholtz Research Programme “Changing Earth – Sustaining our Future” Topic 6, Subtopic 6.4.

In all publications, based on this cruise, the Grant No. **AWI_ PS136_01** will be quoted and the following publication will be cited:

Alfred-Wegener-Institut Helmholtz-Zentrum für Polar- und Meeresforschung (2017). Polar Research and Supply Vessel POLARSTERN Operated by the Alfred-Wegener-Institute. Journal of large-scale research facilities, 3, A119. http://dx.doi.org/10.17815/jlsrf-3-163.

References

Allen D, Allen S, Abbasi S, Baker A, Bergmann M, Brahney J, Butler T, Duce RA, Eckhardt S, Evangeliou N, Jickells T et al. (2022) Microplastics and nanoplastics in the marine-atmosphere environment. Nature Reviews Earth & Environment, 3 (6), 393-405.

Allen S, Allen D, Moss K, Le Roux G, Phoenix VR, Sonke JE (2020) Examination of the ocean as a source for atmospheric microplastics. PLoS ONE, 15, e0232746.

Allen S, Allen D, Phoenix V, Le Roux G, Durantez Jimenez P, Simonneau A, Binet S, Galop D (2019) Atmospheric transport and deposition of microplastics in a remote mountain catchment. Nature Geosciences, 12, 339-344.

Bergmann M, Allen S, Krumpen T, Allen, D (2023) High Levels of Microplastics in the Arctic Sea Ice Alga Melosira arctica, a Vector to Ice-Associated and Benthic Food Webs. Environmental Science & Technology, 57 (17), 6799-6807.

Bergmann M, Mützel S, Primpke S, Tekman MB, Trachsel J, Gerdts G (2019) White and wonderful? Microplastics prevail in snow from the Alps to the Arctic. Science Advances, 5, eaax1157.

Bergmann M, Tekman MB, Gutow L (2017a) Marine litter: Sea change for plastic pollution. Nature, 544, 297-297.

Bergmann M, Wirzberger V, Krumpen T, Lorenz C, Primpke S, Tekman MB et al. (2017b) High Quantities of Microplastic in Arctic Deep-Sea Sediments from the HAUSGARTEN Observatory. Environmental Science and Technology, 51, 11000–11010.

Botterell ZLR, Bergmann M, Hildebrandt N, Krumpen T, Steinke M, Thompson RC, Lindeque PK (2022) Microplastic ingestion in zooplankton from the Fram Strait in the Arctic. Science of the Total Environment, 831, 154886. doi: 10.1016/j.scitotenv.2022.154886.

Kühn S, Schaafsma FL, van Werven B, Flores H, Bergmann M, Egelkraut-Holtus M et al. (2018) Plastic ingestion by juvenile polar cod (Boreogadus saida) in the Arctic Ocean. Polar Biology, 41, 1269-1278.

Liu K, Wu T, Wang X, Song Z, Zong C, Wei N, Li D (2019) Consistent transport of terrestrial microplastics

to the ocean through atmosphere. Environmental Science and Technology, 53(18), 10612-10619.

Parga Martínez KB, Tekman MB, Bergmann M (2020) Temporal trends in marine litter at three stations of the HAUSGARTEN observatory in the Arctic deep sea. Frontiers in Marine Science, 7.

Peeken I, Primpke S. Beyer B, Gütermann J, Katlein C, Krumpen T et al. (2018) Arctic sea ice is an important temporal sink and means of transport for microplastic. Nature Communications, 9, 1505.

Ryan PG (2015) A Brief History of Marine Litter Research. In: Marine Anthropogenic Litter (eds. Bergmann M, Gutow L, Klages M). Springer Berlin, pp. 1-25.

Tekman MB, Wekerle C, Lorenz C, Primpke S, Hasemann C, Gerdts G et al. (2020) Tying up loose ends of microplastic pollution in the Arctic: Distribution from the sea surface, through the water column to deep-sea sediments at the HAUSGARTEN observatory. Environmental Science and Technology, 54, 4079-4090.

Trevail AM, Gabrielsen GW, Kühn S, Van Franeker JA (2015) Elevated levels of ingested plastic in a high Arctic seabird, the northern fulmar (Fulmarus glacialis). Polar Biology, 38, 975-981.

Wang X, Li C, Liu K, Zhu L, Song Z, Li D (2020) Atmospheric microplastic over the South China Sea and East Indian Ocean: abundance, distribution and source. Journal of Hazardous Materials, 121846

Zhang Y, Kang S, Allen S, Allen D, Gao T, Sillanpää M (2020) Atmospheric microplastics: A review on current status and perspectives. Earth-Science Reviews, 203, 103118.

9. FLUX-ON-SITE – GREENHOUSE GAS FLUXES AT OCEAN-SEA ICE INTERFACES IN THE ARCTIC OCEAN

Marei Pohlmann[1], Archana Sebastian[1];
not on board: Damian L. Arévalo-Martínez[1,2], Hermann W. Bange[1]

[1]DE.GEOMAR
[2]NL.URAD

Grant-No. AWI_PS136_05

Objectives

The Arctic Ocean is exceptionally susceptible to Climate Change. It reacts strongly to greenhouse gases (GHG)-driven warming since sea ice melting increases heat absorption through reduced albedo ("Arctic Amplification"). Hence, GHG observations are crucial to monitor the ocean's state and its role in the production and exchange of climate-relevant compounds with the atmosphere. During FLUX-ON-SITE we investigated the dynamics of the GHGs nitrous oxide (N_2O) and methane (CH_4) across the water column in the Fram Strait sector of the Arctic Ocean, as well the spatial variability of the exchange fluxes of both gases across the sea-ice-air interfaces.

The main foci of the project were (i) the gas exchange across interfaces, (ii) the emissions from the region and their share to the global GHG budget, (iii) the role of sub-mesoscale dynamics in shaping the water column variability of N_2O and CH_4, and (iv) the spatial variability of gas source-sink dynamics in the Fram Strait.

Work at sea

In order to fulfil the overarching goal of the BMBF project PETRA (Pathways and emissions of climate-relevant trace gases in a changing Arctic Ocean), we combined along-track surface and water column discrete sampling along the 79°N transect, which was occupied by our group in 2018, 2019, and 2021.

Along-track discrete sampling in surface waters

Discrete samples for N_2O and CH_4 measurements in surface waters (~ 10 m water depth) were collected in 6 h intervals by collecting water from the ship's seawater distribution system. To this end, bubble-free triplicate samples were collected and immediately sealed by means of butyl stoppers and aluminium crimps. Subsequently 50 µL of a saturated mercuric chloride ($HgCl_2$) solution were added. The samples will be analysed by means of a gas chromatographic setup at the Chemical Oceanography department of GEOMAR.

Water column sampling

The sampling for N_2O and CH_4 measurements was carried out in conjunction with nutrient concentrations and other biogeochemical measurements by drawing water directly from 10 L Niskin bottles mounted on a standard CTD/Rosette Water Sampler. Glass vials of 20 mL were used and the samples were treated as explained above and will be analysed at GEOMAR.

The sampling scheme consisted in full coverage of the main features from the surface until approx. 1,000 m water depth. Figure 9.1 shows an overview of the sampling locations during the cruise.

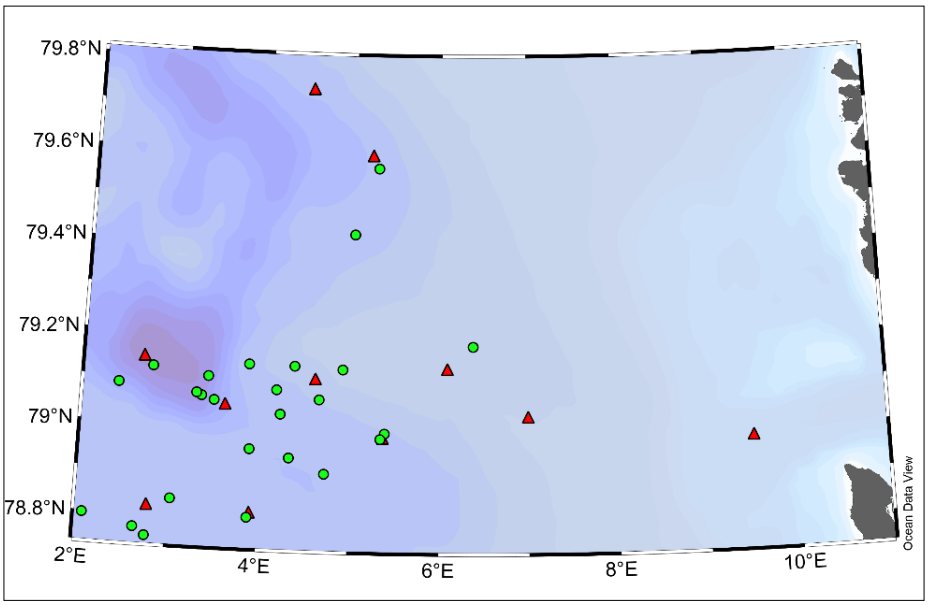

Fig. 9.1: Sampling locations for trace gases during PS136. The red triangles indicate CTD/Rosette Water Sampler stations and the green dots indicate along-track sampling conducted in surface waters.

Preliminary (expected) results

The field work conducted during the PS136 cruise will allow quantifying N_2O and CH_4 sea-ice-fluxes along spatially variable gradients within relatively small areas. Moreover, we expect to resolve significant physically-driven changes in the basin-wide distribution of N_2O and CH_4. In particular, we expect to be able to determine at what extent the polar outflow provides a source of GHG-undersaturated waters to the subpolar North Atlantic. By addressing these scales of variability (sub-km), we expect to contribute to an improved representation of GHG sea-ice-air fluxes in climate models, and more accurate estimates of the relative weight of this area for the Arctic and global N_2O and CH_4 budgets. Likewise, the planned work at 79°N builds upon surveys conducted by the group in 2018, 2019, and 2021 in the region.

Data management

The data derived from this project (as well as the corresponding metadata) will be stored at the Ocean Science Information System (OSIS; https://portal.geomar.de/osis), which is the central information and research data sharing facility for marine research projects at GEOMAR. OSIS is publicly accessible and can be utilized by all team members as well as national and international collaborators. Final quality-controlled data will be uploaded to OSIS after 12 months. Moreover, final data will be submitted to the public repository PANGAEA (https://www.pangaea.de/) with a 2-year moratorium.

In all publications based on this expedition, the Grant No. **AWI_PS136_05** will be quoted and the following publication will be cited:

Alfred-Wegener-Institut Helmholtz-Zentrum für Polar- und Meeresforschung (2017) Polar Research and Supply Vessel POLARSTERN Operated by the Alfred-Wegener-Institute. Journal of large-scale research facilities, 3, A119. http://dx.doi.org/10.17815/jlsrf-3-163.

APPENDIX

A.1 TEILNEHMENDE INSTITUTE / PARTICIPATING INSTITUTES

A.2 FAHRTTEILNEHMER:INNEN / CRUISE PARTICIPANTS

A.3 SCHIFFSBESATZUNG / SHIP'S CREW

A.4 STATIONSLISTE / STATION LIST

A.1 TEILNEHMENDE INSTITUTE / PARTICIPATING INSTITUTES

Adresse	Address
DE.AWI	Alfred-Wegener-Institut Helmholtz-Zentrum für Polar- und Meeresforschung Am Handelshafen 12 27570 Bremerhaven Germany
DE.DRF	DRF Stiftung Luftrettung gemeinnützige AG Rita-Maiburg-Straße 2 70794 Filderstadt Germany
DE.DWD	Deutscher Wetterdienst Geschäftsbereich Wettervorhersage Seeschifffahrtsberatung Bernhard-Nocht-Straße 76 20359 Hamburg Germany
DE.GEOMAR	GEOMAR Helmholtz-Zentrum für Ozeanforschung Wischhofstraße 1-3 24148 Kiel Germany
DE.HS-BHV	Hochschule Bremerhaven An der Karlstadt 8 27568 Bremerhaven Germany
DE.HZH	Institut für Umweltchemie des Küstenraumes Helmholtz-Zentrum Hereon Max-Planck-Straße 1 21502 Geesthacht Germany
DE.MPIMM	Max-Planck-Institut für Marine Mikrobiologie Celsiusstraße 1 28359 Bremen Germany
DE.NHC	Northern Helicopter GmbH Gorch-Fock-Straße 103 26721 Emden Germany

Adresse	Address
DE.SENCKENBERG	Senckenberg am Meer DZMB Fachgebiet Epifauna c/o Biozentrum Grindel Martin-Luther-King Platz 3 20146 Hamburg Germany
DE.UNI-Bremen	Institut für Umweltphysik Universität Bremen Otto-Hahn-Alle 1 28359 Bremen Germany
DE.UNI-DUE	Universität Duisburg-Essen Universitätsstraße 2 45141 Essen Germany
DE.UNI-Hamburg	Universität Hamburg Mittelweg 177 20148 Hamburg Germany
DE.UNI-Rostock	Universität Rostock 18051 Rostock Universitätsplatz 1 Germany
IT.ISMAR	ISMAR – Istituto di Scienze Marine Consiglio Nazionale delle Ricerche (CNR) Via del Fosso del Cavaliere 100 00133 Rome Italy
NL.URAD	Radboud Universiteit Department of Ecological Microbiology Heyendaalseweg 135 6525AJ Nijmegen The Netherlands
NZ.UCANT	University of Canterbury 20 Kirkwood Avenue Upper Riccarton Christchurch 8041 New Zealand
UK.BAS	British Antarctic Survey High Cross Madingley Road Cambridge CB3 0ET United Kingdom

Adresse	Address
UK.NOC	National Oceanography Centre European Way Southampton SO14 3ZH United Kingdom
US.WHOI	Woods Hole Oceanographic Institution 266 Woods Hole Road Woods Hole MA 02543-1050 USA

A.2 FAHRTTEILNEHMER:INNEN / CRUISE PARTICIPANTS

Name/ Last name	Vorname/ First name	Institut/ Institute	Beruf/ Profession	Fachrichtung/ Discipline
Andres	Maikani	US.WHOI	Student (Master)	Biology
Asendorf	Volker	DE.MPIMM	Technician	Biology
Alexandra	Aves	NZ.UCANT	Scientist	Biology
Bergmann	Melanie	DE.AWI	Scientist	Biology
Breunig	Emelie	DE.UNI-Hamburg	Student (Master)	Oceanography
Brix	Saskia	DE.SENCKENBERG	Scientist	Biology
Bryan	Natasha	DE.AWI	Scientist	Biology
Busack	Michael	DE.AWI	Engineer	Engineering Sciences
Dannheim	Jennifer	DE.AWI	Scientist	Biology
Flegar	Konstantin	DE.AWI	Student (Bachelor)	Engineering Sciences
Freer	Jennifer	UK.BAS	Scientist	Biology
Hagemann	Jonas	DE.AWI	Engineer	Engineering Sciences
Hasemann	Christiane	DE.AWI	Scientist	Biology
Hecken	Timo	DE.DRF	Technician	Helicopter Service
Hirschmann	Sophia	DE.GEOMAR	PhD Student	Biology
Isler	Tea	DE.AWI	PhD Student	Bathymetry
Jack	Harding	DE.NHC	Pilot	Helicopter Service
Kistrup	Katharina	DE.AWI	Volunteer	Biology
Klüver	Tania	DE.GEOMAR	Technician	Biology
Knüppel	Nadine	DE.AWI	Technician	Biology
Kraberg	Alexandra	DE.AWI	Scientist	Biology
Lehmenhecker	Sascha	DE.AWI	Engineer	Engineering Sciences
Linse	Katrin	UK.BAS	Scientist	Biology
Lochthofen	Normen	DE.AWI	Engineer	Engineering Sciences
Ludszuweit	Janine	DE.AWI	Technician	Biology
McPherson	Rebecca	DE.AWI	Scientist	Oceanography
Metfies	Katja	DE.AWI	Scientist	Biology
Neber	Anneke	DE.HS-BHV	Student (Bachelor)	Engineering Sciences
Niehoff	Barbara	DE.AWI	Scientist	Biology
Pohlmann	Marei	DE.GEOMAR	Student (Master)	Chemistry
Pontiller	Benjamin	DE.GEOMAR	Scientist	Biology
Purser	Autun	DE.AWI	Scientist	Biology
Rehder	Linda	DE.AWI	PhD Student	Biology
Rohleder	Christian	DE.DWD	Scientist	Meteorology

Name/ Last name	**Vorname/ First name**	**Institut/ Institute**	**Beruf/ Profession**	**Fachrichtung/ Discipline**
Rückert	Sonja	DE.UNI-DUE	Scientist	Biology
Schewe	Ingo	DE.AWI	Scientist	Biology
Schmidt	Lydia	DE.SENCKENBERG	Student (Master)	Biology
Scholz	Daniel	DE.AWI	Engineer	Chemistry
Schrade	Maximilian	DE.AWI	Student (Master)	Biology
Schrage	Kharis	US.WHOI	PhD Student	Biology
Sebastian	Archana	DE.GEOMAR	Student (Master)	Oceanography
Seifert	Michael	DE.DRF	Technician	Helicopter Service
Soltwedel	Thomas	DE.AWI	Lead Scientist	Biology
Thielecke	Antonia	DE.AWI	PhD Student	Biology
Torres-Valdés	Sinhué	DE.AWI	Scientist	Oceanography
Vane	Kim	DE.AWI	Scientist	Biology
Vaupel	Lars	DE.NHC	Pilot	Helicopter Service
Volpe	Gianluca	IT.ISMAR	Scientist	Oceanography
Wenzel	Anna Julia	DE.DWD	Scientist	Meteorology
Xi	Hongyan	DE.AWI	Scientist	Oceanography

A.3 SCHIFFSBESATZUNG / SHIP‘S CREW

Name / Last name	Vorname / First name	Position / Rank
Wunderlich	Thomas Wolf	Master
Langhinrichs	Jacob	Chiefmate
Eckenfels	Hannes	Chiefmate Cargo
Peine	Lutz	2nd Mate
Weiß	Daniel	2nd Mate
Peine	Lutz Gerhard	2nd Mate
Dr. Guba	Klaus	Ships Doc
Grafe	Jens	1 Eng
Ehrke	Tom	2nd. Eng
Krinfeld	Oleksandr	2nd. Eng
Rusch	Torben	2nd. Eng
Pommerencke	Bernd	SET
Müller	Andreas	ELO
Schwedka	Thorsten	ELO
Winter	Andreas	ELO
Krüger	Lars	ELO
Brück	Sebastian	Bosun
Keller	Eugen Jürgen	Carpen.
Möller	Falko	MP Rat.
Buchholz	Joscha	MP Rat.
Schade	Tom	MP Rat.
Decker	Jens	MP Rat.
Fink	Anna-Maria	MP Rat.
Niebuhr	Tim	MP Rat.
Lutz	Johannes	MP Rat.
Luckhardt	Arne	MP Rat.
Jassmann	Marvin	MP Rat.
Probst	Lorenz	MP Rat.
Clasen	Nils	MP Rat.
Münzenberger	Börge	MP Rat
Plehn	Marco Markus	Storek.
Matter	Sebastian Udo	Cook
Bogner	Christoph Friedemann	Cooksm.
Lang	Gerd Martin	Cooksm.
Witusch	Petra	Chief Stew.
Ilk	Romy	2nd Stew
Fehrenbach	Martina	2nd Stew
Golla	Gerald	2nd Stew

Name / Last name	Vorname / First name	Position / Rank
Shi	Wubo	2nd Stew
Chen	Jirong	2nd Stew
Chen	Quan	Laundrym
Deutschbein	Felix Maximilian	Apprent.
Schroeder	Paul	Apprent.

A.4 STATIONSLISTE / STATION LIST PS136

Station list of expedition PS136 from Bremerhaven to Bremerhaven;
the list details the action log for all stations along the cruise track.

See https://www.pangaea.de/expeditions/events/PS136 to display the station (event) list for expedition PS136.
This version contains Uniform Resource Identifiers for all sensors listed under https://sensor.awi.de. See https://www.awi.de/en/about-us/service/computing-centre/data-flow-framework.html for further information about AWI's data flow framework from sensor observations to archives (O2A).

Event label	Optional label	Date/Time	Latitude	Longitude	Depth [m]	Gear	Action	Comment
PS136_0_Underway-53		2023-05-22T14:00:00	53.56401	8.55899		SWEAS	Station start	
PS136_0_Underway-53		2023-06-19T05:59:22	69.80625	19.42964	143	SWEAS	Station end	
PS136_0_Underway-31		2023-05-22T14:00:00	53.56401	8.55899		NEUMON	Station start	
PS136_0_Underway-31		2023-06-19T05:58:53	69.80666	19.43358	141	NEUMON	Station end	
PS136_0_Underway-11		2023-05-22T14:00:00	53.56401	8.55899		MYON	Station start	
PS136_0_Underway-11		2023-06-19T05:58:23	69.80709	19.43765	145	MYON	Station end	
PS136_0_Underway-44		2023-05-24T07:00:00	59.25294	4.17605	271	TSG	Station start	Keel 2
PS136_0_Underway-44		2023-06-19T00:29:30	70.61986	20.03471	230	TSG	Station end	Keel 2
PS136_0_Underway-24		2023-05-24T07:00:00	59.25294	4.17605	271	GRAV	Station start	
PS136_0_Underway-24		2023-06-19T00:30:00	70.61871	20.03612	228	GRAV	Station end	
PS136_0_Underway-13		2023-05-24T07:00:00	59.25294	4.17605	271	FBOX	Station start	
PS136_0_Underway-13		2023-06-19T00:28:33	70.62206	20.03181	211	FBOX	Station end	
PS136_0_Underway-23		2023-05-24T07:00:00	59.25294	4.17605	271	MAG	Station start	
PS136_0_Underway-23		2023-06-19T00:30:03	70.61859	20.03626	227	MAG	Station end	
PS136_0_Underway-43		2023-05-24T07:00:00	59.25294	4.17605	271	TSG	Station start	Keel 1
PS136_0_Underway-43		2023-06-19T00:29:10	70.62063	20.03375	226	TSG	Station end	Keel 1
PS136_0_Underway-42		2023-05-24T07:00:01	59.25298	4.17606	271	SNDVELPR	Station start	

** Comments are limited to 130 characters. See https://www.pangaea.de/expeditions/events/PS136 to show full comments in conjunction with the station (event) list for expedition PS136*

Event label	Optional label	Date/Time	Latitude	Longitude	Depth [m]	Gear	Action	Comment
PS136_0_Underway-42		2023-06-19T00:29:00	70.62102	20.03325	222	SNDVELPR	Station end	
PS136_0_Underway-35		2023-05-24T07:00:01	59.25298	4.17606	271	pCO2	Station start	
PS136_0_Underway-35		2023-06-19T00:29:00	70.62102	20.03325	222	pCO2	Station end	
PS136_0_Underway-3		2023-05-24T07:00:01	59.25298	4.17606	271	ADCP	Station start	
PS136_0_Underway-3		2023-06-19T00:15:20	70.65123	19.98921	169	ADCP	Station end	
PS136_0_Underway-20		2023-05-28T07:49:00	75.21038	5.09662	3306	ICERAD	Station start	
PS136_0_Underway-20		2023-06-16T17:00:00	78.81355	6.51158	1895	ICERAD	Station end	
PS136_0_Underway-34		2023-05-29T13:30:16	78.60035	5.14672	2338	pCO2	Station start	Values before 2023-05-29T13:30 are wrong, profile starts at this point
PS136_0_Underway-34		2023-06-19T00:27:00	70.62573	20.02714	241	pCO2	Station end	Values before 2023-05-29T13:30 are wrong, profile starts at this point
PS136_1-1		2023-05-23T00:57:22	54.76130	6.98958	23	LR-ADCP	Station start	
PS136_1-1		2023-05-24T00:56:42	58.34691	4.45257		LR-ADCP	Station end	
PS136_2-1		2023-05-27T03:01:15	69.99962	3.81126	3252	CTD-RO	max depth	
PS136_3-1		2023-05-28T05:54:54	75.00417	5.10437	3163	CTD-RO	max depth	
PS136_4-1		2023-05-29T01:04:36	78.60262	5.00445	2342	B_LANDER	Station start	Recovery
PS136_4-1		2023-05-30T05:20:36	78.61453	4.98255	2353	B_LANDER	Station end	Recovery
PS136_4-3		2023-05-29T02:01:15	78.60976	5.06773	2325	HN	Station start	
PS136_4-3		2023-05-29T02:04:30	78.60961	5.06735	2325	HN	Station end	
PS136_4-4		2023-05-29T02:04:55	78.60960	5.06730	2325	HN	Station start	
PS136_4-4		2023-05-29T02:08:40	78.60954	5.06702	2325	HN	Station end	
PS136_4-2		2023-05-29T02:24:16	78.60979	5.06756	2325	CTD-RO	max depth	
PS136_4-5		2023-05-29T03:39:07	78.60968	5.06831	2325	MSN	Station start	AWI030

Event label	Optional label	Date/Time	Latitude	Longitude	Depth [m]	Gear	Action	Comment
PS136_4-5		2023-05-29T05:34:59	78.60987	5.06750	2325	MSN	Station end	AWI030
PS136_4-6		2023-05-29T05:35:36	78.60990	5.06749	2325	MSN	Station start	AWI030
PS136_4-6		2023-05-29T07:20:10	78.61047	5.07216	2325	MSN	Station end	AWI030
PS136_4-7		2023-05-29T07:23:16	78.61055	5.07284	2325	LOKI	Station start	
PS136_4-7		2023-05-29T08:58:31	78.61102	5.07603	2326	LOKI	Station end	
PS136_4-8		2023-05-29T09:07:53	78.61087	5.07564	2326	RAMSES	Station start	
PS136_4-8		2023-05-29T10:49:12	78.61141	5.07430	2326	RAMSES	Station end	
PS136_4-9		2023-05-29T10:08:13	78.61110	5.07573	2326	CTD-RO	max depth	
PS136_4-10		2023-05-29T10:50:29	78.61137	5.07440	2326	AUV_lab	Station start	AUV "Paul", rubber boat "Laura"
PS136_4-10		2023-05-29T13:08:38	78.60939	5.09586	2325	AUV_lab	Station end	AUV "Paul", rubber boat "Laura"
PS136_4-11		2023-05-29T13:56:37	78.60055	5.15023	2339	EBS	Station start	
PS136_4-11		2023-05-29T18:17:25	78.61736	5.12614	2328	EBS	Station end	
PS136_4-12		2023-05-29T19:47:17	78.61017	5.06735	2325	TVMUC	max depth	
PS136_4-13		2023-05-29T21:34:39	78.61070	5.06228	2326	BC	max depth	
PS136_4-14		2023-05-30T00:04:00	78.61729	5.14365	2338	OFOBS	Station start	
PS136_4-14		2023-05-30T03:00:57	78.61735	5.00324	2350	OFOBS	Station end	
PS136_5-1		2023-05-30T09:15:27	79.06390	4.19088	2448	CTD-RO	max depth	
PS136_5-2		2023-05-30T09:18:34	79.06374	4.19133	2448	HN	Station start	
PS136_5-2		2023-05-30T09:19:28	79.06367	4.19176	2448	HN	Station end	
PS136_5-3		2023-05-30T09:49:05	79.06799	4.18816	2438	RAMSES	Station start	
PS136_5-3		2023-05-30T10:35:18	79.06670	4.19828	2433	RAMSES	Station end	
PS136_5-4		2023-05-30T10:40:43	79.06685	4.20054	2430	RAMSES	Station start	
PS136_5-4		2023-05-30T11:08:32	79.06783	4.21375	2420	RAMSES	Station end	
PS136_5-5		2023-05-30T11:18:39	79.06795	4.22026	2416	MSN	Station start	EL30
PS136_5-5		2023-05-30T13:17:57	79.07386	4.24159	2384	MSN	Station end	EL30
PS136_5-6		2023-05-30T13:31:17	79.07489	4.24055	2383	MSN	Station start	EL30
PS136_5-6		2023-05-30T15:28:40	79.07454	4.25933	2369	MSN	Station end	EL30

Event label	Optional label	Date/Time	Latitude	Longitude	Depth [m]	Gear	Action	Comment
PS136_5-7		2023-05-30T15:46:40	79.07323	4.26041	2372	LOKI	Station start	
PS136_5-7		2023-05-30T17:23:06	79.07255	4.25809	2377	LOKI	Station end	
PS136_5-8	Larvae Lander	2023-05-30T17:27:16	79.07282	4.25835	2375	B_LANDER	Station start	LARVAE-Lander
PS136_5-8	Larvae Lander	2023-05-31T20:19:16	79.06550	4.25750	2405	B_LANDER	Station end	LARVAE-Lander
PS136_5-9		2023-05-30T19:00:28	79.07431	4.25571	2372	EBS	Station start	
PS136_5-9		2023-05-30T22:18:41	79.09353	4.25370	2279	EBS	Station end	
PS136_5-10		2023-05-30T23:48:44	79.06590	4.16153	2462	BC	max depth	
PS136_5-11		2023-05-31T02:04:39	79.06488	4.18013	2450	TVMUC	max depth	
PS136_5-12		2023-05-31T03:57:42	79.06615	4.17615	2450	BC	max depth	
PS136_6-1	fat boy	2023-05-31T05:50:00	79.02951	4.31244	2543	MOOR	Station start	Mooring: fat boy, problems with recovery, no signal
PS136_6-1	fat boy	2023-05-31T06:46:10	79.02930	4.30972		MOOR	Station end	Mooring: fat boy, problems with recovery, no signal
PS136_6-2		2023-05-31T07:06:32	79.03600	4.27707		TRAMPER	Station start	Placeholder for Crawler III, no signal
PS136_6-2		2023-05-31T07:18:19	79.03641	4.28104		TRAMPER	Station end	Placeholder for Crawler III, no signal
PS136_6-3	FEVI-44	2023-05-31T07:53:02	78.99799	4.31365		MOOR	max depth	Recovery
PS136_6-4		2023-05-31T12:22:42	79.03485	4.17099	2607	OFOBS	max depth	
PS136_7-2		2023-05-31T21:26:05	79.10692	4.59711	1899	HN	Station start	
PS136_7-2		2023-05-31T21:28:14	79.10697	4.59667	1896	HN	Station end	
PS136_7-3		2023-05-31T21:26:30	79.10693	4.59698	1901	HN	Station start	
PS136_7-3		2023-05-31T21:29:33	79.10699	4.59659	1895	HN	Station end	
PS136_7-1		2023-05-31T21:31:08	79.10703	4.59656	1893	CTD-RO	max depth	
PS136_7-4		2023-05-31T23:00:52	79.10721	4.60434	1909	TVMUC	max depth	

Event label	Optional label	Date/Time	Latitude	Longitude	Depth [m]	Gear	Action	Comment
PS136_7-5		2023-06-01T00:52:57	79.10861	4.60674	1887	BC	max depth	
PS136_8-1		2023-06-01T03:54:45	78.99359	4.31289	2618	CTD-RO	max depth	
PS136_8-2	FEVI-46	2023-06-01T06:00:23	78.99915	4.32949	2602	MOOR	Station start	Deployment
PS136_8-2	FEVI-46	2023-06-01T09:23:09	79.00037	4.33102	2600	MOOR	Station end	Deployment
PS136_8-3		2023-06-01T10:50:55	79.03723	4.18514	2590	B_LANDER	Station start	Recovery
PS136_8-3		2023-06-01T12:05:54	79.02348	4.21117	2602	B_LANDER	Station end	Recovery
PS136_8-4		2023-06-01T12:32:12	79.03014	4.32014	2537	MOOR	Station start	Problems with recovery
PS136_8-4		2023-06-01T13:30:38	79.02972	4.32184	2537	MOOR	Station end	Problems with recovery
PS136_8-5	Crawler III	2023-06-01T13:55:22	79.03681	4.29281	2528	B_LANDER	Station start	Crawler III recovery
PS136_8-5	Crawler III	2023-06-01T15:37:24	79.03003	4.30011	2548	B_LANDER	Station end	Crawler III recovery
PS136_8-6		2023-06-01T16:31:32	79.07420	4.15143	2457	AUV_lab	Station start	AUV "Paul", rubber boat "Luisa"
PS136_8-6		2023-06-02T07:57:22	79.04183	5.02769	2179	AUV_lab	Station end	AUV "Paul", rubber boat "Luisa"
PS136_9-1		2023-06-01T19:47:32	79.10815	4.59021	1828	CTD-RO	max depth	
PS136_9-2		2023-06-01T21:00:13	79.10788	4.59186	1851	RAMSES	Station start	
PS136_9-2		2023-06-01T21:43:31	79.10807	4.59134	1834	RAMSES	Station end	
PS136_9-3		2023-06-01T21:46:38	79.10803	4.59226	1857	RAMSES	Station start	
PS136_9-3		2023-06-01T22:29:06	79.10858	4.59659	1858	RAMSES	Station end	
PS136_10-2		2023-06-01T23:32:44	79.13109	4.91688	1523	HN	Station start	
PS136_10-2		2023-06-01T23:37:27	79.13125	4.91603	1523	HN	Station end	
PS136_10-1		2023-06-01T23:32:53	79.13110	4.91684	1523	CTD-RO	max depth	
PS136_10-3		2023-06-02T00:05:50	79.13076	4.91028	1530	RAMSES	Station start	
PS136_10-3		2023-06-02T00:51:05	79.13191	4.89621	1534	RAMSES	Station end	
PS136_10-4		2023-06-02T01:36:50	79.13171	4.91256	1523	TVMUC	max depth	

Event label	Optional label	Date/Time	Latitude	Longitude	Depth [m]	Gear	Action	Comment
PS136_10-5		2023-06-02T02:58:10	79.13037	4.90139	1538	BC	max depth	
PS136_10-6	arcFOCE Lander	2023-06-02T03:50:14	79.13072	4.89940	1538	B_LANDER	Station start	arcFOCE Lander recovery
PS136_10-6	arcFOCE Lander	2023-06-07T19:31:05	79.13172	4.88586	1546	B_LANDER	Station end	arcFOCE Lander recovery
PS136_11-2		2023-06-02T09:31:14	79.13420	6.09412	1273	HN	Station start	
PS136_11-2		2023-06-02T10:08:42	79.13440	6.09391	1273	HN	Station end	
PS136_11-3		2023-06-02T09:38:51	79.13423	6.09395	1273	HN	Station start	
PS136_11-3		2023-06-02T09:41:54	79.13421	6.09329	1273	HN	Station end	
PS136_11-1		2023-06-02T09:55:21	79.13433	6.09366	1273	CTD-RO	max depth	
PS136_11-4		2023-06-02T11:17:57	79.13529	6.08503	1273	RAMSES	Station start	
PS136_11-4		2023-06-02T11:45:57	79.13705	6.07820	1276	RAMSES	Station end	
PS136_11-5		2023-06-02T11:47:34	79.13706	6.07795	1276	RAMSES	Station start	
PS136_11-5		2023-06-02T12:08:48	79.13619	6.07575	1275	RAMSES	Station end	
PS136_11-6		2023-06-02T12:34:55	79.13584	6.08169	1274	SPRA	Station start	SAMIP_5063
PS136_11-6		2023-06-02T13:11:00	79.13797	6.07974	1277	SPRA	Station end	SAMIP_5063
PS136_11-7		2023-06-02T13:19:36	79.13828	6.07817	1278	LOKI	Station start	
PS136_11-7		2023-06-02T14:57:54	79.13693	6.07519	1276	LOKI	Station end	
PS136_11-8		2023-06-02T15:03:14	79.13552	6.07959	1273	MSN	Station start	
PS136_11-8		2023-06-02T17:36:13	79.13371	6.09051	1271	MSN	Station end	
PS136_11-9		2023-06-02T18:23:28	79.13346	6.09118	1271	BC	max depth	
PS136_11-10		2023-06-02T19:35:26	79.13331	6.09159	1272	TVMUC	max depth	
PS136_11-11		2023-06-02T21:08:57	79.13317	6.09191	1272	BC	max depth	
PS136_11-12		2023-06-02T23:39:49	79.13246	6.11626	1267	OFOBS	Station start	
PS136_11-12		2023-06-03T03:21:00	79.13251	6.29469	1335	OFOBS	Station end	
PS136_11-13		2023-06-03T04:29:58	79.13380	6.08834	1271	CTD-RO	max depth	
PS136_11-14		2023-06-03T05:15:19	79.12695	6.09410	1266	EBS	Station start	
PS136_11-14		2023-06-03T08:04:28	79.11996	6.18729	1251	EBS	Station end	

Event label	Optional label	Date/Time	Latitude	Longitude	Depth [m]	Gear	Action	Comment
PS136_12-1	F4W-4	2023-06-03T09:25:21	79.00817	7.04146	1267	MOOR	Station start	Recovery
PS136_12-1	F4W-4	2023-06-03T11:56:05	78.99961	7.04372	1253	MOOR	Station end	Recovery
PS136_12-2	F4S-6	2023-06-03T12:17:36	79.00926	6.95871		MOOR	Station start	Recovery
PS136_12-2	F4S-6	2023-06-03T14:02:37	79.00382	6.94885		MOOR	Station end	Recovery
PS136_12-4		2023-06-03T14:37:02	79.02922	6.99878	1296	HN	Station start	
PS136_12-4		2023-06-03T14:40:28	79.02927	6.99925	1296	HN	Station end	
PS136_12-3		2023-06-03T14:40:48	79.02927	6.99925	1296	CTD-RO	max depth	
PS136_12-5		2023-06-03T14:56:49	79.02931	6.99889	1296	HN	Station start	
PS136_12-5		2023-06-03T15:02:49	79.02962	6.99950	1297	HN	Station end	
PS136_12-6		2023-06-03T15:15:41	79.02937	6.99807	1296	RAMSES	Station start	
PS136_12-6		2023-06-03T16:04:11	79.02818	6.99794	1294	RAMSES	Station end	
PS136_12-7		2023-06-03T16:05:08	79.02822	6.99795	1293	RAMSES	Station start	
PS136_12-7		2023-06-03T16:31:47	79.02868	6.99631	1294	RAMSES	Station end	
PS136_12-8		2023-06-03T17:21:50	79.02954	6.99970	1296	TVMUC	max depth	
PS136_12-9		2023-06-03T18:37:43	79.02969	6.99867	1296	BC	max depth	
PS136_13-2		2023-06-03T21:02:16	79.00013	8.22600	916	HN	Station start	
PS136_13-2		2023-06-03T21:05:45	79.00008	8.22555	917	HN	Station end	
PS136_13-3		2023-06-03T21:10:06	79.00011	8.22524	917	HN	Station start	
PS136_13-3		2023-06-03T21:13:32	79.00015	8.22555	916	HN	Station end	
PS136_13-1		2023-06-03T21:16:39	79.00014	8.22608	916	CTD-RO	max depth	
PS136_13-4		2023-06-03T22:24:41	79.00068	8.22870	916	BONGO	Station start	
PS136_13-4		2023-06-03T22:36:41	79.00132	8.23309	914	BONGO	Station end	
PS136_13-5		2023-06-03T22:43:53	79.00145	8.23454	912	RAMSES	Station start	
PS136_13-5		2023-06-03T23:11:53	79.00174	8.23596	911	RAMSES	Station end	
PS136_13-6		2023-06-04T00:04:18	78.99990	8.16119	976	OFOBS	Station start	
PS136_13-6		2023-06-04T02:26:57	79.00046	8.23362	910	OFOBS	Station end	
PS136_14-2		2023-06-04T06:36:43	79.02785	11.07763	287	HN	Station start	

Event label	Optional label	Date/Time	Latitude	Longitude	Depth [m]	Gear	Action	Comment
PS136_14-2		2023-06-04T06:39:38	79.02787	11.07770	286	HN	Station end	
PS136_14-1		2023-06-04T06:39:00	79.02787	11.07768	286	CTD-RO	max depth	
PS136_14-4		2023-06-04T07:09:50	79.02802	11.07827	286	RAMSES	Station start	
PS136_14-4		2023-06-04T08:02:27	79.02817	11.07691	286	RAMSES	Station end	
PS136_14-3		2023-06-04T07:16:58	79.02806	11.07844	287	HN	Station start	
PS136_14-3		2023-06-04T07:19:53	79.02818	11.07837	286	HN	Station end	
PS136_14-5		2023-06-04T08:30:22	79.02832	11.07637	287	CTD-RO	max depth	
PS136_14-6		2023-06-04T09:18:24	79.02807	11.07600	287	BONGO	Station start	
PS136_14-6		2023-06-04T09:28:45	79.02839	11.07647	287	BONGO	Station end	
PS136_14-7		2023-06-04T09:54:38	79.02842	11.07700	287	TVMUC	max depth	
PS136_15-1		2023-06-04T12:28:23	78.97981	9.42956	223	OFOBS	Station start	
PS136_15-1		2023-06-04T15:10:46	78.97777	9.53016	233	OFOBS	Station end	
PS136_15-2		2023-06-04T15:28:41	78.97987	9.51284	229	RAMSES	Station start	
PS136_15-2		2023-06-04T16:22:03	78.98038	9.51425	230	RAMSES	Station end	
PS136_15-3		2023-06-04T15:41:30	78.97950	9.51285	229	HN	Station start	
PS136_15-3		2023-06-04T15:44:37	78.97979	9.51292	229	HN	Station end	
PS136_15-4		2023-06-04T15:45:37	78.97988	9.51296	229	HN	Station start	
PS136_15-4		2023-06-04T15:48:28	78.97995	9.51299	229	HN	Station end	
PS136_15-5		2023-06-04T16:39:00	78.97998	9.51480	230	TVMUC	max depth	
PS136_16-1		2023-06-04T21:01:45	79.13190	6.10564	1272	MSN	Station start	
PS136_16-1		2023-06-04T22:51:02	79.13760	6.08305	1277	MSN	Station end	
PS136_17-1		2023-06-05T02:40:43	79.60725	5.14744	2775	CTD-RO	max depth	
PS136_17-2		2023-06-05T03:10:59	79.60712	5.12978	2789	RAMSES	Station start	
PS136_17-2		2023-06-05T03:58:48	79.60589	5.10596	2800	RAMSES	Station end	
PS136_17-3		2023-06-05T03:59:28	79.60587	5.10558	2801	MSN	Station start	
PS136_17-3		2023-06-05T06:14:19	79.59979	5.01671	2864	MSN	Station end	
PS136_17-4		2023-06-05T04:59:53	79.60433	5.06907	2837	HN	Station start	

Event label	Optional label	Date/Time	Latitude	Longitude	Depth [m]	Gear	Action	Comment
PS136_17-4		2023-06-05T05:03:41	79.60409	5.06696	2838	HN	Station end	
PS136_17-5		2023-06-05T08:07:10	79.61384	5.20190	2736	TVMUC	max depth	
PS136_17-6		2023-06-05T10:19:26	79.61153	5.13707	2769	BC	max depth	
PS136_17-8		2023-06-05T12:40:02	79.62252	5.07396	2788	HN	Station start	
PS136_17-8		2023-06-05T12:43:17	79.62239	5.07318	2789	HN	Station end	
PS136_17-9		2023-06-05T12:45:01	79.62238	5.07265	2789	HN	Station start	
PS136_17-9		2023-06-05T12:47:50	79.62243	5.07166	2790	HN	Station end	
PS136_17-7		2023-06-05T12:54:10	79.62277	5.06853	2793	CTD-RO	max depth	
PS136_18-1		2023-06-05T16:20:53	79.73896	4.47409	2613	CTD-RO	max depth	
PS136_18-2		2023-06-05T16:27:15	79.73926	4.47382	2612	HN	Station start	
PS136_18-2		2023-06-05T16:32:06	79.73951	4.47501	2611	HN	Station end	
PS136_18-3		2023-06-05T16:51:52	79.74007	4.47680	2607	RAMSES	Station start	
PS136_18-3		2023-06-05T17:44:13	79.74120	4.48379	2595	RAMSES	Station end	
PS136_18-4		2023-06-05T17:00:04	79.74028	4.47797	2605	HN	Station start	
PS136_18-4		2023-06-05T17:11:38	79.74066	4.48030	2601	HN	Station end	
PS136_18-5		2023-06-05T17:51:12	79.74135	4.48499	2593	FRRF	max depth	
PS136_18-6		2023-06-05T19:46:46	79.75856	4.42920	2552	LOKI	Station start	
PS136_18-6		2023-06-05T21:23:06	79.75984	4.43363	2542	LOKI	Station end	
PS136_18-7		2023-06-05T21:26:35	79.76000	4.43350	2541	MSN	Station start	
PS136_18-7		2023-06-05T23:36:19	79.76771	4.44037	2489	MSN	Station end	
PS136_18-8		2023-06-05T23:43:26	79.76879	4.44220	2483	MSN	Station start	
PS136_18-8		2023-06-06T02:19:35	79.78662	4.45146	2380	MSN	Station end	
PS136_18-9		2023-06-06T03:16:42	79.79358	4.45855	2356	TVMUC	max depth	
PS136_18-10		2023-06-06T05:16:20	79.80737	4.46884	2288	BC	max depth	
PS136_18-11		2023-06-06T07:04:04	79.81075	4.46829	2280	CTD-RO	max depth	
PS136_19-1		2023-06-06T11:40:44	79.61757	5.34731	2523	EBS	Station start	
PS136_19-1		2023-06-06T14:29:19	79.61244	5.30274	2608	EBS	Station end	

Event label	Optional label	Date/Time	Latitude	Longitude	Depth [m]	Gear	Action	Comment
PS136_20-1	F4S-7	2023-06-06T19:28:44	79.01116	6.96227	1253	MOOR	Station start	Deployment
PS136_20-1	F4S-7	2023-06-06T21:27:52	79.01158	6.96149	1254	MOOR	Station end	Deployment
PS136_21-1	Larvae Lander	2023-06-06T23:46:02	79.33443	6.00144	1715	B_LANDER	Station start	Deployment Larvae Lander; recovery
PS136_21-1	Larvae Lander	2023-06-07T16:53:05	79.33757	6.00957	1715	B_LANDER	Station end	Deployment Larvae Lander; recovery
PS136_22-1		2023-06-07T02:41:25	79.04264	6.69005	1229	OFOBS	Station start	
PS136_22-1		2023-06-07T06:19:43	79.02574	6.77842	1225	OFOBS	Station end	
PS136_22-2		2023-06-07T07:21:32	79.04252	6.69738	1229	AUV_lab	Station start	
PS136_22-2		2023-06-07T14:01:32	79.04178	6.70415	1230	AUV_lab	Station end	
PS136_23-2		2023-06-07T22:16:23	79.05639	3.66187		HN	Station start	
PS136_23-2		2023-06-07T22:22:03	79.05576	3.66493	1874	HN	Station end	
PS136_23-1		2023-06-07T22:18:07	79.05612	3.66267		CTD-RO	max depth	
PS136_23-3		2023-06-07T22:29:20	79.05521	3.66920		HN	Station start	
PS136_23-3		2023-06-07T22:36:47	79.05459	3.67196		HN	Station end	
PS136_23-4		2023-06-07T22:49:48	79.05339	3.67603	1567	RAMSES	Station start	
PS136_23-4		2023-06-07T23:21:18	79.05044	3.68988	2950	RAMSES	Station end	
PS136_23-5		2023-06-07T23:44:03	79.04845	3.70623	2879	CTD-RO	max depth	
PS136_23-6		2023-06-08T01:15:29	79.05318	3.67753	3031	TVMUC	max depth	
PS136_23-7		2023-06-08T03:44:53	79.05578	3.69516	2993	BC	max depth	
PS136_24-1		2023-06-08T05:58:14	79.04204	3.54467	3573	CTD-RO	max depth	
PS136_24-2		2023-06-08T06:05:59	79.04199	3.54442	3580	HN	Station start	
PS136_24-2		2023-06-08T06:08:21	79.04200	3.54451	3585	HN	Station end	
PS136_24-3		2023-06-08T06:09:46	79.04201	3.54452	3586	HN	Station start	
PS136_24-3		2023-06-08T06:17:19	79.04202	3.54441	3581	HN	Station end	
PS136_24-4		2023-06-08T07:08:32	79.04241	3.54327	3576	RAMSES	Station start	

Event label	Optional label	Date/Time	Latitude	Longitude	Depth [m]	Gear	Action	Comment
PS136_24-4		2023-06-08T07:51:40	79.04393	3.54014	3592	RAMSES	Station end	
PS136_24-5		2023-06-08T09:16:06	79.04697	3.53894	3601	TVMUC	max depth	
PS136_24-6		2023-06-08T12:33:42	79.03627	3.56640	3519	BC	max depth	
PS136_25-2		2023-06-08T14:53:53	79.05991	3.44434	4103	HN	Station start	
PS136_25-2		2023-06-08T15:01:08	79.05950	3.44655	4103	HN	Station end	
PS136_25-1		2023-06-08T15:01:26	79.05949	3.44658	4113	CTD-RO	max depth	
PS136_25-3		2023-06-08T15:01:59	79.05948	3.44666	4100	HN	Station start	
PS136_25-3		2023-06-08T15:04:05	79.05941	3.44698	4112	HN	Station end	
PS136_25-4		2023-06-08T15:29:28	79.05808	3.45704	4070	RAMSES	Station start	
PS136_25-4		2023-06-08T16:13:37	79.05619	3.47718	3981	RAMSES	Station end	
PS136_25-5		2023-06-08T16:23:32	79.05583	3.48203	3975	BONGO	Station start	
PS136_25-5		2023-06-08T16:35:18	79.05537	3.48766	3959	BONGO	Station end	
PS136_25-6		2023-06-08T18:36:17	79.05232	3.44151		TVMUC	max depth	
PS136_25-7		2023-06-08T21:35:18	79.04608	3.48282		BC	max depth	
PS136_25-8		2023-06-09T01:04:27	79.05094	3.44317	4126	BC	max depth	
PS136_26-1		2023-06-09T03:26:31	79.06245	3.33882	5075	RAMSES	Station start	
PS136_26-1		2023-06-09T04:04:00	79.06006	3.33912	4210	RAMSES	Station end	
PS136_26-2		2023-06-09T06:11:46	79.06603	3.33137	5032	TVMUC	max depth	
PS136_27-2		2023-06-09T09:55:11	79.12761	2.96598	5520	HN	Station start	
PS136_27-2		2023-06-09T09:59:31	79.12682	2.96724	5519	HN	Station end	
PS136_27-1		2023-06-09T09:57:41	79.12717	2.96664	5520	CTD-RO	max depth	
PS136_27-3		2023-06-09T10:05:37	79.12560	2.96855	5517	HN	max depth	
PS136_27-4		2023-06-09T10:24:11	79.12400	2.97009	5514	RAMSES	Station start	
PS136_27-4		2023-06-09T11:08:26	79.11916	2.97158	5507	RAMSES	Station end	
PS136_27-5		2023-06-09T11:27:10	79.11717	2.97047	5501	FRRF	Station start	LWL not working
PS136_27-5		2023-06-10T01:59:01	79.13497	2.93737	5533	FRRF	Station end	LWL not working
PS136_27-6		2023-06-09T12:00:04	79.11484	2.96200	5463	LOKI	Station start	
PS136_27-6		2023-06-09T13:12:54	79.11266	2.93569	5410	LOKI	Station end	

Event label	Optional label	Date/Time	Latitude	Longitude	Depth [m]	Gear	Action	Comment
PS136_27-7		2023-06-09T13:30:36	79.12477	2.95236	5519	BONGO	Station start	
PS136_27-7		2023-06-09T13:39:15	79.12429	2.95139	5518	BONGO	Station end	
PS136_27-8		2023-06-09T13:50:47	79.12411	2.95108	5518	MSN	Station start	
PS136_27-8		2023-06-09T16:01:16	79.12258	2.97291	5511	MSN	Station end	
PS136_27-9		2023-06-09T16:51:58	79.12278	2.98227	5510	CTD-RO	max depth	
PS136_27-10		2023-06-09T20:23:06	79.13290	2.94117	5529	TVMUC	max depth	
PS136_27-11		2023-06-10T00:13:57	79.13571	2.94215	5531	BC	max depth	
PS136_27-12		2023-06-10T02:49:02	79.12546	2.72375	5420	EBS	Station start	
PS136_27-12		2023-06-10T08:14:03	79.12511	2.77464	5426	EBS	Station end	
PS136_28-2		2023-06-10T10:21:29	79.06830	3.25766	5182	HN	Station start	
PS136_28-2		2023-06-10T10:28:24	79.06861	3.25743	5180	HN	Station end	
PS136_28-1		2023-06-10T10:22:35	79.06842	3.25741	5179	CTD-RO	max depth	
PS136_28-3		2023-06-10T11:04:33	79.06995	3.26336	5175	MSN	Station start	Test LWL
PS136_28-3		2023-06-10T13:42:34	79.06715	3.30037	5124	MSN	Station end	Test LWL
PS136_29-1		2023-06-10T15:48:13	79.21492	3.66928	3532	B_LANDER	Station start	Seaweed Project
PS136_29-1		2023-06-10T15:49:55	79.21497	3.66972	3462	B_LANDER	Station end	Seaweed Project
PS136_30-1		2023-06-11T07:56:48	78.77024	-2.64611	2618	CTD-RO	max depth	
PS136_30-4		2023-06-11T07:58:58	78.76996	-2.64624	2619	HN	Station start	
PS136_30-4		2023-06-11T08:02:38	78.76954	-2.64624	2619	HN	Station end	
PS136_30-5		2023-06-11T08:15:24	78.76751	-2.64468	2620	HN	Station start	
PS136_30-5		2023-06-11T08:20:14	78.76778	-2.64515	2619	HN	Station end	
PS136_30-2		2023-06-11T08:27:04	78.76713	-2.64352	2620	RAMSES	Station start	
PS136_30-2		2023-06-11T09:09:44	78.76235	-2.63659	2621	RAMSES	Station end	
PS136_30-3		2023-06-11T09:25:00	78.75176	-2.64515	2623	LOKI	Station start	
PS136_30-3		2023-06-11T10:53:32	78.74104	-2.62467	2631	LOKI	Station end	
PS136_30-6		2023-06-11T11:04:47	78.73695	-2.61797	2635	MSN	Station start	
PS136_30-6		2023-06-11T13:23:50	78.71170	-2.68047	2630	MSN	Station end	
PS136_30-7		2023-06-11T14:10:36	78.70084	-2.70614	2620	CTD-RO	max depth	

Event label	Optional label	Date/Time	Latitude	Longitude	Depth [m]	Gear	Action	Comment
PS136_30-8		2023-06-11T17:05:32	78.66477	-2.80931	2524	TVMUC	max depth	
PS136_30-9		2023-06-11T19:01:15	78.64156	-2.81703	2513	GKG	max depth	
PS136_30-10		2023-06-11T19:55:26	78.62875	-2.78686	2533	EBS	Station start	
PS136_30-10		2023-06-12T00:21:16	78.55081	-2.77215	2564	EBS	Station end	
PS136_31-2		2023-06-12T06:21:07	78.81219	-3.91640	1963	HN	Station start	
PS136_31-2		2023-06-12T06:23:32	78.81195	-3.91663	1963	HN	Station end	
PS136_31-1		2023-06-12T06:22:15	78.81208	-3.91653	1963	CTD-RO	max depth	
PS136_31-3		2023-06-12T06:24:15	78.81186	-3.91674	1963	HN	Station start	
PS136_31-3		2023-06-12T06:27:44	78.81146	-3.91657	1962	HN	Station end	
PS136_31-4		2023-06-12T07:01:09	78.81207	-3.91599	1963	RAMSES	Station start	
PS136_31-4		2023-06-12T07:42:42	78.81225	-3.91572	1964	RAMSES	Station end	
PS136_31-5		2023-06-12T08:43:37	78.80963	-3.90583	1970	TVMUC	max depth	
PS136_31-6		2023-06-12T10:18:40	78.78638	-3.80785	2011	BC	max depth	
PS136_31-7		2023-06-12T11:54:49	78.76924	-3.74602	2048	CTD-RO	max depth	
PS136_32-2		2023-06-12T23:00:24	78.92720	-4.72523	1477	HN	Station start	
PS136_32-2		2023-06-12T23:00:43	78.92714	-4.72525	1477	HN	Station end	
PS136_32-1		2023-06-12T23:04:26	78.92635	-4.72544	1476	CTD-RO	max depth	
PS136_32-3		2023-06-12T23:06:11	78.92596	-4.72543	1476	HN	Station start	
PS136_32-3		2023-06-12T23:06:38	78.92587	-4.72541	1476	HN	Station end	
PS136_32-4		2023-06-13T00:23:31	78.90913	-4.72412	1432	TVMUC	max depth	
PS136_32-5		2023-06-13T01:29:26	78.90125	-4.70107	1443	BC	max depth	
PS136_33-1		2023-06-13T08:43:17	78.99019	-5.38830	1021	CTD-RO	max depth	
PS136_33-4		2023-06-13T09:15:15	78.98966	-5.37934	1027	RAMSES	Station start	
PS136_33-4		2023-06-13T10:01:42	78.98838	-5.37462	1027	RAMSES	Station end	
PS136_33-2		2023-06-13T09:27:05	78.98898	-5.38037	1025	HN	Station start	
PS136_33-2		2023-06-13T09:33:42	78.98887	-5.37904	1025	HN	Station end	
PS136_33-3		2023-06-13T09:34:11	78.98886	-5.37895	1025	HN	Station start	Deployment
PS136_33-3		2023-06-13T09:38:11	78.98877	-5.37818	1026	HN	Station end	Deployment

Event label	Optional label	Date/Time	Latitude	Longitude	Depth [m]	Gear	Action	Comment
PS136_33-5		2023-06-13T10:16:21	78.98794	-5.37148	1028	LOKI	Station start	
PS136_33-5		2023-06-13T11:38:22	78.98492	-5.35337	1040	LOKI	Station end	
PS136_33-6		2023-06-13T11:52:52	78.98411	-5.34987	1043	MSN	Station start	
PS136_33-6		2023-06-13T13:24:27	78.97745	-5.33265	1047	MSN	Station end	
PS136_33-7	EGC-9	2023-06-13T13:55:25	78.99042	-5.41544	973	MOOR	Station start	Deployment
PS136_33-7	EGC-9	2023-06-13T16:06:58	78.97847	-5.42718	949	MOOR	Station end	Deployment
PS136_33-8		2023-06-13T16:28:28	78.97566	-5.42032	948	BONGO	Station start	
PS136_33-8		2023-06-13T16:37:14	78.97484	-5.42218	945	BONGO	Station end	
PS136_33-9		2023-06-13T17:17:26	78.97217	-5.42786	938	CTD-RO	max depth	
PS136_33-10		2023-06-13T19:09:47	78.96615	-5.43017	927	TVMUC	max depth	
PS136_33-11		2023-06-13T19:59:04	78.96408	-5.42498	925	BC	max depth	
PS136_34-1		2023-06-14T06:25:08	78.83735	-3.03690	2427	OFOBS	Station start	
PS136_34-1		2023-06-14T10:00:00	78.80334	-3.12374	2417	OFOBS	Station end	
PS136_34-2		2023-06-14T10:20:36	78.79963	-3.11885	2421	BONGO	Station start	
PS136_34-2		2023-06-14T10:32:13	78.79853	-3.11625	2433	BONGO	Station end	
PS136_35-1		2023-06-15T03:03:27	79.04653	3.67822	2891	CTD-RO	max depth	
PS136_36-1		2023-06-15T13:15:02	79.57034	5.24030	2590	OFOBS	Station start	
PS136_36-1		2023-06-15T15:22:17	79.58307	5.21138	2619	OFOBS	Station end	
PS136_37-1	arcFOCE Lander	2023-06-15T21:28:05	79.13570	4.88639	1485	B_LANDER	Station start	arc-FOCE deployment
PS136_37-1	arcFOCE Lander	2023-06-15T21:37:00	79.13484	4.87918	1496	B_LANDER	Station end	arc-FOCE deployment
PS136_38-1		2023-06-15T23:50:38	79.03099	4.22216	2516	B_LANDER	Station start	Deployment Long Term Lander
PS136_38-1		2023-06-15T23:53:17	79.03064	4.22223	2516	B_LANDER	Station end	Deployment Long Term Lander
PS136_39-1		2023-06-16T04:55:15	79.10863	3.38748	4989	OFOBS	Station start	
PS136_39-1		2023-06-16T08:16:07	79.10368	3.42241		OFOBS	Station end	

** Comments are limited to 130 characters. See https://www.pangaea.de/expeditions/events/PS136 to show full comments in conjunction with the station (event) list for expedition PS136.*

Abbreviation	Method/Device
ADCP	Acoustic Doppler Current Profiler
AUV_lab	Autonomous underwater vehicle Polar Autonomous Underwater Laboratory
BC	Box corer
BONGO	Bongo net
B_LANDER	Bottom lander
CTD-RO	CTD/Rosette
EBS	Epibenthic sledge
FBOX	FerryBox
FRRF	Fluorometer, fast repetition rate
GKG	Giant box corer
GRAV	Gravimetry
HN	Hand net
ICERAD	Ice radar
LOKI	Light frame on-sight keyspecies investigation
LR-ADCP	Acoustic Doppler Current Profiling, LongRanger
MAG	Magnetometer
MOOR	Mooring
MSN	Multiple opening/closing net
MYON	DESY Myon Detector
NEUMON	Neutron monitor
OFOBS	Ocean Floor Observation and Bathymetry System
RAMSES	RAMSES hyperspectral radiometer
SNDVELPR	Sound velocity probe
SPRA	Spectral radiometer
SWEAS	Ship Weather Station
TRAMPER	TRAMPER
TSG	Thermosalinograph
TVMUC	Multicorer with television
pCO2	pCO2 sensor
ZODIAC	Rubber boat, Zodiac
pCO2	pCO2 sensor

Die **Berichte zur Polar- und Meeresforschung** (ISSN 1866-3192) werden beginnend mit dem Band 569 (2008) als Open-Access-Publikation herausgegeben. Ein Verzeichnis aller Bände einschließlich der Druckausgaben (ISSN 1618-3193, Band 377-568, von 2000 bis 2008) sowie der früheren **Berichte zur Polarforschung** (ISSN 0176-5027, Band 1–376, von 1981 bis 2000) befindet sich im electronic Publication Information Center **(ePIC)** des Alfred-Wegener-Instituts, Helmholtz-Zentrum für Polar- und Meeresforschung (AWI); see https://epic.awi.de. Durch Auswahl “Reports on Polar- and Marine Research“ (via “browse”/”type”) wird eine Liste der Publikationen, sortiert nach Bandnummer, innerhalb der absteigenden chronologischen Reihenfolge der Jahrgänge mit Verweis auf das jeweilige pdf-Symbol zum Herunterladen angezeigt.

The **Reports on Polar and Marine Research** (ISSN 1866-3192) are available as open access publications since 2008. A table of all volumes including the printed issues (ISSN 1618-3193, Vol. 377-568, from 2000 until 2008), as well as the earlier **Reports on Polar Research** (ISSN 0176-5027, Vol. 1–376, from 1981 until 2000) is provided by the electronic Publication Information Center **(ePIC)** of the Alfred Wegener Institute, Helmholtz Centre for Polar and Marine Research (AWI); see URL https://epic.awi.de. To generate a list of all Reports, use the URL http://epic.awi.de and select “browse”/”type” to browse ”Reports on Polar and Marine Research”. A chronological list in declining order will be presented, and pdf-icons displayed for downloading.

Zuletzt erschienene Ausgaben:

Recently published issues:

780 (2023) The Expedition PS136 of the Research Vessel POLARSTERN to the Fram Strait in 2023, edited by Thomas Soltwedel with contributions of the participants

779 (2023) The Expedition PS135/1 and PS135/2 of the Research Vessel POLARSTERN to the Atlantic Ocean in 2023, edited by Yvonne Schulze Tenberge and Björn Fiedler with contributions of the participants

778 (2023) The MOSES Sternfahrt Expeditions of the Research Vessels ALBIS, LITTORINA, LUDWIG PRANDTL, MYA II and UTHÖRN to the Elbe River, Elbe Estuary and German Bight in 2022, edited by Ingeborg Bussmann, Norbert Anselm, Holger Brix, Norbert Kamjunke, Matthias Koschorreck, Björn Raupers, Tina Sanders with contributions of the participants

777 (2023) The Expedition PS134 of the Research Vessel POLARSTERN to the Bellingshausen Sea in 2022/2023, edited by Karsten Gohl with contributions of the participants

776 (2023) The Expedition PS129 of the Research Vessel POLARSTERN to the Weddell Sea in 2022, edited by Mario Hoppema with contributions of the participants

775 (2023) The Expedition PS133/2 of the Research Vessel POLARSTERN to the Scotia Sea in 2022, edited by Sabine Kasten with contributions of the participants

774 (2023) The Expedition PS133/1 of the Research Vessel POLARSTERN to the Atlantic Ocean in 2022, edited by Christine Klaas with contributions of the participants

773 (2023) A computational approach of locomotion, energy demand and dispersal of the common comatulid crinoid *Promachocrinus kerguelensis* (Echinodermata) and its circum-Antarctic success, by Nils Owsianowski

772 (2023) Russian-German Cooperation: Expeditions to Siberia in 2021, edited by Anne Morgenstern, Birgit Heim, Luidmila A. Pestryakova, Dmitry Yu. Bolshiyanov, Mikhail N. Grigoriev, Dmitry Ayunov, Antonia Dill, and Iuliia Jünger

ALFRED-WEGENER-INSTITUT
HELMHOLTZ-ZENTRUM FÜR POLAR-
UND MEERESFORSCHUNG

BREMERHAVEN

Am Handelshafen 12
27570 Bremerhaven
Telefon 0471 4831-0
Telefax 0471 4831-1149
www.awi.de

HELMHOLTZ